



UNIVERSIDADE DE ÉVORA

Inputs and yield optimization on irrigated maize

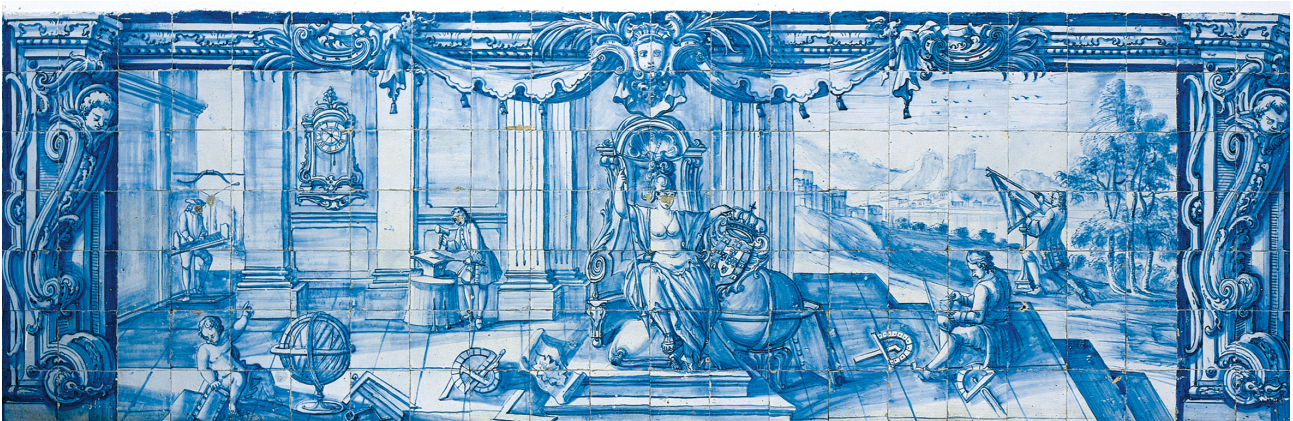
Otimização da produtividade e dos fatores de produção no milho de regadio

Anabela Dias Ramalho Vale Leitão Grifo

Tese apresentada à Universidade de Évora
para obtenção do Grau de Doutor em Ciências Agrárias
na especialidade Agronomia

Orientadores *José Rafael Marques da Silva*
Maria Manuela Melo Oliveira
Carlos Alberto de Jesus Alexandre

Évora, setembro de 2015



INSTITUTO DE INVESTIGAÇÃO E FORMAÇÃO AVANÇADA

À minha família

“Everything is related to everything else, but near things are more related than distant things.”

Waldo Tobler, 1979

Acknowledgements/Agradecimentos

No final deste trabalho gostaria de testemunhar o meu agradecimento a diversas pessoas e instituições que, direta ou indiretamente, contribuíram de forma significativa para sua realização.

Ao meu orientador, Professor Doutor José Rafael Marques da Silva, pela excelente orientação científica, incansável ajuda e apoio em todas as tarefas e fases do trabalho. Obrigada pelos seus ensinamentos, pela dinâmica de trabalho e constante estímulo e pela sua pronta e inesgotável disponibilidade. Não posso ainda deixar de referir a sua enorme paciência e compreensão, entusiasmo, simpatia e amizade demonstrada ao longo destes anos e que foram decisivos para ultrapassar algumas situações difíceis. Mesmo nos momentos mais complicados fez-me sempre acreditar que era possível.

Aos meus coorientadores científicos, Professora Doutora Maria Manuela Melo Oliveira e Professor Doutor Carlos Alberto de Jesus Alexandre pela orientação, incentivo, esclarecimentos e sugestões, confiança, enorme disponibilidade e simpatia com que sempre me receberam. Há momentos que fazem a diferença.

Ao Professor Doutor Gottlieb, director do curso de doutoramento em Ciências Agrárias da Escola de Ciência e Tecnologia da Universidade de Évora pelo acolhimento no curso de doutoramento.

Ao Instituto de Ciências Agrárias e Ambientais Mediterrânicas (ICAAM) por ter sido a minha unidade de acolhimento durante a realização da investigação desenvolvida nesta dissertação.

Ao Engenheiro Castro Duarte e seus colaboradores por todas as condições que me proporcionaram para desenvolver o trabalho de campo.

À Escola Superior Agrária de Santarém (ESAS) e em particular ao Professor Coordenador José Mira de Villas Boas Potes, diretor da ESAS, ao Professor Coordenador António do Patrocínio Amaral de Azevedo, na qualidade de ex-diretor da ESAS, ao Professor Coordenador Manuel Mendes de Sousa Adaixo, presidente do Departamento de Ciências Agrárias e Ambiente da ESAS e ao Professor Adjunto António Mendes Marques, presidente da Unidade Laboratorial de Ciências Agrárias e Ambiente da ESAS, pela amizade, entusiasmo e por me proporcionarem total liberdade em utilizar a Unidade Laboratorial de Ciências Agrárias e Ambiente.

Ao meu marido, Luís Grifo, um dos pilares da minha vida, por acreditar em mim mais do que eu própria, e ser sempre a minha estrutura de apoio de forma incondicional. Trabalhou de forma incansável na recolha de dados de campo, muitas vezes em condições adversas e sempre com alegria e boa disposição. Conseguiu transformar momentos complicados em momentos felizes. É a minha fonte de força que me incutiu a determinação em querer chegar mais longe.

x

À Mestre Albertina Ferreira, colega de trabalho e grande amiga, que me acompanhou ao longo de todo este percurso, me auxiliou em muitos momentos e com quem partilhei algumas lágrimas mas também muitas gargalhadas e muitas horas de trabalho tornando este trajeto muito mais ameno. Emocionalmente, a boa disposição que partilhámos foi relevante para a realização deste estudo.

À minha irmã, Esmeralda Cristina que, com o seu amor incondicional, me fez a revisão dos textos em inglês, muitas vezes com prejuízo próprio. O seu apoio, carinho e compreensão foram essenciais para tornar os meus dias mais harmoniosos.

Às colegas e amigas, Professora Adjunta Ana Cláudia Charana e Professora Adjunta Ana Ambrósio Paulo que me apoiaram em termos de serviço letivo, ouviram os meus lamentos e me proporcionaram bom ambiente de trabalho e um alegre convívio.

À Mestre Maria Fernanda Rebelo, colega e grande amiga, pelo entusiasmo e preciosa ajuda na determinação, coordenação e orientação de todas as análises de solos. À equipa de funcionários da Unidade Laboratorial de Ciências Agrárias e Ambiente da ESAS (Rute Sales Costa, José Manuel Saragoça, Maria Madalena Mascarenhas e Maria José Maia) e às alunas Ana Catarina Rebelo e Ana Rita Pereira que disponibilizaram o seu tempo para colaborar amavelmente na realização de algumas tarefas, revelando sempre boa disposição.

Ao Laboratório Químico Agrícola (LQA) da Universidade de Évora pela ajuda na determinação de alguns parâmetros do solo.

Ao meu colega e amigo Mestre Rodrigo Rodrigues que com amabilidade que o caracteriza me acompanhou e ajudou em alguns trabalhos de campo.

Ao jovem, Luís Marques da Silva que ajudou na recolha de dados de campo com energia e entusiasmo.

Aos meus queridos filhos, Eduardo Grifo e Bruno Grifo pelo seu carinho e amor e por compreenderem as inúmeras ausências. Trabalharam de forma incansável na recolha de dados de campo mostrando sempre compreensão e entusiasmo mesmo em condições hostis. Que este trabalho lhes sirva de motivação e exemplo de que vale sempre a pena investirmos em nós próprios e em novos desafios, independentemente da nossa idade.

Aos meus pais, Maria Celeste e António Leitão, pelo seu amor sem dimensão, pelos princípios e valores que me inculcaram, por me “mimarem” durante toda a vida, por estarem presentes de forma incondicional nos momentos mais difíceis, por me ensinarem a importância dos “estudos” e acreditarem em mim.

À minha família, especialmente sogros, cunhados e sobrinhos por compreenderem o meu afastamento e ausências e por toda a alegria e carinho que me proporcionaram.

Aos meus amigos, Lúcia Coelho, Alexandre Coelho e Dra. Maria Pilar Rosinha pela boa disposição, incentivo, amizade e disponibilidade com os meus filhos, dando o apoio necessário sempre que lhes solicitava.

Às minhas amigas Doutora Maria Encarnação Marcelo, Mestre Iris Crispim, Doutora Rita Neres, Doutora Marta Madeira, Professora Adjunta Maria Adelaide Oliveira, Doutora Ana Mafalda Ferreira, Professora Adjunta Paula Lúcia Ruivo, Professora adjunta Rosa Santos Coelho, Especialista José Manuel Carvalho, Professora Adjunta Helena Mira que em muitos dos momentos mais sensíveis me ouviram, compreenderam e incentivaram. A todos os colegas e funcionários da ESAS e amigos que tiveram sempre uma palavra de estímulo.

Ao Professor Doutor Francisco Coelho pelo trabalho e disponibilidade em adequar o “template do latex” à situação desta dissertação.

A todos

Um muito obrigado ...

Contents

Contents	xi
List of Figures	xv
List of Tables	xvii
Acronyms	xix
Abstract	xxi
Sumário	xxiii
1 Introduction	1
1.1 Objectives	2
2 Scientific background	3
2.1 Precision agriculture	3
2.2 Spatial and temporal variability	4
2.2.1 Yield	4
2.2.2 Soil	5
2.2.3 Topography	6
2.2.4 Other sources	7
2.3 Management zones	7
2.4 Evaluating variability	8
2.4.1 Grid sampling	8
2.4.2 Sensors	9
2.5 Variable-rate technology	12

3	Exploratory Field Risk Analysis Considering Space and Multi-Year Maize Yield	13
3.1	Introduction	14
3.2	Materials and Methods	15
3.2.1	Collecting and processing yield data	15
3.2.2	Data analysis	16
3.3	Results	18
3.3.1	Grain yield descriptive statistics	18
3.3.2	Grain yield spatial dependence	19
3.3.3	Principal Components Analysis	19
3.4	Discussion	21
3.5	Conclusions	28
4	Stochastic simulation of maize productivity: spatial and temporal uncertainty in order to manage crop risks	29
4.1	Introduction	30
4.2	Materials and Methods	31
4.2.1	Details of the field experimental site and the collection of yield data	31
4.2.2	Data processing and analysis	32
4.3	Results and Discussion	33
4.3.1	Exploratory and spatial structure analyses	33
4.3.2	Real Yield Data	36
4.3.3	Yield Stochastic Simulations	36
4.3.4	Yield classes and their occurrence probability	50
4.4	Conclusions	51
5	Maize fertilization: soil phosphorous and potassium optimization - yield/input ratio	53
5.1	Introduction	54
5.2	Materials and methods	56
5.2.1	Study field	56
5.2.2	Digital elevation model	56
5.2.3	Apparent soil electrical conductivity measurements (EC_a survey)	56
5.2.4	Soil sampling and laboratory procedures	57
5.2.5	Data analysis	57
5.2.6	Yield/input ratio	60
5.2.7	Crop budget	60
5.3	Results	60
5.3.1	Productivity maps of P and K	60

CONTENTS	xiii
5.3.2 Yield/nutrient input ratio of phosphorus and potassium	63
5.4 Discussion	66
5.4.1 Differential fertilization - decision making	66
5.4.2 Differential fertilization - economic aspects	67
5.5 Conclusions	69
6 General Discussion, Future Work and Conclusions	71
6.1 General discussion	71
6.2 Future work	73
6.3 Conclusions	74
A Figures	77
B Maize production costs	87
Bibliography	89

List of Figures

3.1	(a) 2002 yield variogram for the Azarento field; (b) 2006 yield variogram for the Bemposta field. . .	19
3.2	Standardized maize yield maps for the Azarento field: (a) yield in 2002; (b) yield in 2003; (c) yield in 2004; (d) yield in 2007.	22
3.3	Azarento field: (a) temporal yield standard deviation; (b) average temporal maize yield; (c) first principal component scores; (d) second principal component scores.	23
3.4	Standardized maize yield maps for the Bemposta field: (a) yield in 2002; (b) yield in 2003; (c) yield in 2004; (d) yield in 2006; (e) yield n 2007; (f) yield in 2008; (g) yield in 2010.	24
3.5	Bemposta field: (a) Temporal yield standard deviation; (b) Average temporal maize yield; (c) First principal component scores; (d) Second principal component scores.	25
3.6	Plot of the first principal component scores (PC1) vs. the average temporal yield of 300 random yield observations in the Azarento and Bemposta fields.	26
3.7	Plot of the second principal component scores (PC2) vs. the temporal yield standard deviation for 300 random yield observations in the Azarento and Bemposta fields.	27
4.1	Maize yield variogram - 2002.	34
4.2	Field area percentage according to different standard yield classes and different initial point densities for stochastic simulation: (a) Azarento field; (b) Bemposta field.	42
4.3	Real and simulated yield ($\approx 65\%$ points ha^{-1}) field area percentage according to different standard yield classes (Azarento field): (a) 2002; (b) 2003; (c) 2004; (d) 2007.	43
4.4	Average real yield and simulated yield ($\approx 65\%$ points ha^{-1}) field area percentage according to different standard yield classes and considering 4 years (Azarento field).	44
4.5	Below-average yield areas with 80% confidence considering 2002, 2003, 2004 and 2007 simulation data analyzed independently (Azarento field).	47
4.6	Above average yield areas with 80% confidence considering 2002, 2003, 2004 and 2007 simulation data analyzed independently (Azarento field).	48
4.7	Below-average (a) and above-average (b) yield areas with 80% confidence considering 2002, 2003, 2004 and 2007 simulation yield data grouped together (Azarento field).	49

5.1	(a) Digital elevation model (DEM): contour, slope and soil sampling points; (b) EC_a spatial distribution.	58
5.2	Maize yield spatial statistics: (a) yield average and (b) yield standard deviation.	61
5.3	The soil (a) phosphorus and (b) potassium spatial distribution.	62
5.4	Spatial distribution of the yield/input ratio of (a) phosphorus (P_{yr}) and (b) potassium (K_{yr}).	63
5.5	Yield/phosphorus ratio zones (Z1, Z2, Z3, Z4 and Z5) according the 2007 maize yield; (Y+ higher yield; Y- lower yield; P+ higher phosphorus soil concentration; P- lower phosphorus soil concentration).	64
5.6	One-to-one straight line comparison between yield/phosphorus ratio (P_{yr}) and yield/potassium ratio (K_{yr}).	67
5.7	Management zones (Z1, Z2, Z3, Z4 and Z5) according to the 2007 maize yield and yield/input ratio of $0.12 \text{ t ha}^{-1} (\text{mg Kg}^{-1})^{-1}$	68
A.1	DEMs for: (a) Azarento field; b) Bemposta field.	78
A.2	Real and simulated yield ($\approx 65 \text{ points ha}^{-1}$) field area percentage according to different standard yield classes Bemposta field: (a) 2002; (b) 2003; (c) 2004; (d) 2006.	79
A.3	Real and simulated yield ($\approx 65 \text{ points ha}^{-1}$) field area percentage according to different standard yield classes Bemposta field: (e) 2007; (f) 2008; (g) 2010.	80
A.4	Average real yield and simulated yield ($\approx 65 \text{ points ha}^{-1}$) field area percentage according to different standard yield classes and considering 7 years (Bemposta field).	81
A.5	Below average yield areas with 80% of confidence considering 2002, 2003, 2004 and 2006, simulation data analyzed independently (Bemposta field)	82
A.6	Below average yield areas with 80% of confidence considering 2007, 2008 and 2010 simulation data analyzed independently (Bemposta field)	83
A.7	Above average yield areas with 80% of confidence considering 2002, 2003, 2004 and 2006 simulation data analyzed independently (Bemposta field).	84
A.8	Above average yield areas with 80% of confidence considering 2007, 2008 and 2010 simulation data analyzed independently (Bemposta field).	85
A.9	Below average (a) and above average (b) yield areas with 80% of confidence considering 2002, 2003, 2004, 2006, 2007, 2008 and 2010 simulation yield data grouped together (Bemposta field)	86

List of Tables

3.1	Summary statistics for grain yield at the Azarento and Bemposta agricultural fields.	18
3.2	Maize yield data variogram parameters for Azarento (2 structures) and Bemposta agricultural fields.	20
3.3	Values of the eigenvector loadings for each variable and percentage of explained variance by the first two axes for Bemposta and Azarento fields.	21
4.1	Summary statistics for grain yield in Azarento and Bemposta agricultural fields.	34
4.2	Maize yield data variogram parameters for Azarento (2 structures) and Bemposta agricultural fields.	35
4.3	Percentages of yield standard classes for real yield in the Azarento field.	36
4.4	Percentages of yield standard classes for real yield in the Bemposta field.	37
4.5	Percentages of yield standard classes for the 2002 simulated yield data in the Azarento field considering 30, 65, 125 and 200 points ha^{-1} of yield data positions randomly.	38
4.6	Percentages of yield standard classes for the 2002 simulated yield data in the Bemposta field considering 30, 65, 125 and 200 points ha^{-1} of yield data positions randomly.	38
4.7	Percentages of the yield standard classes for simulated yield data in the Azarento field considering 65 points ha^{-1} of yield data positions for 2002, 2003, 2004 and 2007.	39
4.8	Percentages of yield standard classes for simulated yield data in the Bemposta field considering 65 points ha^{-1} of yield data positions for 2002, 2003, 2004, 2006, 2007, 2008 and 2010.	40
4.9	Percentage differences between real yield and yield simulation classes considering $\approx 65\%$ points ha^{-1} of yield data positions (Azarento).	41
4.10	Percentage differences between real yield and yield simulation classes considering $\approx 65\%$ points ha^{-1} of yield data positions (Bemposta).	41
4.11	Percentage differences of minimum, maximum and average yield values per yield class between real yield data and simulated yield data, considering $\approx 65\%$ points ha^{-1} of yield data.	44
4.12	Field area percentage below the yield average according to 95%, 90%, 80%, 70%, 60% and 50% confidence levels, considering yield simulations from $\approx 65\%$ points ha^{-1} of real yield data.	45

4.13	Field area percentage above-yield average according to 95%, 90%, 80%, 70%, 60% and 50% confidence levels, considering yield simulations from $\approx 65\%$ points ha^{-1} of real yield data.	46
5.1	Phosphorus, potassium, apparent soil electrical conductivity and yield of 2007 data variogram parameters.	59
5.2	Grain yield summary statistics for the Azarento field.	61
5.3	Soil P levels and yield/P ratio according to Z1, Z2, Z3, Z4 and Z5 zones.	65
5.4	Soil K levels and yield/K ratio according to Z1, Z2, Z3, Z4 and Z5 zones.	66
5.5	Fertilization scenarios.	70
5.6	Fertilizer units applied in each scenario.	70
B.1	Maize production costs	88

Acronyms

CEC	Cation exchange capacity
DEM	Digital elevation model
DGNSS	Differential Global Navigation Satellite System
Ca	Calcium
CEC	Cation exchange capacity
EC _a	Apparent electrical conductivity
EMI	Electromagnetic Induction
ER	Electrical resistivity method
GIS	Geographic Information Systems
GNSS	Global Navigation Satellite System
K	Potassium
Mg	Magnesium
N	Nitrogen
NDVI	Normalized difference vegetation index
PA	Precision agriculture
OM	Organic matter
P	Phosphorous
PCA	Principal component analysis
PC1	1 st principal componente
PC2	2 nd principal componente
SGS	Sequential Gaussian Simulation
VRA	Variable rate application
VRT	Variable rate technology

Abstract

This dissertation describes efforts to move toward the study of soil and the management of yield variability through research that explored and evaluated the potential of some techniques to provide greater understanding and knowledge of an agricultural field, even in situations where there is no prior knowledge of its behavior. The first experiment used a principal components analysis (PCA) in the study of the spatial and temporal variability of maize grain yield. The results of this experiment demonstrated that the 1st and 2nd principal components could be used to identify field zones with different spatial and temporal behaviors. The second experiment applied stochastic and sequential Gaussian simulation techniques to spatially and temporally forecast and model maize productivity. This technique enabled the modeling of spatial uncertainty in maize productivity based on probabilistic maps with different confidence levels. The third experiment examined different fertilization input scenarios based on yield/nutrient inputs ratio and break-even yields to optimize agronomic, economic and environmental support decisions. According to the results, it is possible to reduce agricultural production costs through the differential management of inputs. The outcomes showed that differential management decisions can maximize returns and reduce activity risk without having to implement major changes on the farm.

Keywords: maize yield; yield principal components analysis; yield stochastic simulation; differential inputs distribution; management zones

Sumário

Otimização da produtividade e dos fatores de produção no milho de regadio

O presente trabalho de investigação, que considerou três estudos, explora e avalia o potencial de alguns modelos no estudo da gestão da variabilidade espacial e temporal da produtividade e dos nutrientes no âmbito da produção de regadio. O primeiro estudo focou a utilização da técnica estatística Análise de Componentes Principais (ACP) no estudo da variabilidade temporal da produtividade da cultura do milho na região do Alto Alentejo. Os resultados desta experiência mostraram que as duas primeiras componentes principais permitem identificar zonas da parcela agrícola com diferente comportamento espacial e ambiental. No segundo estudo avaliou-se o desempenho da simulação sequencial Gaussiana na previsão e modelação da produtividade da cultura do milho. Esta técnica permitiu modelar a incerteza espacial da produtividade com base em mapas de probabilidade com diferentes níveis de confiança. O terceiro estudo avaliou diferentes cenários de fertilização a partir do rácio produtividade/nutrientes e do breakeven da produtividade de forma a otimizar, em termos agronómicos, económicos e ambientais, as tomadas de decisão. De acordo com os resultados obtidos, foi possível obter uma redução substancial dos custos de produção através da sugestão da aplicação diferenciada da fertilização. Os resultados mostraram que é possível reduzir os riscos, quer económicos quer ambientais, da atividade agrícola sem grandes alterações no processo produtivo da exploração agrícola.

Palavras-chave: produtividade da cultura milho, análise de componentes principais, simulação estocástica, fertilização diferenciada, zonas de gestão localizada

1

Introduction

To produce more food and reduce economic and environmental costs, agricultural activities need to combine smart technologies with smart agro-processes. Traditional farming considers the management of agronomic fields to be uniform despite the spatial variability that can be found within a field. Precision agriculture accounts for the spatial variability of fields and promotes site-specific management to increase economic returns and minimize environmental impacts [BBSM07, MTM10].

In Portugal, little research has been done on the delineation of management zones, and there is a general lack of literature on this subject. However, some researchers have developed studies of variable rate pasture applications (e.g., [PSM⁺05, SSMds14]), spatial yield variability (e.g., [Mar06, MRSM12]), topography (e.g., [MA05]) and soil mechanical resistance (e.g., [CaEF⁺12]).

Every day, agriculture is confronted with numerous challenges, so the adoption of modern technology by global agriculture is inevitable, and Portugal is not an exception. In the future, agriculture will be severely competitive and challenging, and all of the available tools, technology and knowledge will be necessary to sustainably intensify this activity.

Geographic information systems and geostatistical tools can be used to develop thematic maps of soils, yields and other parameters, which are extremely important for spatially and temporally efficient agricultural management.

The accurate mapping of yield-limiting factors remains a challenge for researchers [CC08]. Topographic attributes, soil properties and climate constraints interact to influence the spatial and temporal variability in yields. However, this variability is not an independent phenomenon; it reflects within-field variation of the soil yield potential [PJABa06] and can be an important factor for the delineation of within-field management zones [Bla00, FWWB00, Mar06].

Applying site-specific practices will improve net returns and minimize environmental impacts [LWHT10, SPdS⁺10, SSS14]. In other words, modern agriculture is technologically demanding, so there is a need for more research, and farm managers must exercise best practices to achieve yield and environmental targets.

1.1 Objectives

The purpose of this work is to explore several useful strategies that have been developed to assess the spatial and temporal variability in yield. These strategies are intended to improve future agronomical prescriptions and allow for a more accurate estimation of variable rate management to reduce risks and enhance environmental and economic benefits.

This dissertation is divided into three parts:

i) The first part (Chapter 2) is an introduction to the problems addressed in the manuscripts on which this thesis is based, and it provides an overview of the theoretical foundation of the dissertation;

ii) The second part (Chapters 3, 4, 5) is comprised of three scientific manuscripts that have already been published or submitted for publication in international peer-reviewed journals, and they were developed to answer several research questions:

- a) Chapter 3 describes how the multivariate principal components analysis technique can be simultaneously used to delineate yield management zones and to identify specific locations inside a field with temporal yield resilience, i.e., to calculate the temporal risk associated with maize yield;
- b) Chapter 4 explores the possibility of using stochastic simulation techniques to forecast maize productivity and model spatial and temporal uncertainty using probabilistic yield maps when there is a lack of data;
- c) Finally, Chapter 5 presents a yield/input ratio approach and yield break-even as potential tools to help farmers and managers 1) optimize agronomic inputs, 2) delineate management zones, and 3) reduce economic and environmental risks from production;

iii) The third part (Chapter 6) integrates all of the scientific discussions and conclusions presented in this document and considers the implications for further research.

2

Scientific background

2.1 Precision agriculture

Precision agriculture (PA) is also known as precision farming or site-specific crop management. The term first appeared in 1990 as the title of a workshop in Great Falls, Montana, which was sponsored by Montana State University, but researchers had previously used the terms “site-specific crop management” or “site-specific agriculture” [Oli10].

There are many definitions for precision agriculture (PA), but all of them describe a crop production system with low inputs and high efficiency as well as environmental and economic benefits.

According to Schellberg et al. [SHG⁺08], PA is “an innovative, integrated and internationally standardized approach that aims to increase the efficiency of resource use and to reduce the uncertainty of decisions required to control variation on farms”.

Another example is the more detailed definition by Sudduth [Sud99], who defined PA as “a management system of crop production practices and inputs such as seed, fertilizers and pesticides that are variably applied within a field. Input rates are based on the needs for optimum production at each within-field location. Since

over-application and under-application of agrochemicals are both minimized, this strategy has the potential for maximizing profitability and minimizing environmental impacts”.

In fact, PA is as old as agriculture itself. In the early days, each farmer knew each portion of his land well and cultivated and devoted his attention to fields based on their characteristics, thus ensuring enough food to sustain his family. However, in recent decades, the need to produce more food and the growth of cultivated areas has led farmers to treat fields as homogeneous zones, so management is based on the average needs for fertilizer, water and pesticide inputs. For a long time, site-specific crop management was ignored.

The adoption of PA gradually occurred over many years, but PA is currently a fact thanks to a set of technologies such as Global Navigation Satellite Systems (GNSS), geographic information systems (GIS), remote sensing, sensors and data-acquisition systems, computer science, simulation models, agricultural machinery, and variable rate application systems (VRT), as well as the interest of humans in better practices .

The spatial and temporal variability of soil and crop factors are the basis for PA [ZWW02]. Spatial variability refers to how soil properties and production vary in space. Temporal variation is a major source of production risk because it is difficult to control; it occurs over years due to weather or seasonal events [Toz09]. However, the power of new technologies in the collection, storage, processing and display of spatial data makes it possible to obtain comprehensive information about yield variability in space and time [ZWW02].

However, the way forward is not to present PA as a solution for all or to impose the system on farmers but to assist them and share information so that they can put questions to PA experts.

As reported by Schellberg et al. [SHG⁺08], “the key to successful future PA is not only to collect relevant data but also to convert them into useful information and then derive consequential decisions and rigorously evaluate risks and benefits”.

2.2 Spatial and temporal variability

The spatial and temporal variability of the soil, yield and crop attributes are the basis for PA, and several approaches can be used to study yield variability. It is challenging to identify and comprehend spatial and temporal variability because there are many parameters involved in the production process. Therefore, some authors consider the spatial and temporal variability of different factors, such as yield variability, crop variability, field variability, soil variability, variability in anomalous factors, and management variability [ZWW02]. Other researchers incorporate different types of data sets to define zones with more or less uniform production potential [KZN⁺14].

2.2.1 Yield

The goal of the spatial and temporal analysis of yield variability is to delineate areas with consistent yield patterns to develop practices that can optimize crop production.

The availability of yield monitors equipped with GNSS, which can generate spatially dense data at relatively low cost, has stimulated the study of spatial and temporal yield variability and interest in the site-specific application of crop inputs [LCD99]. This simple method of data collection has encouraged several researchers to analyze yield variability over space and time. Diker et al. [DHB04] showed that spatial and temporal yield can be analyzed with multi-year data to detect broad patterns that are preserved over time. With only a few years of yield data, a farmer or manager can try to identify the yield-limiting factors in similar and dissimilar zones. If possible, the farmer should amend the problem in the subsequent years of production, but the causes of vari-

ability can change with time and the type of crop [VPG03]. As evidenced by Blackmore et al. [BGF03], temporal variability is generally much higher than spatial variability, so care must be taken when defining areas of low and high productivity as potential zones for site-specific management.

According to Diacono et al. [DCT⁺12], when crops grow in a rain-fed Mediterranean environment, the different spatial yield distributions from one cropping season to another may be mainly due to the influence of meteorological conditions. This conclusion is in agreement with other results, such as those of Link et al. [LGC04] in Germany, who found that maize grain yield was affected by climatic variations from year to year over six years, or those of Basso et al. [BCC⁺09], who concluded that soil water content was the main factor affecting spatial variability in yield.

When a temporal trend in yield is identified in a given part of a field over multiple years, its effect can be calculated, and Blackmore et al. [BGF03] and Marques da Silva [Mar06] proposed a modified standard deviation function to quantify this variance. This function was able to detect spatial changes over time, e.g., parts of a field where yield is always close to the mean (low temporal variance) and parts that are temporally unstable because they sometimes produce above-average yields but produce below-average yields at other times (high temporal variance). Consequently, Blackmore et al. [BGF03] and Marques da Silva [Mar06] divided their temporal variance and spatial variability maps into four homogeneous classes: (1) high yielding areas – zones in which the yield is above the inter-annual mean; (2) low yielding areas – zones in which the yield is below the inter-annual mean; (3) stable areas – zones with low inter-annual spatial variance (based on an arbitrarily defined threshold) and (4) unstable areas – zones with high inter-annual spatial variance (based on an arbitrarily defined threshold).

The analysis of different patterns of yield in space and time can be further applied to the analysis of other factors, such as crop density, crop height, crop nutrient stress, crop water stress, crop biophysical properties, crop leaf chlorophyll content, and crop grain quality [ZWW02, DMV07]. Crop models can be used to better understand the effects of these factors, which are directly related to the plants, and the processes involved in crop growth and thus identify the spatial and temporal variability in yield. The study of the daily growth of crops under a few stresses, such as water, nitrogen (N), temperature or pests, with different models has been used to identify the causes of spatial variability in yield [BBP02].

In Italy, Basso et al. [BBSM07] studied the growth of corn, soybeans and wheat (under crop rotation) using models that simulate the responses of crop growth and development to different environmental conditions. These models incorporate different types of information, such as soil data (sand, silt and clay content, bulk density, organic carbon and water limits), the standard deviations of temporal yield data calculated according to Blackmore [Bla00] and Blackmore et al. [BGF03], weather data (incoming solar radiation, air temperature and rainfall), and yield data from yield monitoring systems during different growing seasons. The models were applied to two areas identified as stable, i.e., with higher or lower than average yields and lower temporal variance over time. The difference between the annual simulated and measured yield data was acceptable, but the long-term simulated yield data varied for all crops, which confirmed the influence of climatic data and soil properties on the average yield [BBSM07].

2.2.2 Soil

The spatial variability of crop production reflects the variability in soil fertility, which depends on physical and chemical soil properties [AHMU04, PGZ⁺07].

Although the geological and pedological processes of soil formation determine the spatial variability in the soil, some physical soil properties can be altered over time due to soil erosion and management practices, such as tillage [ITJ⁺05, VVS⁺08]. For example, Iqbal et al. [ITJ⁺05] identified the higher soil bulk density in subsurface

horizons, which restricts downward water movement, as perhaps being due to the compaction of fine sandy or fine silt layers by heavy machinery.

In 2005, a study of the spatial variability of the physical soil properties of three fields over three years became important to the delineation of different zones with distinct maize yield potentials. Soil properties were relatively homogeneous inside each zone but were significantly different between zones, so the available water, and thus nutrient uptake, may have differed from zone to zone, reflecting the potential productivity of each area [MKR⁺05]. Cox et al. [CGWA03] and Guo et al. [GMB12] made similar observations and found that the clay content was an adequate criterion for dividing fields into areas of equal productivity. These authors suggested that the higher yield in areas with higher clay content is related to the availability of more plant-available water during the dry periods of the growing season [CGWA03, GMB12] because soil texture is one of the most important factors influencing the water-holding capacity of the soil [SSL⁺04, GMB12].

In addition to the physical soil properties, other researchers have studied chemical properties and/or nutrient status to better understand the variability in yield across fields. Ping et al. [PGZ⁺07] found low temporal variability in pH, cation exchange capacity (CEC), calcium (Ca) and texture over time, and other studies [KB00, LGC04] have found that soil properties, such as organic matter (OM), pH, phosphorous (P), potassium (K), magnesium (Mg) and nitrogen content do not directly explain the spatial variability in yield. In fact, the nutrient response patterns within a field often do not mimic yield patterns, which implies that there are other factors, such as topographic attributes, that affect crop yields [KB00, LGC04].

2.2.3 Topography

Actually, some researches have shown that, in general, the spatial variabilities in soil and yield are very closely associated with their position on the landscape. For instance, Aimrun et al. [AAR⁺09] studied the distribution of several chemical soil properties, and the lowest positions in the study area exhibited high total N, available P, exchangeable K, Ca, Mg and total organic carbon values compared with the highest positions, which is probably due to the dynamics of surface runoff water.

Guo et al. [GMB12] found that topography, combined with other factors, explained up to 70.1% of the variability in cotton yield, which agrees with the results of Kaspar et al. [KCJ⁺03], who, in a study over four dry years in Iowa, found that topography explained 78% of the spatial variability in maize yield due to the effects of soil properties, soil erosion and water availability.

Curvature is an important topographic factor that determines the movement of water and nutrients in the soil, and the influence of the curvature profile on yield is more obvious in dry years than in wet years [KKKM11, KZN⁺14]. Usually, a convex curvature is associated with soil erosion, and a concave curvature is associated with soil, water and nutrient deposition [GMB12]. Although this does not always happen, concave areas should theoretically have greater water and nutrient availability and thus be more productive [KB02, SSL⁺04, BCC⁺09, GMB12].

This conclusion is supported by the work of Kravchenko and Bullock [KB00] and Lund et al. [LWH01], who found that several fields, which were located lower in the landscape and in depressions (concave surface), had higher OM and moisture contents, which are very important during periods of drought. In some fields, these depression zones also had higher P, K and CEC values [LWH01]. On the other hand, the excessive amounts of water that accumulate in concave surfaces during wet periods can reduce yield [KB00]. The same result was observed by Kitchen et al. [KSM⁺05] and Vitharana et al. [VVS⁺08], i.e., greater crop productivity occurred lower in the landscape, although the crops in lower landscape positions could be destroyed during extreme rain events or under predominantly wet climatic conditions. According to Vitharana [VVS⁺08], crop production is likely to be more variable between years in such areas than in other areas.

These findings were also similar to those of Marques da Silva [Mar06], who in seven trial fields in a Mediterranean environment, observed that yield stability is related to the distance to flow accumulation lines. Maize yield increased with a decrease in this distance.

Nevertheless, some studies have found inconsistent or insignificant correlations between landscape position and yield, OM, P, K, Mg, Ca and CEC (e.g., [CGWA03, KPF⁺04, SCMaC08, GMB12]). Presumably, this is due to changes in the parent material across the landscape [KB00] or to erosion processes at positions higher in the landscape; the additional moisture stored in the clay in the upper layer of eroded soil may produce better yields [LWH01, MS08, GMB12, KZN⁺14]. Machado et al. [MBA⁺02] also observed higher productivity in sorghum grain at high elevations where there was high water availability and higher clay and silt fractions compared with low elevations. These examples show that there are many soil properties that can promote yield variability, and these factors vary from one location to another.

2.2.4 Other sources

There are many other factors that contribute to spatial and temporal variability. For example, between-year variations in solar radiation, air temperature, air humidity, and precipitation may affect the temporal variation in yield.

Crop pests and/or diseases may also play an important role in spatial and temporal yield variability, and diseases in the soil can have a huge impact on the sustainability of yields and crops. Blackmore et al. [BGF03], Jaynes [JCK05], Di Virgilio et al. [DMV07] and Zhang et al. [ZWW02] also reported that weed infestations, damage from wild animals (birds, wild boars, etc.), and wind damage are factors that can cause anomalous variabilities in crop production.

Other anomalous factors, such as malfunctioning irrigation systems (e.g., a damaged sprinkler) or poorly designed irrigation systems can cause a high degree of yield variability as shown by Marques da Silva [Mar06].

2.3 Management zones

A management zone is a part of an agricultural field that is homogeneous in terms of yield-limiting factors and in which a specific crop input is applied at a single rate with the objective of providing economic and/or environmental benefits. The variability in the field determines the size and number of subdivisions that might justify different management regimes [ZWW02]. As opposed to traditional, uniform management, site-specific management is based on a field data set that allows for the differentiation of management practices, such as fertilization, crop-seeding rate, hybrid crops, tillage, and weed and pest control, [ZWW02, OSn07, WS⁺08].

Obtaining reliable information about the distribution of soil properties to produce representative maps is the greatest challenge to progress in site-specific management [KO03]. Several studies have evaluated the potential of different approaches (numerous methods based on one or multiple information sources) to identify zones that justify different management strategies to achieve the effective implementation of variable rate application technology [CLS⁺08, FWWB00, PCCB13]. For example, in the study by Miao et al. [MMRS05], an approach that integrated soil and landscape variability, spatial trends in yields and temporal stability proved to be more effective than other strategies in which researchers only used information about the soil, landscape or yield to identify management zones. Kravchenko and Bullock [KB00] and Peralta et al. [PCCB13] also suggested that integrating soil properties with topography was useful for understanding yield variability and delineating site-specific management zones.

Combining topographic attributes, such as elevation, slope, flow accumulation lines, and curvature with infor-

mation about yield variability is more comprehensive [MS06], but topography may not be enough to delineate site-specific management units [CGWA03, SSL⁺04].

Kitchen et al. [KSM⁺05] reported that the combination of elevation variables and apparent electrical conductivity were promising for delineating management zones on claypan soil. These variables generated 60-70% agreement between yield productivity and elevation-based productivity zones [KSM⁺05].

Other authors have proposed the use of detailed soil surveys based on a high density of observations (intensive sampling) or target soil sampling using an appropriate technology, such as EC_a patterns, to define the different management zones [LCD99, FB04, TL05].

Diker et al. [DHB04] used only the variability in yield over time and space as the basis for delineating management zones; a zone was identified by the number of years in which yield was equal to or greater than the average yield in a given year. The combination of statistically similar yield classes made it possible to define three response zones with low, medium and high yields.

Some authors [ZSJ⁺10, KKKM11, DCT⁺12, KZN⁺14] have also highlighted that integrating remote sensing imagery with yield and field data provides reliable tools to support zone management delineation and to estimate the optimal number of zones.

Ortega and Santibáñez [OSn07] proposed three methods based on cluster analysis, principal component analysis and coefficients of variation to delineate homogeneous management zones using manually collected yield samples and soil chemical properties. The three methods were adequate and similar, and because the spatial and temporal variability in yield is affected by several factors, the authors noted that the identification of the variables responsible for this variability is as important as the methodology. Therefore, because it is impossible to determine all of the factors that affect yield, Ortega and Santibáñez [OSn07] suggested identifying and measuring only those variables that are most relevant to yield determination when building different management zones.

2.4 Evaluating variability

2.4.1 Grid sampling

Several authors have tested different methods for the management of yield variability (e.g., [HMC03, JCK05, KSM⁺05, CLS⁺08]), and the most common approach is the intensive sampling of the field to identify different soil fertility levels and to estimate the capacity of the soil to supply nutrients. It is important to note that the samples must be representative so that experts can recommend a fertilizer with accuracy and precision.

In general, grid sampling is based on the subdivision of a field into a systematic arrangement of small areas or cells, and it can provide an accurate basis for variable rate application. However, there is no grid size that is suitable for the entire extent of a farm with so many diverse features [FWWB00]. For example, some studies [LGC04, LGBC06] have shown that larger grids better describe temporal yield variability, and smaller grids adequately describe spatial yield variability. Another study in a cool temperate grassland in Ireland with sandy clay loam soil, demonstrated that to estimate K and P, the optimal sample size for soil K was about twice as large as that for soil P [SWB⁺00]. Shi et al. [SWB⁺00] also noted that, in addition to sample size, a combination of field size, arrangement and shape ought to be considered when developing sampling schemes to map soil nutrient distributions. Because of this, some authors (e.g., [SWB⁺00, PGZ⁺07, HABF13, PdJBBA14]) have experimented with different grid sizes and schemes, such as triangular grids. Fields that express high spatial variability over a small scale may require fine grid-spacing as exemplified by Cambardella and Karlen [CK99] for an organic field.

Nanni et al. [NPD⁺11] evaluated several grid resolutions to sample the soil attributes in a field that was usually

cultivated with sugarcane, and a sampling density finer than 1 sample ha⁻¹ was necessary to capture the spatial variability of P and K. According to these authors, the need for a higher sampling density for P and K is related to the fact that these attributes are more sensitive to management practices than others (e.g., clay). Taylor et al. [TWE03], Peralta and Costa [PC13] and Nanni et al. [NPD⁺11] also suggested partitioning the field into specific management zones as well as the use of stratified sampling to reduce the number of soil samples or the use of other tools, such as soil electrical conductivity.

2.4.2 Sensors

Monitoring and control systems allow for the assessment of yield or physical-chemical soil characteristics, and they simultaneously reduce the amount of work needed in the laboratory to improve yield efficiency [SKW⁺]. These systems consist of devices with sensors that can quickly measure a large number of sample points in real time and thus provide a description of the spatial variability of the soil and yield [Ada06]. To improve the quality of the information and to facilitate data acquisition, a wide variety of sensors have been developed with an emphasis on yield and soil sensors [ZWW02]. Maps can be generated from these sensors and processed with other layers with spatial information [AHMU04].

Thus, harvesting equipment with yield sensor systems have been or are being developed, and they are widely available for many of the major crops. Yield sensors can instantaneously record georeferenced yield data at harvest, and the yield monitoring systems permit the yield variability to be displayed. The resulting yield maps represent the interaction between many soil properties and production inputs, so they provide important information for the development of crop management strategies [DHB04, SD07]. These yield maps make it possible to measure the variability in yield over time and space, and when yield data are collected over multiple years, the maps can be used to measure temporal variability. For example, yield maps enable researchers to identify areas where the yield has been equal, greater or lower than the average yield over time [DHB04].

A wide variety of soil sensors that are involved in the real time (on-the-go) detection and acquisition of data for specific soil attributes have been described in the literature and are commercially available or in development. Adamchuk et al. [AHMU04] and Adamchuk [Ada06] highlighted the following measurement systems: i) electrical and electromagnetic sensors that measure the effect of soil composition on resistivity/conductivity or electrical capacitance; ii) optical and radiometric sensors that use electromagnetic waves to detect the level of energy absorbed/reflected by soil particles; iii) mechanical sensors that measure the resulting forces through a tool that engages with the soil; iv) acoustic sensors that quantify the sound produced by a tool that interacts with the soil; v) pneumatic sensors that assess the ease of injecting air into the soil; vi) electrochemical sensors that use ion-selective membranes that produce voltage in response to the activity of selected ions.

Despite the existence of various soil sensors, the electrical and electromagnetic sensors are commercially available and commonly used in agriculture. These sensors provide measurements that cannot be used directly because their absolute value is dependent on the physical and chemical properties of the soil. However, these sensors provide valuable information about soil differences and similarities that make it possible to divide the soil into management zones with common features [AHMU04].

Soil electrical conductivity sensors

Although the relationship between yield and EC_a is not simple, measurements of soil EC_a have demonstrated a close relationship between soil CEC and soil texture, which influences the water-holding capacity/drainage of the soil. In this way, EC_a maps can be a very interesting tool when there is a strong relationship with the crop yield maps [LWH01, PC13].

Traditionally, soil-paste electrical conductivity measurements were used to assess soil conductivity and to determine its salinity and moisture content [RMSA89], but this process is slow, labor-intensive, expensive and suffers from high local-scale variability associated with small soil core samples [CL05a].

To determine the most accurate and precise fertilizer application, an intensive and representative approach to soil core sampling is required, but this method depends on laboratory analysis of the representative soil samples and is time consuming and costly [EDNW00, HMC03]. Therefore, detailed soil mapping requires the use of more expeditious tools to identify and assess the spatial variability of the soil properties that influence the spatial variability in yield. The fact that EC_a sensors are fast, simple, accurate and reasonably priced makes them some of the most interesting and widely used tools in the investigation of the relationship between EC_a and soil properties [AHMU04, CLOK06]. The theories and principles of the measurement of soil EC_a and a description of the methods underlying these sensors are well documented by Rhoades et al. [RCL99], Corwin and Lesch [CL03, CL05b, CL05a, CL05c] and Friedman [Fri05].

The commercially available sensors that enable direct, instantaneous measurements of bulk EC_a in situ are essentially based on two types of methods: direct contact with the soil (e.g., Veris[®] 3100 sensor, Veris Technologies[®], Salina, Kansas, US) and indirect contact with the soil by means of electromagnetic induction (EMI) (e.g., Geonics EM38[®], Mississauga, Ontario, Canada) [CL05a, JED⁺05, RCL99].

The measurement of electrical conductivity by direct contact relies on the creation of an electrical circuit through one pair of coulter-electrodes that injects a known voltage into the soil. Another pair of coulter-electrodes, in direct contact with the soil, measure the voltage from the first pair [AHMU04, CL03, CL05a, GAHT09]. As the coulters roll through a field, the distance between them defines the effective measurement depth [AHMU04], which measures the degree of difficulty that a material imposes on the passage of a given electric current. This method is also called the electrical resistivity method (ER).

The electromagnetic induction method uses a transmitter coil to induce a magnetic field in the soil and a receiver coil to measure the response; there is no direct contact with the soil [AHMU04, CL03, CL05a, GAHT09].

The electrical resistivity method is an invasive technique that is less susceptible to metal interference when compared to EMI. The depth of the measurements can be easily changed by altering the spacing between the electrodes, and it is well suited for field-scale applications and does not require daily calibration. The disadvantage of this system is that it requires good contact between the soil and the coulter-electrodes, so it may not work properly in dry or stony soils. Furthermore, ER sensors are usually much heavier than EMI sensors [CL05a, GAHT09, LCD00].

The electromagnetic induction method is a non-invasive technique that is well suited for field-scale applications, and it works well in dry or stony soils and is able to collect data on soils covered with vegetation preferably when the crop is not very densely developed. The disadvantages of this system are that i) it needs daily calibration; ii) it is susceptible to outside metal interference, and iii) it is hard to change the depth of the measurements [CL05a, GAHT09, LCD00].

Even though Fleming et al. [FWWB00] documented differences in the conductivity values from both methods, other authors have found the results of these methods to be similar in terms of conductivity and their relationship with the physical and chemical soil properties [SSM13, SSdS14, SKB⁺03]. Some studies have found that the EC_a values measured by direct contact were much lower than those measured by the electromagnetic induction method, which is probably due to i) the complex EC_a spatial patterns caused by texture variability; ii) the influence of bedrock weathering; iii) the erosion of certain high-elevation areas of the landscape; iv) different measurement depths; v) variation in the depth of the clay content and/or vi) variation in the vegetation layer and its moisture content [PCCB13, SSM13, SSdS14, SPC13, SKW⁺]. Some authors have also observed that the ER method presents the greatest temporal stability under wide variations in the moisture contents of the soil and vegetative ground cover [SSM13, SSdS14, SPC13, SKW⁺]. Although both methods measure EC_a magnitudes

differently, they both provide useful and consistent information about EC_a spatial patterns [AES06, PPCA13].

Relationship between EC_a and soil properties

Although the first agricultural studies using electrical conductivity were related to the salinity of the soil [CL05a], conductivity has recently been used to successfully measure some physical and chemical soil properties that often determine the productivity of a field [Ame07, HMC03, RPPLS11].

The continuous macro- and micro-pores, which exist between soil particles and are filled with water, are responsible for the transmission of electricity in soils. Thus, soils with more fine particles have a high specific surface area, greater particle-particle contact and a greater number of small pores that retain water for longer periods of time and are better conductors of electricity [CL03, SPC13].

In non-saline soils, EC_a is strongly correlated with texture; sands have low conductivity, silts have medium conductivity, and clays exhibit high conductivity [GMB12, LCD99, LWH01]. This finding is consistent with the results of other studies (e.g., [CO05, JCK05, JKS⁺05, RPPLS11, SPC13, SSdS14]) that showed that EC_a was significantly correlated with clay, silt, and sand contents, as well as CEC, soil moisture, elevation and slope. In general, CEC and soil moisture strongly correlate with clay and consequently are highly correlated with EC_a [BKE09, HYE⁺04, MF11, SKW⁺].

Research has shown that stable soil properties, such as clay, sand, exchange cations and subsoil structure, have a greater impact on the spatial patterns of EC_a than transient properties, such as soil water and temperature [AES06, FB04]. However, Kachanoski et al. [KWG88] and Hartsock [HMT⁺00] found that soil moisture had a greater effect on EC_a in soils with low clay content.

In non-saline soils, the strong relationship between EC_a and texture causes the observed patterns, which remain in place throughout the year [GMB12]. Although the conductivity values change with different soil moisture levels, soil temperatures, and topsoil densities, the EC_a maps maintain similar patterns over time [FB04, KKKM11, LCD99, SSdS14].

However, some authors have reported weak relationships between EC_a and some soil properties such as porosity, pH, clay content, and salinity in some fields [BKE09, SPMS10], and Kühn et al. [KBW⁺09] reported a greater impact by organic matter and $CaCO_3$ than clay in relation to EC_a . This is probably due to a combination of several factors, such as the salt content in relatively dry regions [KBW⁺09] or by variations in the low clay content of the soil [MHS⁺03].

Direct relationships between EC_a and the nutrient levels in the soil, such as phosphorous (P), potassium (K), calcium (Ca), magnesium (Mg), manganese (Mn), zinc (Zn), and copper (Cu) are not always consistent [HMC03], so it is hard to define a single relationship between EC_a and soil properties and soil nutrient concentrations [HMC03]. According to Heiniger et al. [HMC03], salinity, soil texture or soil moisture can mask the response of EC_a to changing nutrient levels in the soil, so they suggest dividing a field into small areas with similar texture, which would improve the accuracy of EC_a for evaluating changes in the concentration of nutrients in the soil.

Rodríguez-Pérez et al. [RPPLS11] and Hartsock et al. [HMT⁺00] found a strong correlation of sodium (Na), Mg, clay and sand with the EC_a measurements, and Peralta and Costa [PC13] demonstrated a negative correlation between Zn^{2+} , Mn^{2+} , Fe^{2+} and Cu^{2+} concentrations and EC_a . In the study by Jung et al. [JKS⁺05], 60% of the variation in silt, clay and CEC could be predicted through the EC_a , and the findings of Heiniger et al. [HMC03] indicated that the cases with a strongly significant relationship (R^2 ranging from 0.51 to 0.75) between EC_a and soil nutrients occurred when the nutrient was associated with those properties that directly influence EC_a : volumetric water content, volumetric content of the soil particles, CEC, and the dissolved salts in the soil solution. For instance, EC_a was directly related to the levels of Ca and Mg when they were associated with differences in

CEC across the field or when EC_a was closely associated with the level of P when it was linked to salinity due to the application of animal manure [HMC03].

The works of Mueller et al. [MHS⁺03], Jung et al. [JKS⁺05] and Peralta et al. [PCCB13] demonstrated a strong relationship between EC_a and Ca, Mg, clay and CEC. Nevertheless, the association between EC_a and P was low, perhaps due to the lower conductance of the inorganic phosphorus ions that are more common in soil ($H_2PO_4^-$ and $H_2PO_4^{2-}$) compared to other ionic species, such as Ca^{2+} and Mg^{2+} , or as a consequence of the type of fertilizer and the tillage system [JKS⁺05, PCCB13]. The strong relationship between EC_a and exchangeable Mg observed by Hedley et al. [HYE⁺04] reflected the dominant clay mineralogy of the soil, i.e., chlorites weathering to illites and releasing Mg into the soil solution.

In 2009, Aimrun et al. [AAR⁺09] found a significant relationship between EC_a values measured by a Veris sensor and clay, available P and exchangeable K. The highest EC_a values were recorded in the lowest position on the landscape, probably due to the accumulation of soluble salts at these places from surface runoff water and to the higher clay and soil moisture contents [AAR⁺09]. This behavior is consistent with the results of Serrano et al. [SPMS10], Basso et al. [BCC⁺09] and Vitharana et al. [VVS⁺08]. An inverse relationship, i.e., higher EC_a values observed in higher positions, was found by Lund et al. [LWH01] and Marques da Silva and Silva [MS08] due to the higher clay content resulting from erosion.

Although productivity is not directly related to EC_a , this can be useful in the study of yield variability, especially in fields where productivity is very dependent on the water-holding capacity of the soil. More clay, silt, CEC and less sand are soil properties that are consistently positively related to productivity [MA05, SKW⁺] due to the higher capacity of the soil to retain moisture and nutrients [MKR⁺05]. These properties can be indirectly measured by EC_a [GMB12].

2.5 Variable-rate technology

Variable-rate technology (VRT) refers to any technology that enables producers to vary the rate of crop inputs, and its aim is to increase crop production profitability, reduce negative environment impacts and promote sustainable management practices. To achieve these goals, it is crucial to assess the spatial and temporal variability of crops and soil attributes to delineate different management zones and to determine how to manage the variable rate inputs [FWWB00, PGZ⁺07].

There are two basic technologies used to implement variable rate application (VRA): sensor-based and map-based. Sensor-based VRA does not require a map or a positioning system; real-time sensors measure soil properties or crop characteristics using sensors “on-the-go”. This information is processed and immediately used to control a variable-rate applicator, so it is not necessary to use a Differential Global Navigation Satellite System (DGNSS) [EMP01, GAHT09].

Map-based VRA is a technology supported by electronic maps, also called prescription maps, and a DGNSS must be used. Therefore, to implement this method, a map of the previously measured target item is required. Thus, the optimal management zone configuration is the key to precision farming because this information is essential to the preparation of the prescription maps used for variable rate inputs.

There are many candidate inputs for variable-rate application, such as N, P, K, lime, seeds, pesticides, manure soil amendments, water and tillage practices. Therefore, spatial variability maps based on a set of field data are important for site-specific farming by variable-rate technology [AKA⁺11, ITJ⁺05, PC13, ZWW02].

It is important to note that not all fields and farms economically benefit by using VRA technology, but even in such situations, the environmental benefits and the possibility of increasing crop production should be carefully evaluated [GAHT09].

3

Exploratory Parcel Risk Analysis Considering Space and Multi-Year Maize Yield

Grifo, A. R. L., Marques da Silva, J. R., & Oliveira, M.M. (2015). Exploratory Field Risk Analysis Considering Space and Multi-Year Maize Yield.

Submitted to Spanish Journal of Agricultural Research

Abstract

Multitemporal yield maps integrate spatial and temporal variability conditioned by different production processes and factors. This is influential to enhance decision making. This study aims at the development of a tool that may quantify a production risk. The emphasis is on the identification and characterization of the spatial and temporal variability of maize yield by means of a Principal Components Analysis (PCA) multivariate technique. PCA of multitemporal maize yield data allowed for the following: a) the comparison of the production risk in different agricultural fields; b) the interpretation of the spatial variation of the average temporal productivity; and c) the temporal productivity resilience. The results showed that it is possible to define four management zones for site-specific treatment: i) zones of high productivity (high PC1 values) and stable over time (intermediate PC2 values); ii) zones of high productivity (high PC1 values) and non-stable over time (low or high PC2 values); iii) zones of low productivity (low PC1 values) and stable over time (intermediate PC2 values); and iv) zones of low productivity (low PC1 values) and non-stable over time (low or high PC2 values). This knowledge can assist producers in two ways: i) between-fields comparison based on field risk, especially when maize prices decrease; and ii) intra-field comparison based on the average temporal yield, indicated by the first PCA axis and temporal yield stability indicated by the second PCA axis.

Keywords: field risk; Principal Components Analysis; maize yield; spatial and temporal analysis

3.1 Introduction

Obtaining georeferenced data of soil physical and chemical properties allows for the delineation of areas with a similar yield (e.g., [AAR⁺09, AZK07, CL05b, CLOK06, Goo98a, ITJ⁺05, LCD00]). However, crop yield is not always correlated with soil physical and chemical properties. The interaction of these factors with i) climate (e.g., [BJCK00, MBA⁺02]); ii) topography (e.g., [JCK05, KKKM11, MS06, MS08, SSL⁺04]); iii) nutrition (e.g., [BJCK00]); and iv) pests and diseases [BJCK00, JCK05] affect the spatial and temporal crop productivity. Thus, multitemporal productivity maps typically reflect the spatial and temporal variability of this set of interactions involved in the production process, thereby constituting a basic tool for decision making. Several studies have been developed to understand spatial variability and its interaction with temporal variability [BGF03, DCT⁺12, LGC04]. Diker et al. [DHB04] studied the maize yield variability in two irrigated fields and although the spatial yield distribution changed over time, it was possible to classify the area into low, medium and high productivity management zones. Other authors also observed multitemporal yield variations based on the factors of water availability and dry and wet years [BJCK00, KKKM11, SSL⁺04]. Blackmore et al. [BGF03] and Marques da Silva and Silva [MS06] analysed the spatial and temporal variability of barley, wheat, rapeseed and maize and found a high degree of inter-annual variability. Marques da Silva and Silva [MS06] proved that the interaction between topography and the irrigation system noticeably affected the spatial and temporal yield variability. These authors showed that increasing the watered area by means of a centre pivot led to an increase in the spatial and temporal production instability. Marques da Silva et al. [MRS12] introduced the Rasch model to study spatial and temporal yield variability. These authors showed how this model allows for the development of yield potential probabilistic maps.

One of the great difficulties in analysing these types of spatial databases is their dimension and redundancy of variables. Principal Components Analysis (PCA) is a multivariate statistical technique that decreases the complexity of the data with the least possible loss of information. This technique makes it possible to better understand the relationships between variables and thus extract information components relevant to the understanding of the phenomenon under investigation.

The PCA method has been used by several authors to study different problems related to yield crops. For example, Carroll and Olivier [CO05] used the PCA method to study spatial relationships between soil physical prop-

erties and soil apparent electrical conductivity (EC_a), and Islam et al. [IVL⁺11] and Vitharana et al. [WS⁺08] applied PCA to identify and extract the main factors affecting soil fertility. Several authors applied PCA and multiple regression analysis to predict soybean and rice yield [CGWA03, KWJ89, YLK⁺01]. Moral et al. [MTM10] used PCA to study the spatial variability of five well-correlated soil properties.

The goal of this work is to verify whether the use of PCA for these types of multi-spatial-temporal yield data allows us to delineate yield management zones for maize and to simultaneously calculate the temporal risk that may be associated with the yield of a given field or a specific location inside a field.

This paper is organized as follows. In section 2, we present the Materials and Methods where we mention the following: i) the collection and processing of yield data; ii) data and geostatistical analysis; and iii) Principal Components Analysis methodology description. In section 3, we present the results and discussion. Finally, in section 4, we provide some concluding comments.

3.2 Materials and Methods

3.2.1 Collecting and processing yield data

This study was conducted using maize yield data collected from two agricultural fields, Azarento and Bemposta, with an area of approximately 60 ha and 30 ha, respectively, irrigated by centre pivot. The fields are located in Herdade do Cego, at Fronteira (Lat: +39.09307; Long: -7.611332), in the Alentejo region of southern Portugal.

According to the FAO [FAO14], the soils of these fields are classified as Luvisols and Vertisols.

The topography of the region can be characterized as undulating. The altitude varies from 196 to 230 m in the Azarento field and from 191 to 220 m in the Bemposta field. The slopes vary from 0 to 12 degrees in the Azarento field and from 0 to 13 degrees in the Bemposta field. The climate of this area is typically Mediterranean (Csa climate according to the Koppen classification). The average annual rainfall is 600 mm (20 years), with a hot dry season from June to September and maximum temperatures that occasionally exceed 40°C. The winters are mild, with minimum temperatures rarely below 0°C.

The considered yield years were 2002-2004 and 2007 for Azarento and 2002-2004, 2006-2008 and 2010 for Bemposta. The maize was sown in late April/early May and harvested in September/October. The farmer used a reduced tillage system, involving a small subsoiler (300 mm in depth) prior to sowing.

A CLAAS Lexion 450 combine harvester (produced by CLAAS, Harsewinkel, Germany) that was equipped with a combine electronic board information system (CEBIS) was used, which provided instantaneous yield and grain moisture data with less than 5% error. The combine harvester was equipped with a 6 m cutting header; a differential GPS Pilot; a grain photoelectric sensing (the magnitude of signal of the light receptor is used to determine the flow rate of the grain); and a grain moisture sensor (by sensing the dielectric properties of the harvested grain), both located near the top of the clean grain elevator. The weight of the collected grain was adjusted for dry grain moisture (140 g kg⁻¹ of moisture).

The resulting yield map not only shows the yield variation across the field but also characteristic errors, then it is important the preparation of the yield maps so that these errors are kept to a minimum. Thus, before data analysis it was applied to the raw data a filtering process in accordance with the methodologies of Blackmoore and More (1999): removal of production values located outside the study field; removal of production values with speed records lower than 1 km h⁻¹ and greater than 10 km h⁻¹; removal of output production values below 0.5 t and above 24 t; and elimination of the production points located at a zero distance between them.

3.2.2 Data analysis

Exploratory data analysis

The SPSS®: software (IBM Corp., Armonk, New York, USA [IBM10]) and ArcGISTM: Geostatistical Analyst tool (ESRI, Redlands, USA [ESR09]) were used in the spatial yield data exploratory analysis to check for the presence of global and local outliers, trends, normality and data directional dependence. Box-plots, histograms and Normal QQPlots were examined to observe extreme values and identify possible outliers. The 1st quartile (Q1) and the 3rd quartile (Q3) yield data indicated values to be eliminated, i.e., the values exceeding $Q3+3(Q3-Q1)$ and those lower than $Q1-3(Q3-Q1)$ (e.g., [MRSP10]). Local outliers were eliminated considering the Voronoi analysis (ArcGISTM: Geostatistical Analyst tool; ESRI, [ESR09]). Voronoi maps were constructed from a number of polygons that formed around each sampling point.

These polygons were created so that every location within a polygon was closer to the sample point in that polygon compared with any other sample point; this is influential to compute a variety of local statistics. The Voronoi Map tool provides a number of methods for calculating and assigning values to polygons.

Cluster method was used to identify possible outliers. The cluster method identifies those cells that are dissimilar to their surrounding neighbours. All of the cells were placed into five class intervals, and if the class interval of a cell was different from each of its neighbours, the cell was coloured grey to distinguish it from its neighbours. When a cluster equalled -1, it was considered a local outlier [ESR09].

Geostatistical analysis

The maize yield spatial dependence analysis was conducted with standardized yield data using SpaceStatTM software (BioMedware, Ann Arbor, USA [Bio12]) and ArcGISTM: Geostatistical Analyst (ESRI, Redlands, USA [ESR09]). The trend analysis tool in Arcmap was used to explore the global trends in the data. The trends were analysed based on direction and the order of the line that fit the trend. The variograms were assessed in different directions to identify whether there were directional influences affecting the data. These directional influences will affect the accuracy of the surface created. The analysis using Geostatistical Analyst tool indicated that the interpolation model should not account for the anisotropy. The data revealed no trend or isotropic behaviour [IS89, Oli10].

The spatial structure of each year of maize data was characterized by experimental variograms that were calculated from experimental data using Matheron's equation [Oli10]:

$$\gamma(h) = \frac{1}{2N(h)} \sum_{i=1}^n [Z(x_i + h) - Z(x_i)]^2 \quad (3.1)$$

where x_i and x_i+h are the sampling locations that are separated by a distance h ; $Z(x_i)$ and $Z(x_i+h)$ are the measured values of variable Z at the corresponding locations that are separated by a distance h , and $N(h)$ is the total number of sample pairs within the distance interval h and the given direction. All of the pairs of points that were separated by distance h (lag) were used to calculate the experimental variogram.

Spherical and exponential theoretical models were fitted to the empirical omni-directional variograms [Goo98b, Oli10]. The models were fitted using the following cross-validation statistics. The best model was the one with a mean error (ME) and standardized mean (MS) nearest to zero, the smallest root mean squared prediction error (RMSE), the average standard error nearest the root mean squared prediction error and the standardized root mean squared prediction error (RMSS) nearest to 1 [IS89, ESR09].

The variogram structural properties were used in the construction of maps using ordinary kriging for each yield year, performed on a regular resolution grid of 6 m. All maps were drawn using ArcGISTM: Spatial/3D analyst tools [ESR09].

A yield surface with a 6 m resolution grid, the same as the combined width, was obtained considering an ordinary kriging interpolator and the variogram structural properties. All maps were drawn using ArcGISTM: Spatial/3D analyst tools [ESR09].

Principal components analysis (PCA)

The fundamental contributions to the development of the PCA were made by Pearson [Pea04] and later by Hotelling [Hot33], and this multivariate approach is now incorporated into mathematical statistics [LMP95]. However, only after the 1960's was it possible to apply PCA to the processing of multivariate data with the use of computing platforms.

In most studies each individual is represented by a large number of variables. The individual study of each variable does not consider the relationships that may exist between them (which is usually the most important aspect). The data analysis techniques must therefore take into account multidimensional data. PCA is a linear factorial method and it is a technique suited to explore the underlying structure of such data.

The main goal of PCA is to search for synthesis variables called principal components. The PCA aims to identify a structure of a set of variables that are related to each other to construct a measurement scale for factors that control the initial variables. PCA is a method of reducing the complexity of the data with the least possible loss of information. If two or more variables are interrelated, it means that they share a common characteristic that may not be directly observable. Thus, through the correlations observed between variables, PCA creates common factors and structural relationships that link the factors to the variables. The most general method is the "measure of sampling adequacy of the Kaiser-Meyer-Olkin" (KMO), proposed by Kaiser [Kai70] and Kaiser and Rice [KR74]. The KMO measures the homogeneity of variables, comparing simple correlations with partial correlations observed between variables.

The new components can then be used as indicators that summarize the available information on the original variables. These components are linear combinations of the initial variables; they are not correlated with each other, and they exhibit maximum variance. The study and interpretation of the variance-covariance structure of a given phenomenon, measured by multiple variables to reveal the relationships between variables, between individuals and between individuals and variables, is the primary objective of the PCA. The reduction of the dimensionality of the representative points of the samples, although the statistical information present in the original p-variables is the same as that of the main p-components, makes it possible to obtain more than 80% of that information in only two or three main components [Pea04].

PCA was performed using ArcGISTM: Spatial/3D analyst tools [ESR09]. The variables used for each field were the maize yield of each year. Standardization to mean 0 and variance 1, using the field mean of each year as a reference, was needed to ensure the multi-temporal data were comparable and to homogenize the variance in the multivariate analysis. PCA was applied to the correlation matrix to extract the eigenvectors and eigenvalues.

Annual normalized maize yield variables were processed to develop new artificial variables using PCA. These new artificial variables consisted of a linear combination of the original variables and were designated as the principal components. In this particular case, each year of production for each tested field had a different weight in each obtained component. The components are mutually orthogonal, that is, each component carries different statistical information [Jac80]. For each component, the ArcGISTM: Spatial Analyst Tool [ESR09] created a raster surface with the same resolution of the original data. All contour lines were obtained using ArcGISTM:

Spatial Analyst Tool [ESR09].

3.3 Results

3.3.1 Grain yield descriptive statistics

All summary statistics of the maize yield are shown in Table 3.1. Considerable variability was found for most variables, with a medium coefficient of variation. The variability was higher in 2002 and 2003 for both fields. In 2003, the Azarento field yield showed a nearly symmetrical distribution, whereas a negative asymmetry was observed in the remaining years. The presence of some values with low productivity in 2002, 2004 and 2007 resulted in a left skewing of the yield distribution but all the skewness coefficients exhibited values <1 or > -1 . Although a linear geostatistic does not require a normal distribution, a variogram is based on variances, and any asymmetry with skewness values higher or lower than these values should be examined [Oli10]. Therefore, although the data did not follow a normal distribution when using the Kolmogorov-Smirnov procedure with Lilliefors Significance Correction, no transformation was used for the geostatistical analyses. In the autocorrelation scale at approximately 60 to 70 m (Fig. 3.1), it was found that yield data had a near normal distribution. In the Bemposta field, the maize yields for 2002, 2003 and 2010 revealed approximately symmetric distributions. The yield data from other years showed a moderate negative asymmetry with a similar magnitude. The data dispersion around the mean was similar to the variation observed in the Azarento field (Table 3.1).

Table 3.1: Summary statistics for grain yield at the Azarento and Bemposta agricultural fields.

Yield Year	Mean (t ha ⁻¹)	Standard deviation (t ha ⁻¹)	Minimum (t ha ⁻¹)	Maximum (t ha ⁻¹)	Coefficient of variation	Skewness
Azarento						
2002	12.57	4.966	0.505	23.986	0.395	-0.292
2003	08.34	3.175	0.504	22.886	0.381	0.008
2004	12.66	3.833	0.506	23.968	0.303	-0.664
2007	12.55	3.582	0.503	23.913	0.285	-0.464
Bemposta						
2002	12.03	4.741	0.500	23.980	0.394	0.134
2003	08.99	3.082	0.502	22.787	0.394	0.343
2004	10.84	2.955	0.544	23.657	0.273	-0.553
2006	12.77	3.446	0.508	23.933	0.270	-0.568
2007	13.28	4.307	0.511	23.951	0.324	-0.288
2008	14.86	3.908	0.565	23.908	0.263	-0.744
2010	12.23	3.282	0.518	23.887	0.268	-0.092

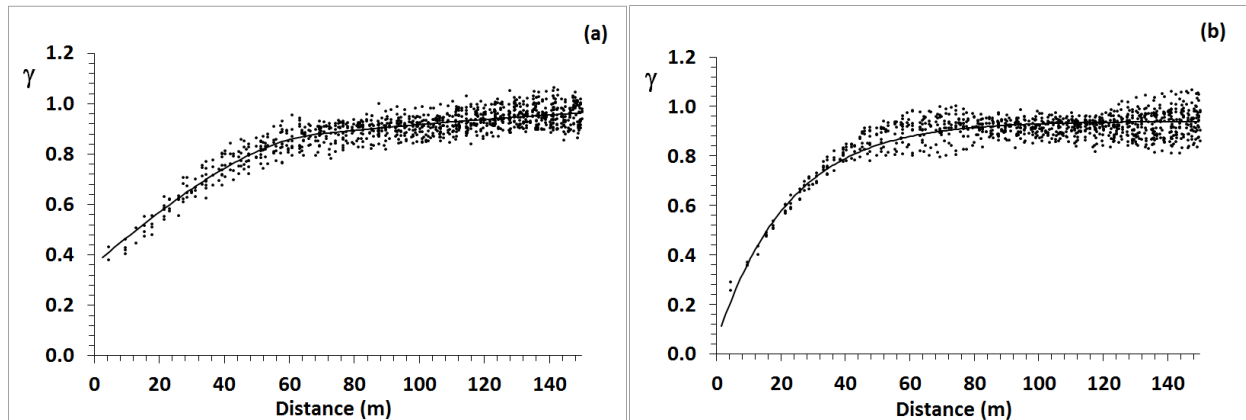


Figure 3.1: (a) 2002 yield variogram for the Azarento field; (b) 2006 yield variogram for the Bemposta field.

3.3.2 Grain yield spatial dependence

The omnidirectional variogram parameters computed for the yearly maize yield data for the Azarento and Bemposta fields displayed in Figures 3.1a and 3.1b are shown in Table 3.2.

Oliver [Oli10] showed that in presence of a large set of data, nested variation is often observed, and a combination of two or more simple models can be used to model such variation. A spherical model with two structures showed the best fit for Azarento (Table 3.2, Fig. 3.1a). In this field, there was a strong spatial autocorrelation in the first 60 m and a smoother autocorrelation from 60 m to 160 m. In the Bemposta field, an exponential model with a single structure was the best fit (Table 3.2, Fig. 3.1b). The variogram ranges had a strong spatial autocorrelation in the first 60 m, which was cancelled or disappeared thereafter.

The yearly maize yield data for Bemposta appeared to vary more consistently than the yearly maize yield data for Azarento, as shown by the smaller nugget effect and the larger range of its variograms. These differences are probably related to differences in topography.

According to the $C0/(C0+C)$ ratio (Table 3.2), all years yield of Azarento and the 2004 yield of Bemposta showed a moderated spatial dependence. The remaining yield years of Bemposta indicated a strong spatial dependence [CMP⁺94]. The spatial dependence better explains the yield variation in the Bemposta field than in the Azarento field, with a higher random error caused by a higher nugget effect.

3.3.3 Principal Components Analysis

The 4 yield years (4 variables) in the Azarento pivot and the 7 yield years (7 variables) in the Bemposta pivot were subjected to a Principal Components Analysis performed on the Pearson's correlation matrix coefficient. In each pivot, all yield years (all variables) showed significant correlations ($P < 0.05$).

In the case of the Azarento field, the higher correlations were always high and positive between the 2002, 2003 and 2004 yields and ranged from 0.75 to 0.81. The correlations of these yields with the 2007 yield were lower but still positive and significant.

In the case of the Bemposta field, positive correlations were found between all years. These years showed correlations from 0.5 to 0.7, but the 2004 yield revealed a weak (0.33) positive correlation with the 2007 and

Table 3.2: Maize yield data variogram parameters for Azarento (2 structures) and Bemposta agricultural fields.

Yield Year	Lag (m)	Nr. Lags	Model	Nugget Effect Co	Sill	Range (m)	SD ¹ (%)	SDD ²
Azarento								
2002	6	40	Spherical	0.37	0.42	69.0 210.7	36.5	Mod
2003	6	40	Spherical	0.34	0.32	55.5 240.7	34.8	Mod
2004	6	40	Spherical	0.31	0.37	57.8 179.3	32.0	Mod
2007	6	40	Spherical	0.37	0.29	49.6 313.1	34.3	Mod
Bemposta								
2002	6	25	Exponential	0.20	0.83	135.0	19.5	Strong
2003	6	25	Exponential	0.21	0.80	108.0	20.8	Strong
2004	6	25	Exponential	0.30	0.73	120.0	29.1	Mod
2006	6	25	Exponential	0.07	0.87	67.5	7.4	Strong
2007	6	25	Exponential	0.10	0.66	99.0	13.2	Strong
2008	6	25	Exponential	0.13	0.64	84.0	16.8	Strong
2010	6	25	Exponential	0.20	0.69	97.5	22.5	Strong

¹SD=Spatial Dependence (Co/Co+C): (SD<25%=strong spatial dependency (Strong); SD between 25 and 75%=moderate spatial dependence (Mod.); SD>75% weak spatial dependence; SD≈ 100%= random); ²SDD=Spatial dependence degree (Cambardella et al. 1994)

2002 yields and a moderate (0.50) correlation with the 2003 and 2010 yields. The eigenvalues and eigenvectors were extracted from the correlation matrix (Table 3.3).

The results of the Kaiser Meyer Olin (KMO) method showed suitability of only one factor, with KMO=0.827 in Azarento and KMO=0.852 in Bemposta, indicating that factor analysis was appropriate. Despite the Principal Components Analysis having revealed that only one component was significant according to the Kaiser criterion (to retain the eigenvalues greater than 1), we considered the first two principal components for the multi-temporal yield database for both fields. The values of the eigenvector loadings for each year and the percentage of the variance explained by the first two axes for the Bemposta and Azarento fields are shown in Table 3.3. Each major component (Table 3.3; Figs. 3.3c, 3.3.d, 3.5c and 3.5d) is a linear combination of all the original variables (Figs. 3.2 and 3.4) and attempts to explain the overall variability. The eigenvalue analysis revealed that the first (PC1) and second components (PC2) together accounted for 88.8% and 77.3% of the yield data variance in the Azarento and Bemposta fields, respectively.

3.4 Discussion

The 1st component, PC1 (Figs. 3.3c and 3.5c), refers to the first orthogonal axis that explained 76.9% and 64.1% of the total variance presented in the original data for the Azarento and Bemposta fields, respectively (Table 3.3). In the Azarento field, the eigenvector loadings (Table 3.3) between PC1 and 2002, 2003 and 2004 (Fig. 3.2) were close to 0.50 and showed a slight increase from the 2002 to the 2004 yield. Although not very different, the 2007 yield showed that something different occurred because it is the only year that PC2 was negatively correlated with yield.

In the Bemposta field, the eigenvector loadings (Table 3.3) between PC1 and the yield ranged between 0.31 and 0.43. Bemposta PC2 correlated negatively with the 2004 and 2008 data. The productivities of 2006 and 2007 contributed the most to PC1, with a 0.43 factor loading (Table 3.3).

Table 3.3: Values of the eigenvector loadings for each variable and percentage of explained variance by the first two axes for Bemposta and Azarento fields.

Yield Variable	PC1	PC2	PC1	PC2
	Bemposta		Azarento	
	Eigenvectors		Eigenvectors	
Yield 2002	0.39	0.49	0.51	0.18
Yield 2003	0.35	0.07	0.52	0.37
Yield 2004	0.31	-0.64	0.54	0.19
Yield 2006	0.43	0.15		
Yield 2007	0.43	0.38	0.43	-0.89
Yield 2008	0.37	-0.41		
Yield 2010	0.35	0.18		
Eigenvalue	2.19	0.45	1.40	0.22
Total explained variance (%)	64.1	13.2	76.9	11.9

With a total explained variance of 100% in the 1st component (PC1), one could say that all studied yield years were equal. Considering this and a comparison between the two different fields, one could say that the higher the explained variance in the 1st component, the more stable a field would be over time. Based on a com-

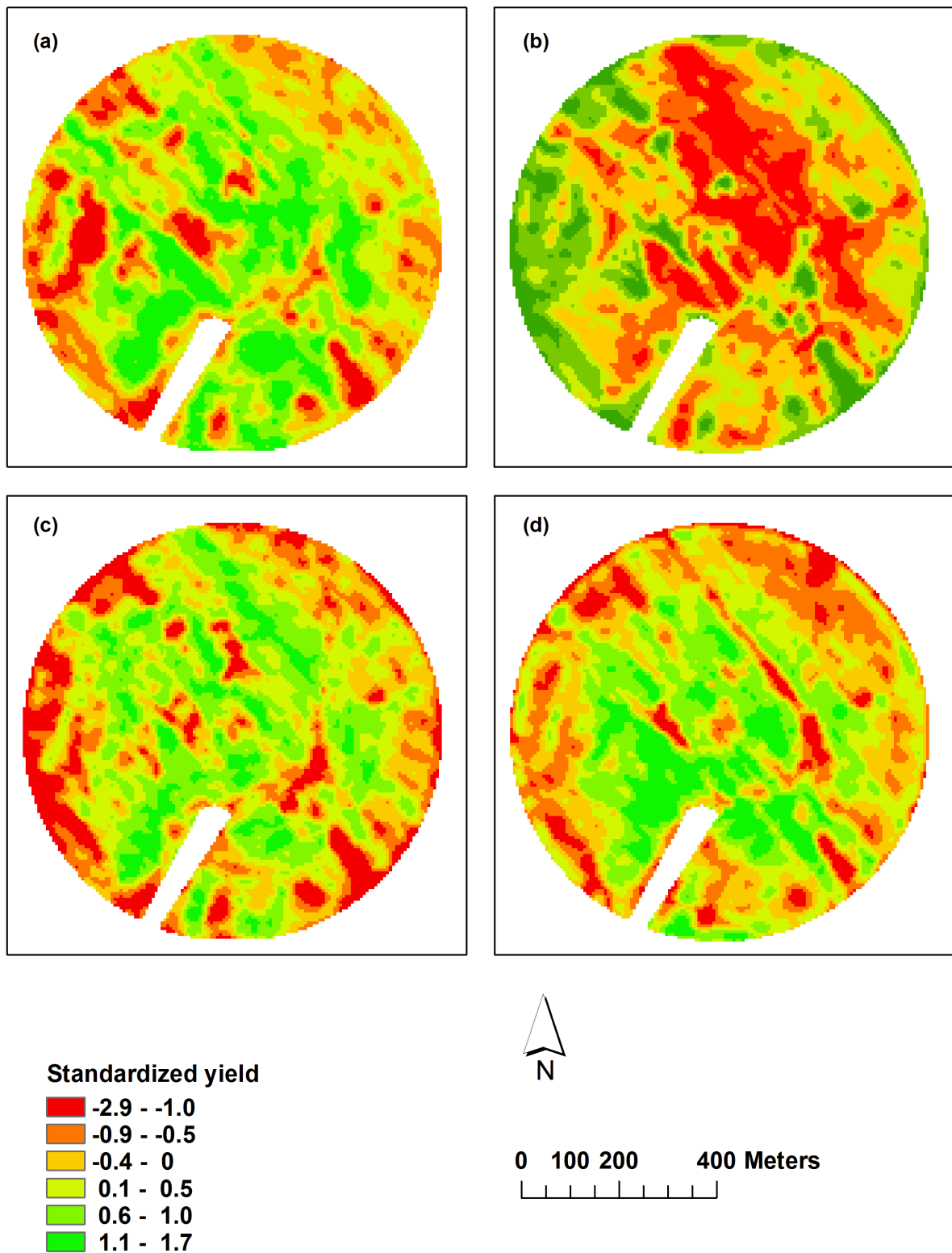


Figure 3.2: Standardized maize yield maps for the Azarento field: (a) yield in 2002; (b) yield in 2003; (c) yield in 2004; (d) yield in 2007.

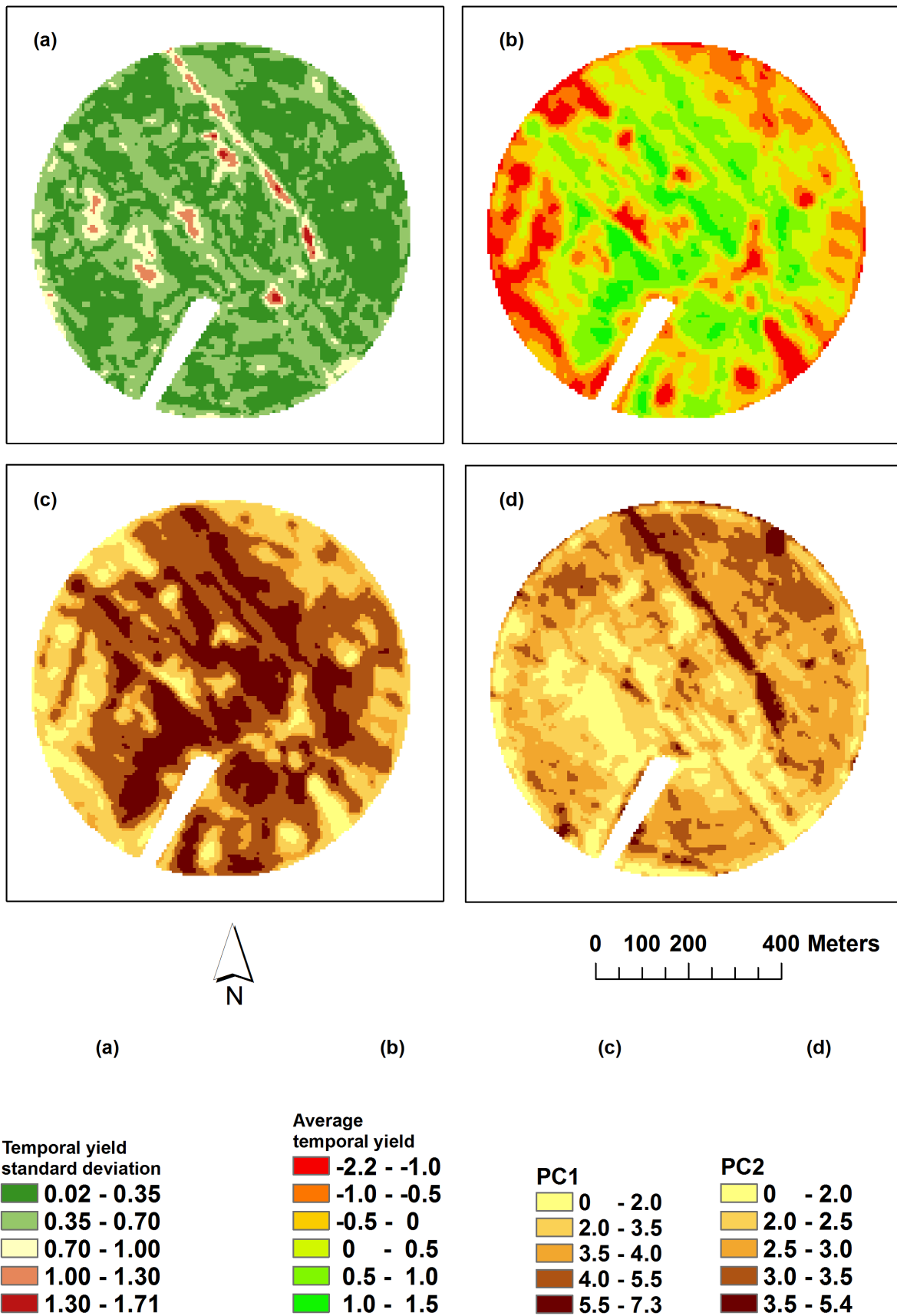


Figure 3.3: Azarento field: (a) temporal yield standard deviation; (b) average temporal maize yield; (c) first principal component scores; (d) second principal component scores.

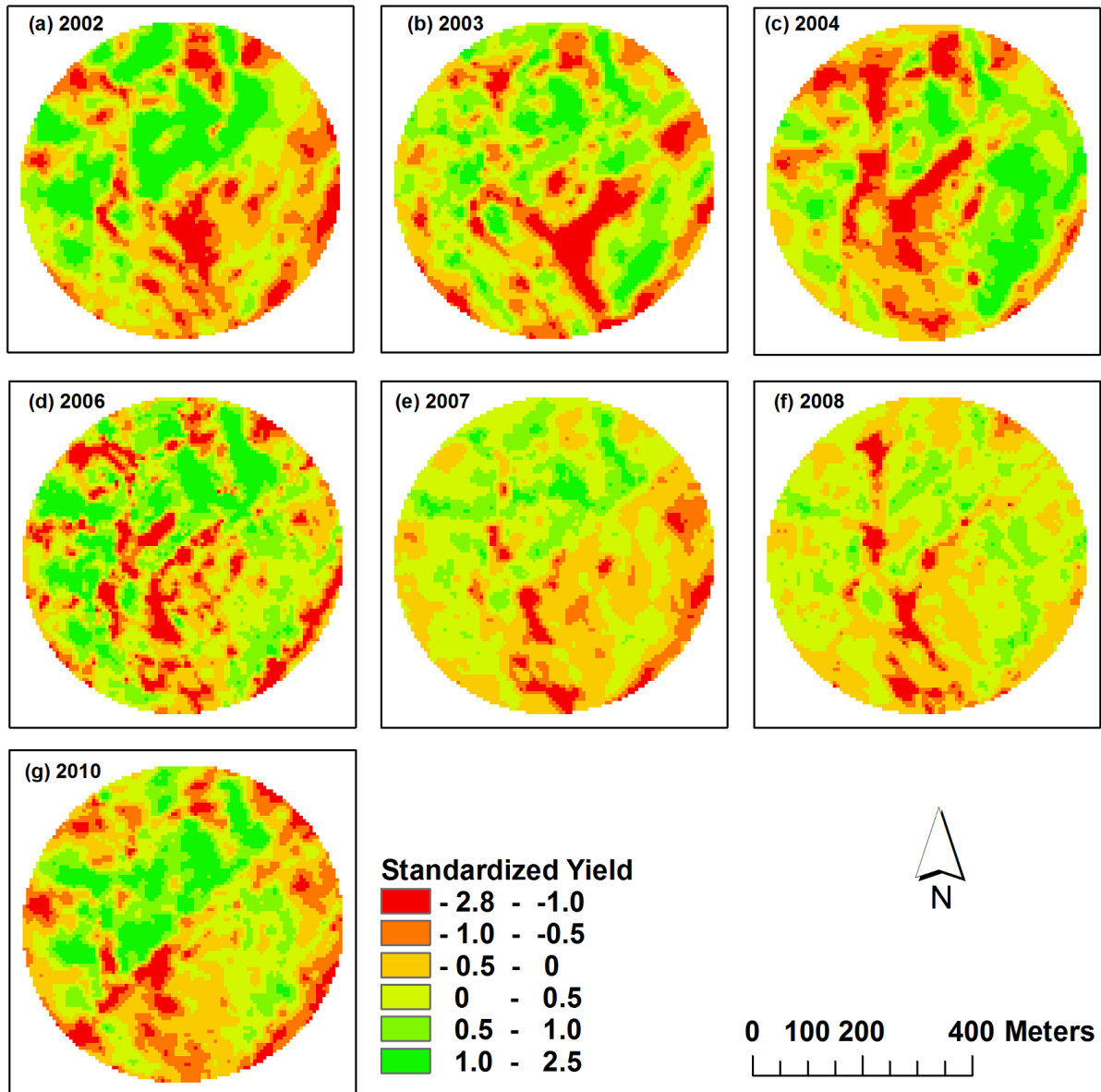


Figure 3.4: Standardized maize yield maps for the Bemposta field: (a) yield in 2002; (b) yield in 2003; (c) yield in 2004; (d) yield in 2006; (e) yield n 2007; (f) yield in 2008; (g) yield in 2010.

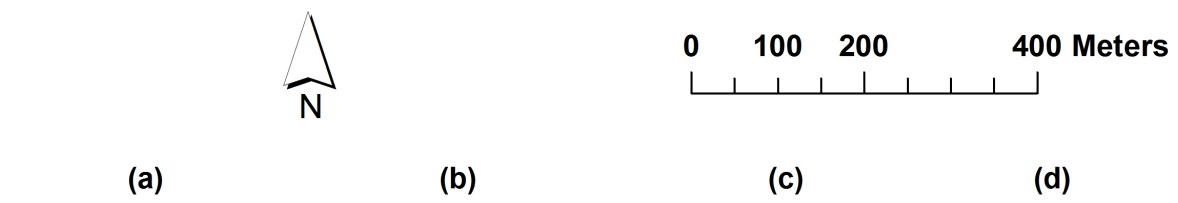
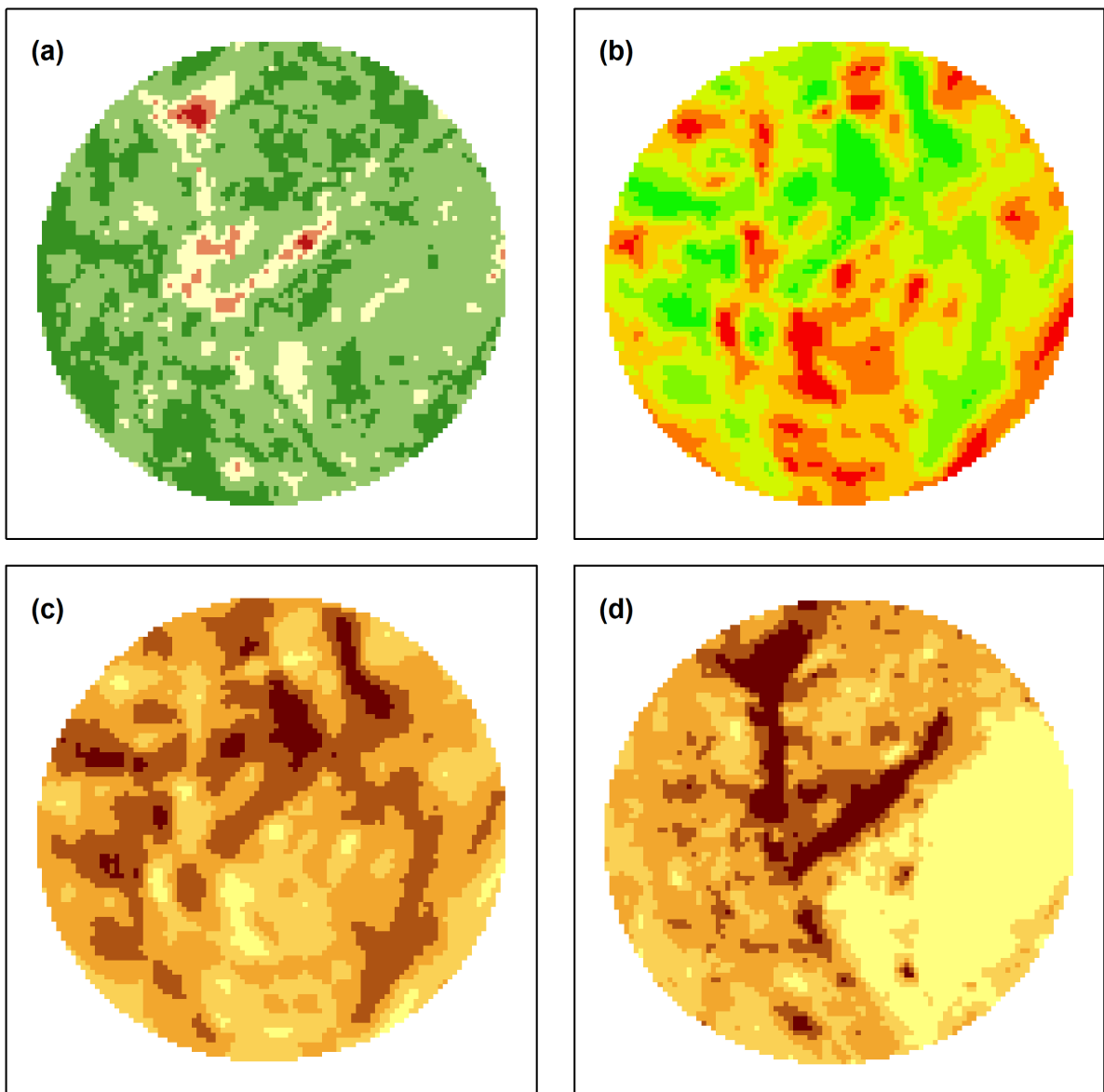


Figure 3.5: Bemposta field: (a) Temporal yield standard deviation; (b) Average temporal maize yield; (c) First principal component scores; (d) Second principal component scores.

parison of the Azarento and Bemposta variance explained by PC1, and if we could consider that the analysis was carried out for the same number of years, we could say that the Azarento field is a more stable field from a temporal perspective because the 1st component explains more variance over time; stating this in another way, the Azarento field becomes more redundant over time and this information is of major importance when producers have to choose between two production fields and want to reduce yield risks.

A PC1 comparative analysis of both fields (Figs. 3.3c and 3.5c) with both of the average temporal yield maps (Figs. 3.3b and 3.5b), allows us to observe that the highest values of PC1 coincide with the highest average temporal yield areas, whereas lower PC1 values coincide with the lower average temporal yield areas. The same can be confirmed in Figure 3.6, which shows 300 random yield observations in each of the fields, where one can see that when PC1 increases, the average temporal yield of the Azarento (4 years) and Bemposta fields (7 years) also increases.

When comparing the PC1 values of the two fields, we found that the PC1 upper limit of the Bemposta field (9.93) was greater than the PC1 upper limit of the Azarento field (7.32) (Figs. 3.3c and 3.5c). A similar discrepancy can be observed considering the 300 random observations (Fig. 3.6).

This means that the Bemposta field reached a higher average temporal yield value and therefore, produced more, on average, than the Azarento field in some years (Table 3.1). PC1 values close to zero indicate lower average temporal yield values, whereas PC1 values close to the maximum indicate the opposite (Fig. 3.6).

As shown in Figure 3.6, the point of intersection of the y-axis was lower for the Azarento field (-2.14) compared with the Bemposta field (-1.86); however, the Azarento field had a higher linear regression slope (0.50), indicating that the average temporal yield per unit of PC1 increased more rapidly compared with the Bemposta field (which exhibited a slope of 0.38).

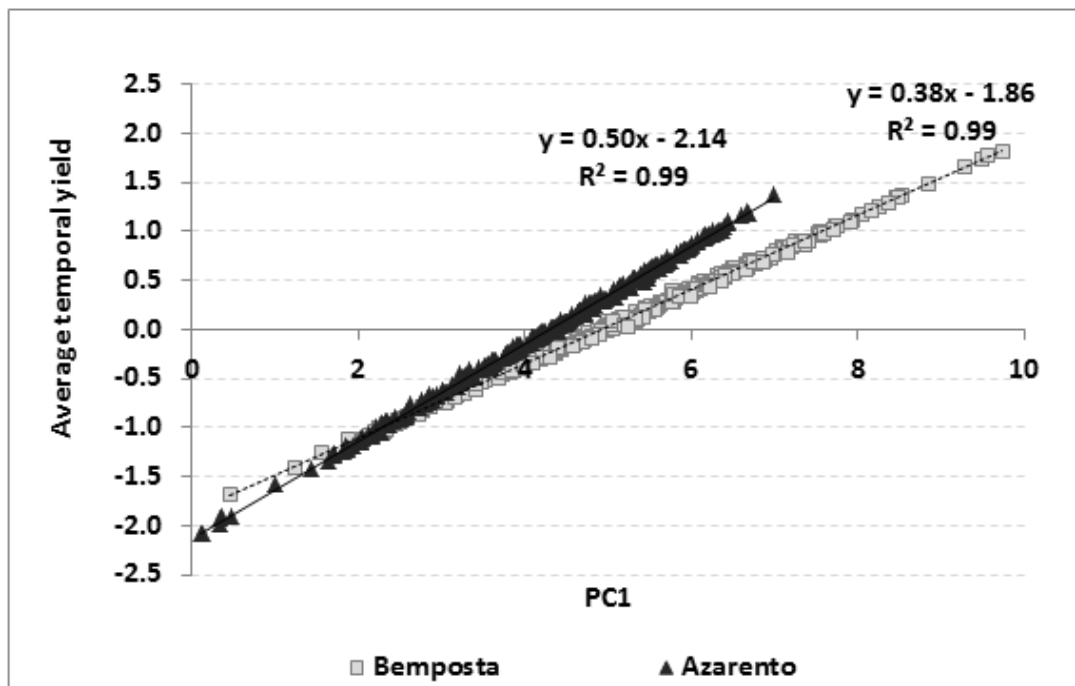


Figure 3.6: Plot of the first principal component scores (PC1) vs. the average temporal yield of 300 random yield observations in the Azarento and Bemposta fields.

Considering the PC1 for intra-field analysis, it is possible to delineate areas of high or low average temporal yield,

which enables site-specific management with consequent economic and environmental benefits. It should be noted that when performing an intra-field analysis, PC1 does not provide any information on the average temporal yield variability.

The 2nd component, PC2 (Figs. 3.3d and 3.5d), refers to the second orthogonal axis, which explained 11.9% and 13.2% of the total variance present in the original Azarento and Bemposta field data, respectively (Table 3.3). In the Azarento field, PC2 (Fig. 3.3d) was positively (0.18 to 0.37) related to the 2002, 2003 and 2004 yield and negatively (-0.89) to the 2007 yield (Table 3.3). In the Bemposta field, PC2 (Fig. 3.5d) was positively related mainly to the 2002 (0.49) and 2007 (0.38) yield and negatively to the 2004 (-0.64) and 2008 (-0.41) yield (Table 3.3).

The 2nd component showed similar PC2 limit values in both fields (0 to 5.4 in Azarento, and 0 to 5.6 in Bemposta; Figs. 3.3d and 3.5d). The second component appeared to have a parabolic association with the temporal yield standard deviation, and showed significant ($P < 0.05$) R^2 values of 0.62 and 0.51 for the Azarento and Bemposta fields, respectively (Figs. 3.3a, 3.5a and 3.7). In the Azarento field, the PC2 values tended to be located primarily around the midpoint of the PC2, while in the Bemposta field, the PC2 values appeared to be more distributed within the confines above (Fig. 3.7). This figure also demonstrates that higher and lower PC2 values show that the temporal yield standard deviation values were consistently higher than 0.5. On the other hand, Figure 3.7 clearly shows that intermediate values of PC2 are related to areas with lower temporal yield variability, i.e., the temporal yield standard deviation values were consistently less than 0.5.

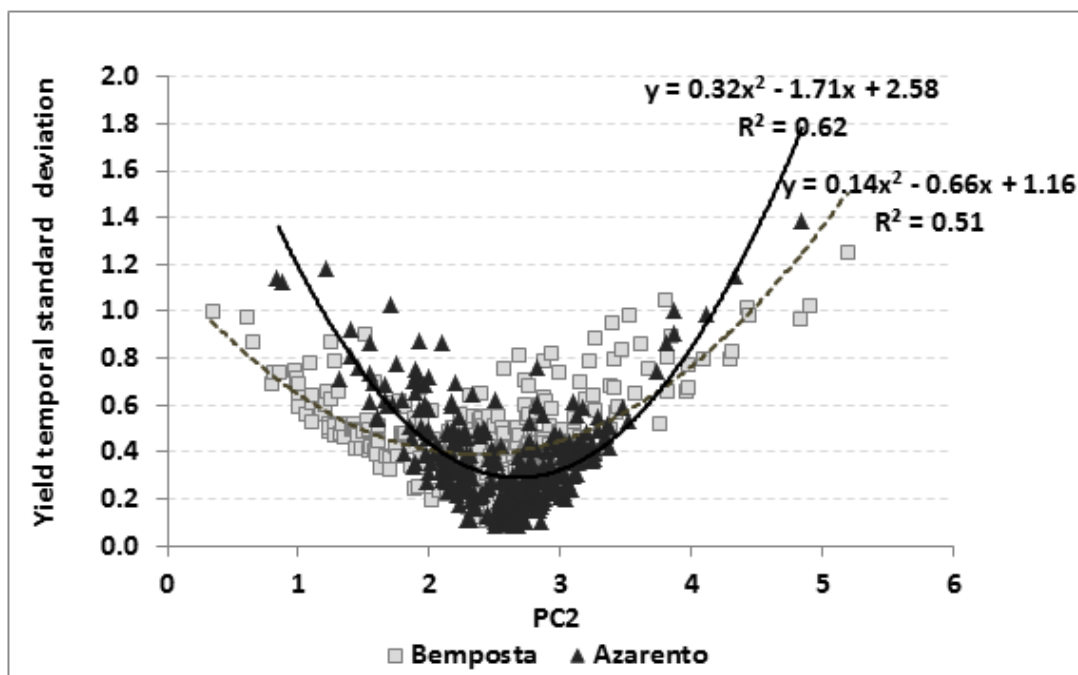


Figure 3.7: Plot of the second principal component scores (PC2) vs. the temporal yield standard deviation for 300 random yield observations in the Azarento and Bemposta fields.

Thereby, this 2nd component (Figs. 3.3d and 3.5d) seems to identify regions of the field where low PC2 values (e.g., between 0 and 2, Figs. 3.3d and 3.5d) and high PC2 values (e.g., between 4 and 6, Figs. 3.3d and 3.5d), with low or high yield, indicate areas of high temporal yield variability. These results lead us to believe that in both fields, temporal instability of productivity occurs mainly in areas with low and high PC2 values, with high or low productivity of the yield area. These areas have a potentially high production risk. Therefore, PC2 identifies areas of higher or lower temporal yield resilience. In other words, if the yield in an intra-field zone changes

readily over time (up or down), PC2 is close to the maximum or minimum; if the yield in an intra-field zone does not change that much over time, PC2 is close to intermediate values.

3.5 Conclusions

Based on results we may conclude that: i) in a between-field average temporal yield comparison, the field with the highest absolute temporal yield average and the highest explained variance by means of PC1, will be the more productive and the least risky. This is fundamental for ranking all agricultural fields in terms of the maize temporal yield risk; ii) in an intra-field yield temporal analysis, the 1st component makes it possible to observe that the highest PC1 values coincide with the highest average temporal yield areas and the lowest PC1 values coincide with the lowest average temporal yield areas; iii) in an intra-field yield temporal analysis, the 2nd component makes it possible to observe that low and high values of PC2 indicate areas of high temporal yield variability, and intermediate values of PC2 indicate areas of low temporal yield variability.

Considering the first two components in an intra-field temporal yield analysis, one can define management zones for site-specific treatment: i) zones of high productivity (high PC1 values) and stable over time (intermediate PC2 values); ii) zones of high productivity (high PC1 values) and non-stable over time (low or high PC2 values); iii) zones of low productivity (low PC1 values) and stable over time (intermediate PC2 values); and iv) zones of low productivity (low PC1 values) and non-stable over time (low or high PC2 values).

This information is valuable for producers as an exploratory study and may enhance decision-making processes and the selection of agricultural fields or parts of agricultural fields considering their temporal redundancy by means of the overall variability explained by PC1. One may choose parts of a field with a higher absolute temporal yield average, higher PC1 values and median PC2 values to optimize production factors and to reduce economic risk of the activity.

4

Stochastic simulation of maize productivity: spatial and temporal uncertainty in order to manage crop risks

Grifo, A. R. L., & Marques da Silva, J. R. (2015). Stochastic simulation of maize productivity: spatial and temporal uncertainty in order to manage crop risks. *Precision Agriculture*, 16 (3). Published online 24 May 2015. doi 10.1007/s11119-015-9401-1
<http://link.springer.com/article/10.1007/s11119-015-9401-1>

Abstract

There is emerging interest in evaluating the uncertainty of agricultural production to support the production process and for guidance in decision making. The main objective of this work was to estimate the spatial and temporal maize yield uncertainty using stochastic simulation techniques to reduce the economic risk considering the producer risk profile and the international prices of maize and inputs. The results showed that i) the class yield percentage variation in yield stochastic simulation depends on the sampling density; ii) higher sampling densities promote an overestimation of low and high yield values compared to those of real yield data; iii) reducing sampling density promotes the low and high values of overestimation reduction while increasing the central classes values compared to those of real yield data; iv) the ideal point density for yield stochastic simulation is approximately 65 points ha⁻¹; v) in Mediterranean environments, more than 3 to 4 years' worth of real yield data considered as a whole do not seem to improve the field level of confidence when cropping irrigated maize; and vi) the number of equi-probable surfaces that were generated by sequential Gaussian simulation helped to calculate the yield class uncertainty and permitted the study of class yield probabilities for a particular position of the field and, therefore, to manage the yield risk and support future decisions. The approach that is presented in this paper may increase prior knowledge of agricultural field behavior in the absence of multi-year data, thereby increasing the possibility of reducing economic risks.

Keywords: stochastic simulation, maize, yield spatial and temporal uncertainty, risk management

4.1 Introduction

The availability of sophisticated technologies that can be applied to agriculture has provided greater guidance in the development of the production process and greater impact on decision making.

Defining low and high potential stable zones for site-specific management is particularly difficult because temporal variability is generally higher than space variability for crops and soil properties [CC08]. Therefore, different tools and large amounts of geo-referenced information have been used to characterize soil differences within crop production fields with accuracy.

According to Batchelor et al. [BBP02], different crop growth models have been used to simulate the effect of management, weather, genetic, water stress and other yield limiting factors. In precision agriculture, these models are used to understand the spatial variability and provide guidance for the site-specific management decisions of crop inputs.

Generally, crop models are developed and tested at the scale of small and homogeneous areas, assuming that inputs are uniform for all spatial area [BBP02, HJ00]. However, as described by Hansen and Jones [HJ00], even under these conditions, new properties and processes appear as a result of new components (e.g., human and economic subsystems) or interactions among neighboring components of the system (e.g., intercrop competition), which may condition the results. These authors indicate potential approaches that are related to input sampling and calibration for controlling or minimizing the effects of those components or interactions.

The connection between crop growth models and climate prediction depends on the assumption that the models can capture the response to climate variability that occurs year to year [HJ00].

Basso et al. [BCC⁺09] used a crop model that simulates plant growth and development responses to environmental conditions, genetics and management strategies. The interactions with plant parameters, topography, soil attributes, and remotely sensed data increased the possibilities of observing yield variability over the years

[BCC⁺09]. The remote sensing imagery provides timely spatial information of soil and crop variability throughout the season [BBP02], which is important to target sampling and to provide spatial input for crop models [BRP⁺01].

To control all of the factors that are involved in the production process through models is not easy, and crop models are not perfect. Others techniques introduce new challenges for accurately defining the spatial and temporal yield and soil variability. The use of geostatistical tools has made it possible to characterize the spatial and temporal distribution of physico-chemical properties of soils e.g., [AKA⁺11, CK99, MTM10, NMMK12], to better understand the complex relationships that occur between soil properties and environmental factors and to sustainability intensify the production process [AZK07, DMV07, DCT⁺12, Goo98b].

Geostatistical techniques, such as kriging, make it possible to estimate attributes in unsampled locations based on the spatial continuity of the data [Goo99, Soa06]. These estimation techniques smooth the details of local spatial variability as shown by Goovaerts [Goo98b] with pH data on pasture. This kriging smoothing algorithm leads to an over-estimation of small values and an underestimation of large values [Goo98b, Goo99]. However, this technique permits the mapping and discriminating of areas where the studied variable had large and small values [Soa06].

The inability of the estimation procedures to produce extreme attributes has made the application of stochastic simulation procedures relevant to the study of soils and plants. In stochastic simulation, the aim is not to minimize the error variance but to reproduce the variability of the attributes being studied in a probabilistic way; that is, it is intended to generate a set of values that reproduce the histogram and variogram model of sample data [Goo98b, Goo99, Goo00].

An intermediate approach, simulated annealing, has been discussed by Goovaerts [Goo98b, Goo99, Goo00]. This approach enabled the author [Goo98b] to create maps of soil contamination by zinc, with a balance between the estimation and simulation, depending on the desired weight constraint (histogram and variogram reproduction or minimum error variance at each location).

Estimating the yield uncertainty in agriculture is somewhat important, especially if one tries to achieve economic optimization. The main objective of this work was to study the stochastic and sequential Gaussian simulation techniques and determine i) if they can be useful in forecasting and modeling maize productivity; ii) if they can be useful in modeling spatial and temporal uncertainty by means of probabilistic yield maps; and iii) if they can help producers to reduce overall risks.

4.2 Materials and Methods

4.2.1 Details of the field experimental site and the collection of yield data

This study was conducted on two center-pivot fields near Fronteira (Lat: +39.09307; Long: -7.611332) in the Alentejo region of southern Portugal. The considered maize yield years were 2002, 2003, 2004 and 2007 for the Azarento field (60 ha) and 2002, 2003, 2004, 2006, 2007, 2008 and 2010 for the Bemposta field (30 ha). Irrigated maize was sown in late April/early May and harvested in September/October. The farmers used a reduced tillage system involving a small subsoiler (300 mm in depth) prior to sowing.

The soils are classified mainly as Luvisols and Vertisols [FAO14]. The altitude varies from 192 m to 230 m and the slope from 0 to 24% (see supplementary material - Appendix A).

A CLAAS LEXION 450 combine harvester (produced by CLAAS, Harsewinkel, Germany) was used and was equipped with a combine electronic board information system (CEBIS), providing instantaneous yield and grain moisture data with a less than 5% error. The combine harvester was equipped with a 6 m cutting header; a differential

GPS Pilot; a grain photoelectric sensing (the magnitude of signal of the light receptor is used to determine the flow rate of the grain); and a grain moisture sensor (by sensing the dielectric properties of the harvested grain), both near the top of the clean grain elevator. To eliminate the identifiable errors, the yield data were processed using the methodology of Blackmore and Moore [BM99] (see subsection 3.2.1), and the weight of the collected grain was adjusted for grain moisture (140 g kg^{-1}). The yearly maize yield data were standardized with a mean equal to zero and a standard deviation equal to one in order to reduce the weather influence from one year to the other.

4.2.2 Data processing and analysis

An exploratory data analysis of maize productivity was performed to detect the presence of global outliers and trends and to test data normality using SPSS[®] software (IBM Corp., Armonk, New York, USA [IBM10]). The yield data did not follow a normal distribution when using procedures of Kolmogorov-Smirnov with Lilliefors significance correction. However, the data transformations did not improve the data distribution, possibly because yield data have an almost symmetric distribution, with skewness near to zero. According to Kroulík et al. [KMKP06] and Panagopoulos et al. [PdJBBA14], data under these conditions can be considered normally distributed because they have a skewness range between -1 and 1.

The severe outliers were eliminated annually using the 1st (Q1) and 3rd (Q3) quartiles yield data; the values exceeding $Q3+3(Q3-Q1)$ and inferiors to $Q1-3(Q3-Q1)$ were eliminated [MRSP10].

The SpaceStatTM (BioMedware, Ann Arbor, USA [Bio12]) and ArcGISTM (ESRI, Redlands, USA [ESR09]) software programs were used to detect the presence of trends, global and local outliers and data directional dependence and to perform a maize yield structural analysis with previously standardized data.

Voronoi maps were constructed considering the polygons that formed around each sampling point, allowing us to compute a variety of local statistics. The detection of outliers consisted of the identification of the cells that were dissimilar to their surrounding neighbors. All of the cells were placed into five class intervals, and if the class interval of a cell was different from each of its neighbors, the cell was considered a local outlier (ArcGISTM: Geostatistical Analyst tool, (ESRI, Redlands, USA [ESR09]).

The spatial structure analysis for each variable was performed using experimental variograms that were calculated from experimental data using Matheron's equation [Oli10]:

$$\gamma(h) = \frac{1}{2N(h)} \sum_{i=1}^n [Z(x_i + h) - Z(x_i)]^2 \quad (4.1)$$

where x_i and x_i+h are the sampling locations that are separated by a distance h ; $Z(x_i)$ and $Z(x_i+h)$ are the measured values of variable Z at the corresponding locations that are separated by a distance h , and $N(h)$ is the total number of sample pairs within the distance interval h and the given direction. All of the pairs of points that were separated by distance h (lag) were used to calculate the experimental variogram.

The experimental omnidirectional variograms were fitted to standard models in order to capture the main characteristics of maize productivity [Goo98b, Goo99, Oli10] by minimizing the weighted sum of squares (WSS) of the differences between the experimental and theoretical variogram models and considering the study area and prior knowledge [Goo98b]. Following cross-validation statistics, the choice of the best model was based on the lowest root mean square error [ESR09, IS89].

The interpolation of the considered maize yield years was performed by ordinary kriging, which estimates values as a linear combination of closer observations considering two criteria: non-bias and minimization of the

estimation variance [Goo98b, Goo99]. The analysis of yield spatial variability was performed in a $6\text{ m} \times 6\text{ m}$ square mesh using the ArcGISTM software geostatistical analyst extension [ESR09].

The spatial dependence was calculated with spatial class ratios that were similar to those that were presented by Cambardella et al. [CMP⁺94].

The forecasting and modeling of maize productivity were performed using sequential Gaussian simulation techniques provided in the SGeMS software suite (Stanford Geostatistical Modeling Software, [Rem02]). The simulation reproduces the variance of input data, both in a univariate sense (via. the histogram) and spatially (through the variogram), therefore it is preferred to kriging for applications where the spatial variation of the measured field must be preserved [Goo99, VBJ02]. The sequential Gaussian simulation assumes that the marginal distribution function of the variable to simulate has a Gaussian distribution. The respective data transformation was accomplished within limits equal to the minimum and maximum sampling before the application of sequential Gaussian simulation. The applied algorithm defines a random path through all grid nodes. Simple kriging of the nodes in the path helps generating a local distribution. A new value is then drawn from this local distribution. This added to the nodes in the random path and the next node is simulated, and so on [Goo99, VBJ02].

Data standardization was performed before the application of sequential Gaussian simulation. Considering the previous knowledge of Sequential Gaussian simulation techniques, one hundred equi-probable scenarios of maize yield were tested and generated using SGeMS (Stanford Geostatistical Modeling Software, [Rem02]) for 30, 65, 125 and 150 to 250 points ha^{-1} of the 2002 real yield, randomly chosen data. Of all of the previous simulations, the best simulation trial was then replicated for all of the years and fields.

All of the yield surfaces that were generated each year and in each simulation were analyzed using ArcGISTM software, [ESR09] and classified into 10 standard distribution yield classes: 1st (< -1); 2nd (-1 to -0.75); 3rd (-0.75 to -0.50); 4th (-0.50 to -0.25); 5th (-0.25 to 0); 6th (0 to 0.25); 7th (0.25 to 0.50); 8th (0.50 to 0.75); 9th (0.75 to 1); and 10th (> 1).

4.3 Results and Discussion

4.3.1 Exploratory and spatial structure analyses

The exploratory data analysis was performed in order to understand the basic features of the yield data. Due to extremely high temperatures during the pollination time, the 2003 yield year (Table 4.1) had a relatively low average yield (8.34 tha^{-1}) compared to those of the other yield years. The coefficient of variation (Table 4.1) showed a low to medium variability in every year.

The spatial behavior of the maize yield was assessed by variogram models whose parameters are shown in Table 4.2. Spatial variation was characterized by spherical (2 structures) and exponential models in the Azarento and Bemposta fields, respectively (Table 4.2).

Within each field, all of the yearly set and subset yield variograms showed a similar shape with a nugget effect and were still on the same order of magnitude (Table 4.2 and Fig. 4.1); however, in 2007, the Azarento field had a greater range of spatial dependence. According to Cambardella et al. [CMP⁺94], the Azarento field showed a moderate maize yield spatial dependency, while the Bemposta field showed a stronger maize yield spatial dependency.

Table 4.1: Summary statistics for grain yield in Azarento and Bemposta agricultural fields.

Yield Year	Mean (t ha ⁻¹)	Standard deviation (t ha ⁻¹)	Minimum (t ha ⁻¹)	Maximum (t ha ⁻¹)	Coefficient of variation	Skewness
Azarento						
2002	12.57	4.966	0.505	23.986	0.395	-0.292
2003	08.34	3.175	0.504	22.886	0.381	0.008
2004	12.66	3.833	0.506	23.968	0.303	-0.664
2007	12.55	3.582	0.503	23.913	0.285	-0.464
Bemposta						
2002	12.03	4.741	0.500	23.980	0.394	0.134
2003	08.99	3.082	0.502	22.787	0.394	0.343
2004	10.84	2.955	0.544	23.657	0.273	-0.553
2006	12.77	3.446	0.508	23.933	0.270	-0.568
2007	13.28	4.307	0.511	23.951	0.324	-0.288
2008	14.86	3.908	0.565	23.908	0.263	-0.744
2010	12.23	3.282	0.518	23.887	0.268	-0.092

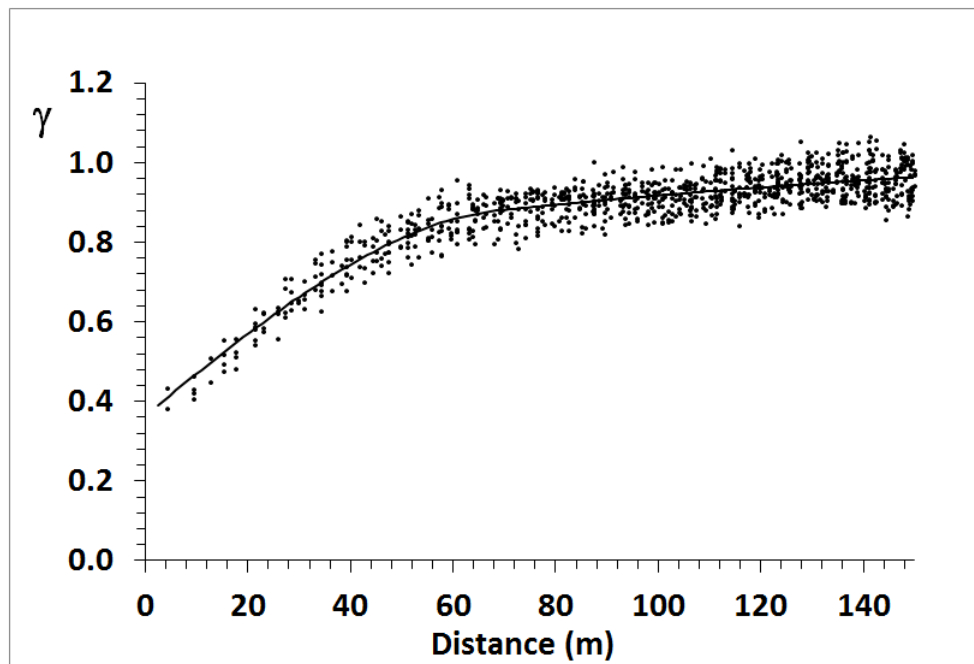


Figure 4.1: Maize yield variogram - 2002.

Table 4.2: Maize yield data variogram parameters for Azarento (2 structures) and Bemposta agricultural fields.

Yield Year	Lag (m)	Nr. Lags	Model	Nugget Effect Co	Sill	Range (m)	SD ¹ (%)	SDD ²
Azarento								
2002	6	40	Spherical	0.37	0.42 0.23	69.0 210.7	36.5	Mod
2003	6	40	Spherical	0.34	0.32 0.31	55.5 240.7	34.8	Mod
2004	6	40	Spherical	0.31	0.37 0.28	57.8 179.3	32.0	Mod
2007	6	40	Spherical	0.37	0.29 0.41	49.6 313.1	34.3	Mod
Bemposta								
2002	6	25	Exponential	0.20	0.83	135.0	19.5	Strong
2003	6	25	Exponential	0.21	0.80	108.0	20.8	Strong
2004	6	25	Exponential	0.30	0.73	120.0	29.1	Mod
2006	6	25	Exponential	0.07	0.87	67.5	7.4	Strong
2007	6	25	Exponential	0.10	0.66	99.0	13.2	Strong
2008	6	25	Exponential	0.13	0.64	84.0	16.8	Strong
2010	6	25	Exponential	0.20	0.69	97.5	22.5	Strong

¹SD=Spatial Dependence (Co/Co+C): (SD<25%=strong spatial dependency (Strong); SD between 25 and 75%=moderate spatial dependence (Mod.); SD>75% weak spatial dependence; SD≈ 100%= random); ²SDD=Spatial dependence degree (Cambardella et al. 1994)

4.3.2 Real Yield Data

Table 4.3 (Azarento field) shows that in 2002, 2003, 2004 and 2007, the percentage of the standard productivity in each class was more or less stable from year to year. In percentage terms, the smallest difference (Ymax-Ymin) for all of the years (0.97 percentage points) occurred in class 2; the biggest difference for all of the years (3.62 percentage points) occurred in class 8; and the global difference average was approximately 2.4 percentage points (Table 4.3, data average of column 10). On average, 65% of the total field production was between classes 3 and 8. With the exception of classes 2, 3, and 9, which showed yield percentages of approximately 7% to 9%, most of the classes had a yield percentage of approximately 10% to 12% while maintaining a reasonable yield percentage stability in each class productivity over time (Table 4.3).

Similar results were found for Bemposta field (Table 4.4); the analysis of 7 yield years confirms that on average, 65% of the total field production is located between classes 3 and 8. Nevertheless, Bemposta field, for which the global difference average is approximately 4.56 percentage points (Table 4.4, data average of column 13), has higher yield values compared to Azarento field (Table 4.3), possibly due to the different number of yield years and their respective yield variability. In percentage terms, the smallest yield difference was also encountered in class 2 (2.46 percentage points), and the biggest was encountered in the two extreme classes (classes 1 and 10).

Table 4.3: Percentages of yield standard classes for real yield in the Azarento field.

Yield classes	Yield standard interval	Y02 (%)	Y03 (%)	Y04 (%)	Y07 (%)	YMin (%) (1)	YMax (%) (2)	YMed (%)	(2) - (1) (%)
1	<-1.00	9.91	11.51	11.67	9.07	9.07	11.67	10.54	2.60
2	-1.00 to -0.75	6.34	6.51	5.89	6.86	5.89	6.86	6.40	0.97
3	-0.75 to -0.50	9.15	7.60	7.77	10.07	7.70	10.07	8.65	2.37
4	-0.50 to -0.25	10.28	9.72	8.65	11.84	8.65	11.84	10.12	3.19
5	-0.25 to 0.00	11.43	12.52	11.00	12.37	11.00	12.52	11.83	1.52
6	0.00 to 0.25	12.69	13.12	11.93	12.19	11.93	13.12	12.48	1.19
7	0.25 to 0.50	10.55	11.54	13.06	10.68	10.55	13.06	11.46	2.51
8	0.50 to 0.75	11.02	9.00	12.62	10.28	9.00	12.62	10.73	3.62
9	0.75 to 1.00	8.90	8.15	10.25	6.83	6.83	10.25	8.53	3.42
10	>1.00	9.73	10.33	7.18	9.82	7.18	10.33	9.27	3.15

YMin - Minimum yield class percentage; YMax - Maximum yield class percentage; YMed - Average real yield class percentage; Y02; Y03; Y04; Y07 - Real yield 2002; 2003; 2004 and 2007

4.3.3 Yield Stochastic Simulations

In order to determine the influence of data density on the stochastic simulation results, 30, 65, 125 and 150 to 250 points ha⁻¹ of the initial data were tested.

From Tables 4.5 and 4.6 and considering all of the simulated yield classes, if a 200 points ha⁻¹ (SY02) density is used, there is an overestimation of the lower yield values (Table 4.5, 14.79%; Table 4.6, 10.94%) and the higher yield values (Table 4.5, 15.35%; Table 4.6, 18.17%) compared to the real yield values, as represented by YMed (Tables 4.5 and 4.6). This phenomenon is also visible in Figures 4.2a and 4.2b when comparing both of the curves. When decreasing the point density in the simulations, the overestimation effect of the border classes

Table 4.4: Percentages of yield standard classes for real yield in the Bemposta field.

Yield classes	Yield standard interval	Y02 (%)	Y03 (%)	Y04 (%)	Y06 (%)	Y07 (%)	Y08 (%)	Y10 (%)	YMin (%) (1)	YMax (%) (2)	YMed (%)	(2) - (1) (%)
1	<-1.00	8.13	9.29	9.43	10.42	12.21	8.47	6.24	6.24	12.21	9.17	5.97
2	-1.00 to -0.75	6.59	5.62	7.20	5.12	6.20	4.75	6.24	4.75	7.20	5.96	2.46
3	-0.75 to -0.50	9.15	8.15	8.34	6.24	8.43	6.96	9.91	6.24	9.91	8.17	3.66
4	-0.50 to -0.25	10.96	9.67	11.75	10.24	9.58	9.73	12.73	9.58	12.73	10.67	3.15
5	-0.25 to 0.00	13.74	12.01	12.46	10.50	9.67	11.36	15.02	9.67	15.02	12.11	5.35
6	0.00 to 0.25	12.59	14.18	12.39	11.71	10.57	13.23	12.33	10.57	14.18	12.43	3.61
7	0.25 to 0.50	9.92	13.26	10.38	13.57	9.96	12.93	11.51	9.92	13.57	11.65	3.65
8	0.50 to 0.75	6.26	11.57	8.97	11.49	9.44	10.90	9.21	6.26	11.57	9.69	5.32
9	0.75 to 1.00	5.37	7.86	8.63	7.61	8.67	9.81	5.69	5.37	9.81	7.66	4.44
10	>1.00	17.29	8.39	10.45	13.09	15.26	11.87	11.13	8.39	17.29	12.50	8.90

YMin - Minimum yield class percentage; YMax - Maximum yield class percentage; YMed - Average real yield class percentage; Y02; Y03; Y04; Y06; Y07; Y08; Y10 - Real yield 2002; 2003; 2004; 2006; 2007; 2008 and 2010

(classes 1 and 10) diminishes, while the central classes increase their weight, as shown in Tables 4.5 and 4.6 and in Figures 4.2a and 4.2b.

Looking at Tables 4.5 and 4.6 and Figures 4.2a and 4.2b, it is possible to perceive that the YMed curve, representing the yield average pattern that was found in the 4 and 7 years of real data, is very similar to the curves that were obtained with the lower simulation data densities, at 30 and 65 points ha^{-1} curves. The average real yield (YMed), with the exception of classes 5 and 6 (Azarento) and classes 7, 8 and 9 (Bemposta), follows a very similar pattern of 65 points ha^{-1} curves. However, the reduction effect of extremely high values (class 10) as observed in low-density data (30 and 65 points ha^{-1}) in the Azarento field (Fig. 4.2a) is not present with the same intensity as in the Bemposta field (Fig. 4.2b). This result may have occurred because, in 2002 (year basis for simulated data), the percentage of the field area with higher yield data was atypically high in the Bemposta field (Table 4.4), and the stochastic simulation addresses the variability of the data [Goo98b]. Considering the above and for these particular fields, it was found that the optimal yield simulation data density is approximately 65 points ha^{-1} .

Thus, for all of the yield years that were considered in Azarento and Bemposta, one hundred stochastic simulations per year were performed considering a simulation data density of 65 points ha^{-1} of real data density. Tables 4.7 and 4.8 present these results.

Tables 4.7 and 4.8 show that the stochastic simulation presented an inter annual consistency considering a simulation data density of approximately 65 points ha^{-1} . In percentage points, the smallest multi-year amplitude (SYmax-SYmin) occurred in class 2, with 1.37 percentage points (Table 4.7, Azarento) and 2.67 percentage points (Table 4.8, Bemposta). In addition, in both fields, the biggest multi-year amplitude (SYmax-SYmin) occurred in class 1, with 4.39 and 5.66 percentage points for Azarento and Bemposta, respectively (Tables 4.7 and 4.8). However, the average multi-year amplitude was lower in Azarento (2.9 percentage points - obtained by averaging, column 9 in Table 4.7) compared to that in Bemposta (3.8 percentage points - obtained by averaging, column 12 in Table 4.8).

Approximately 65% of the total field has a simulated production between classes 3 and 8 (Tables 4.7 and 4.8) in both fields, which is similar to real yield data that were previously reported (Tables 4.3 and 4.4). With the exception of classes 2, 3, and 9, which presented yield percentages of approximately 6% to 9%, all of the other classes presented a yield percentage of approximately 10% to 13%, maintaining a reasonable yield stability

Table 4.5: Percentages of yield standard classes for the 2002 simulated yield data in the Azarento field considering 30, 65, 125 and 200 points ha⁻¹ of yield data positions randomly.

Yield classes	SY02	SY02	SY02	SY02	YMed
	(200 pts ha ⁻¹) (%)	(125 pts ha ⁻¹) (%)	(65 pts ha ⁻¹) (%)	(30 pts ha ⁻¹) (%)	
1	14.79	12.47	11.06	8.47	10.54
2	6.28	6.51	6.4	6.37	6.40
3	7.55	8.68	8.70	9.65	8.65
4	8.45	9.29	9.85	11.73	10.12
5	9.54	9.94	10.76	13.08	11.83
6	10.73	11.30	11.75	12.94	12.48
7	9.75	10.56	11.75	10.88	11.46
8	9.30	9.81	10.80	9.53	10.73
9	8.26	8.93	9.02	8.94	8.53
10	15.35	12.51	9.90	8.42	9.27

SY02 - Simulated yield 2002; YMed - Average real yield class percentage from Table 4.3; pts ha⁻¹ - points ha⁻¹

Table 4.6: Percentages of yield standard classes for the 2002 simulated yield data in the Bemposta field considering 30, 65, 125 and 200 points ha⁻¹ of yield data positions randomly.

Yield classes	SY02	SY02	SY02	SY02	YMed
	(200 pts ha ⁻¹) (%)	(125 pts ha ⁻¹) (%)	(65 pts ha ⁻¹) (%)	(30 pts ha ⁻¹) (%)	
1	10.94	9.96	7.41	6.51	9.17
2	6.34	6.40	7.33	6.30	5.96
3	8.21	8.87	9.78	10.47	8.17
4	10.42	10.42	11.32	13.11	10.67
5	11.94	12.12	12.92	13.81	12.11
6	11.10	11.59	11.21	11.33	12.43
7	9.78	9.81	9.97	10.47	11.65
8	7.23	6.99	7.19	7.16	9.69
9	5.88	5.88	6.17	6.32	7.66
10	18.17	17.96	16.70	14.50	12.50

SY02 - Simulated yield 2002; YMed - Average real yield class percentage from Table 4.3; pts ha⁻¹ - points ha⁻¹

Table 4.7: Percentages of the yield standard classes for simulated yield data in the Azarento field considering 65 points ha⁻¹ of yield data positions for 2002, 2003, 2004 and 2007.

Yield classes	SY02 (65 pts ha ⁻¹) (%)	SY03 (65 pts ha ⁻¹) (%)	SY04 (65 pts ha ⁻¹) (%)	SY07 (65 pts ha ⁻¹) (%)	SYMin (1) (%)	SYMax (2) (%)	SYMed (%)	(2) - (1) (%)
1	11.06	10.42	11.88	7.49	7.49	11.88	10.21	4.39
2	6.4	7.22	5.85	6.51	5.85	7.22	6.50	1.37
3	8.7	8.32	7.53	9.62	7.53	9.62	8.54	2.09
4	9.85	10.26	8.74	12.36	8.74	12.36	10.30	3.62
5	10.76	12.94	10.43	13.1	10.43	13.1	11.81	2.67
6	11.75	13.77	12.52	12.28	11.75	13.77	12.58	2.02
7	11.75	11.12	13.29	11.6	11.12	13.29	11.94	2.17
8	10.8	8.15	11.61	10.86	8.15	11.61	10.36	3.46
9	9.02	6.88	10.34	6.43	6.43	10.34	8.17	3.91
10	9.9	10.92	7.82	9.74	7.82	10.92	9.60	3.1

SY02; SY03; SY04; SY07 - Simulated yield 2002; 2003; 2004 and 2007; SYMin - Simulated yield minimum class percentage; SYMax - Simulated yield maximum class percentage; SYMed - Average simulated yield class percentage; pts ha⁻¹ - points ha⁻¹

percentage throughout the analyzed period.

This result indicates that the point sampling density affects the yield stochastic simulation results: i) a denser sampling stochastic simulation tends to distribute the yield evenly, and ii) a less dense sampling stochastic simulation tends to concentrate the yield in central classes.

Tables 4.9 and 4.10 present the difference between the real yield data (Tables 4.3 and 4.4) and the stochastic simulated yield data (Tables 4.7 and 4.8); the yield percentages differences are minimal. In both of the fields, $\approx 45\%$ of the yield classes showed yield differences lower than $|0.5|$ percentage points; $\approx 37\%$ of the yield classes showed yield differences lower than $|1.0|$ percentage points; and $\approx 19\%$ of the yield classes showed yield differences higher than $|1.0|$ percentage points and lower than $|1.58|$ and $|2.14|$ in Azarento and Bemposta fields, respectively.

This fact can also be observed on Figures 4.3 and 4.4, where there is a strong correlation between the real yield relative percentage curves and the simulated yield relative percentage curves (see supplementary material for the Bemposta field curves - Appendix A).

The differences between the minimum, maximum and average yield values (Table 4.11) per yield class between real yield data (Tables 4.3 and 4.4) and simulated yield data (Tables 4.7 and 4.8) are normally less than 1 percentage point ($\approx 80\%$) for both of the analyzed fields.

These results indicate that the yield stochastic simulation may be an interesting tool for interpreting yield trends over time because it permits a high number of temporal repetitions considering a relatively small spatial and temporal sampling basis.

Table 4.8: Percentages of yield standard classes for simulated yield data in the Bemposta field considering 65 points ha^{-1} of yield data positions for 2002, 2003, 2004, 2006, 2007, 2008 and 2010.

Yield classes	SY02 (65 pts ha^{-1}) (%)	SY03 (65 pts ha^{-1}) (%)	SY04 (65 pts ha^{-1}) (%)	SY06 (65 pts ha^{-1}) (%)	SY07 (65 pts ha^{-1}) (%)	SY08 (65 pts ha^{-1}) (%)	SY10 (65 pts ha^{-1}) (%)	SYMin (1) (%)	SYMax (2) (%)	SYMEd (%)	SY (2) - (1) (%)
1	7.15	7.72	7.72	9.06	11.36	7.99	5.70	5.70	11.36	8.10	5.66
2	6.09	7.31	7.31	5.35	6.55	4.64	6.23	4.64	7.31	6.21	2.67
3	9.84	9.89	9.89	7.15	7.98	7.44	9.09	7.15	9.89	8.75	2.74
4	10.53	11.79	11.79	10.20	9.89	9.54	11.26	9.54	11.79	10.72	2.25
5	14.25	12.17	12.17	11.33	10.91	11.78	13.49	10.91	14.25	12.30	3.34
6	12.81	12.94	12.94	13.03	10.18	14.04	15.05	10.18	15.05	13.00	4.87
7	10.03	11.11	11.11	13.26	9.95	12.51	12.85	9.95	13.26	11.54	3.31
8	7.45	9.62	9.62	10.39	9.15	11.82	8.74	7.45	11.82	9.54	4.37
9	6.47	7.44	7.44	8.47	9.24	9.59	6.02	6.02	9.59	7.81	3.57
10	15.39	10.00	10.00	11.76	14.80	10.65	11.57	10.00	15.39	12.03	5.39

SY02; SY03; SY04; SY06; SY07; SY08; SY10 - Simulated yield 2002; 2003; 2004 and 2007; SYMin - Simulated yield minimum class percentage; SYMax - Simulated yield maximum class percentage; SYMed - Average simulated yield class percentage; pts ha^{-1} - points ha^{-1}

Table 4.9: Percentage differences between real yield and yield simulation classes considering $\approx 65\%$ points ha^{-1} of yield data positions (Azarento).

Yield classes	Y02- SY02	Y03- SY03	Y04- SY04	Y07- SY07
	(%)	(%)	(%)	(%)
1	-1.15	1.09	-0.21	1.58
2	-0.06	-0.71	0.04	0.35
3	0.45	-0.72	0.24	0.45
4	0.43	-0.54	-0.09	-0.52
5	0.67	-0.42	0.57	-0.73
6	0.94	-0.65	-0.59	-0.09
7	-1.2	0.42	-0.23	-0.92
8	0.22	0.85	1.01	-0.58
9	-0.12	1.27	-0.09	0.4
10	-0.17	-0.59	-0.64	0.08

Y02; Y03; Y04; Y07 - Real yield 2002; 2003; 2004 and 2007

SY02; SY03; SY04; SY07 - Simulated yield 2002; 2003; 2004 and 2007

Table 4.10: Percentage differences between real yield and yield simulation classes considering $\approx 65\%$ points ha^{-1} of yield data positions (Bemposta).

Yield classes	Y02- SY02	Y03- SY03	Y04- SY04	Y06- SY06	Y07- SY07	Y08- SY08	Y10- SY10
	(%)	(%)	(%)	(%)	(%)	(%)	(%)
1	0.72	-0.66	-1.17	2.12	1.19	0.90	-0.23
2	-0.73	0.56	0.87	0.61	-0.52	0.07	-0.09
3	-0.64	0.73	0.00	-1.02	-0.16	-0.16	0.07
4	-0.35	-0.34	1.61	-1.04	-0.45	-0.11	1.04
5	0.83	0.08	0.47	-1.66	-0.16	-0.80	0.28
6	1.38	1.17	-1.09	-0.45	0.07	-0.03	0.79
7	-0.05	-1.07	-0.41	0.68	0.14	0.46	0.94
8	-0.94	-0.35	-0.38	-0.57	0.08	-1.22	0.52
9	-0.80	0.52	0.61	-0.47	0.15	0.15	-1.17
10	0.58	-0.62	-0.53	1.80	-0.34	0.75	-2.14

Y02; Y03; Y04; Y06; Y07; Y08; Y10 - Real yield 2002; 2003; 2004; 2006; 2007 and 2010

SY02; SY03; SY04; SY06; SY07; SY08; SY10 - Simulated yield 2002; 2003; 2004; 2006; 2007 and 2010

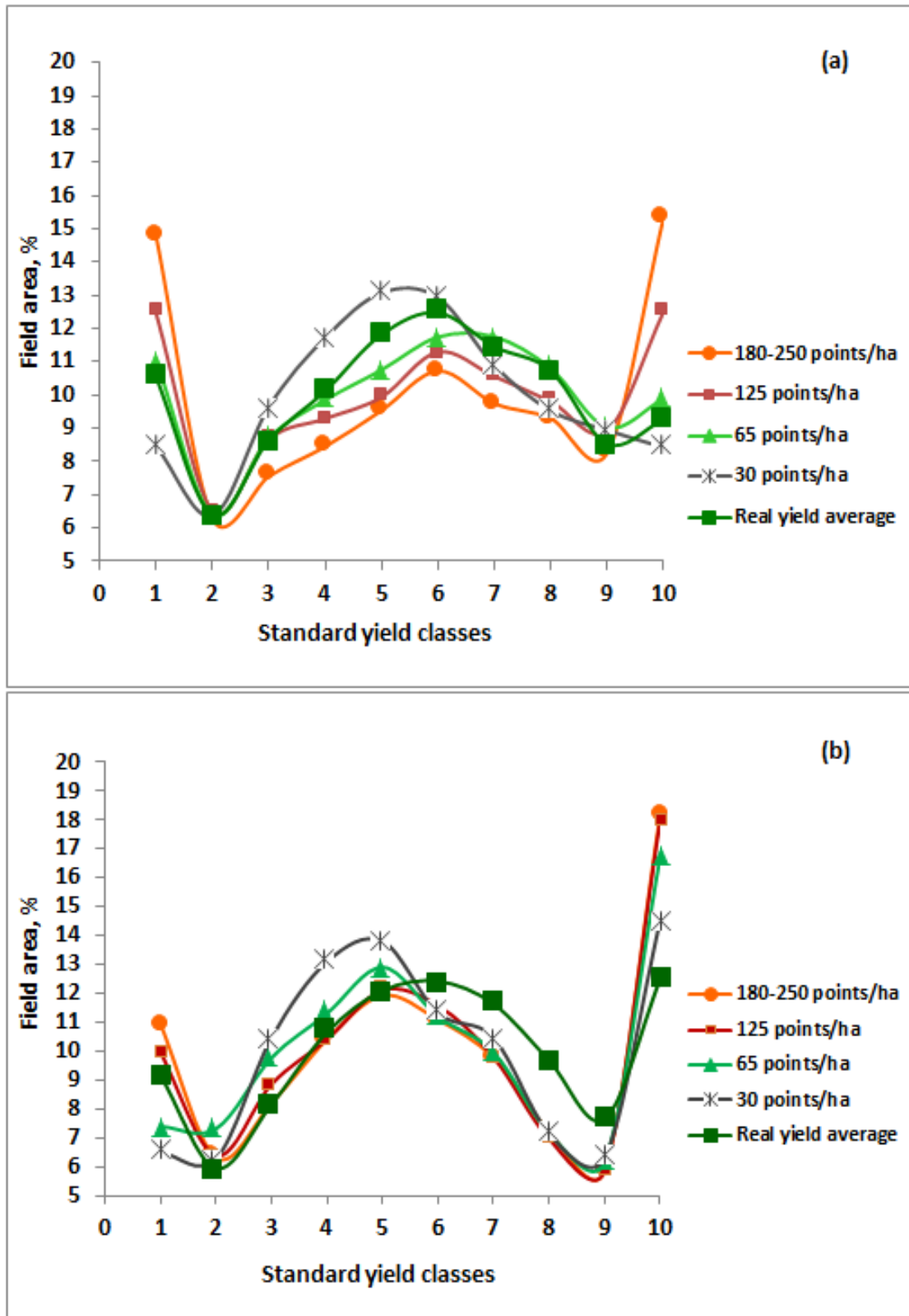
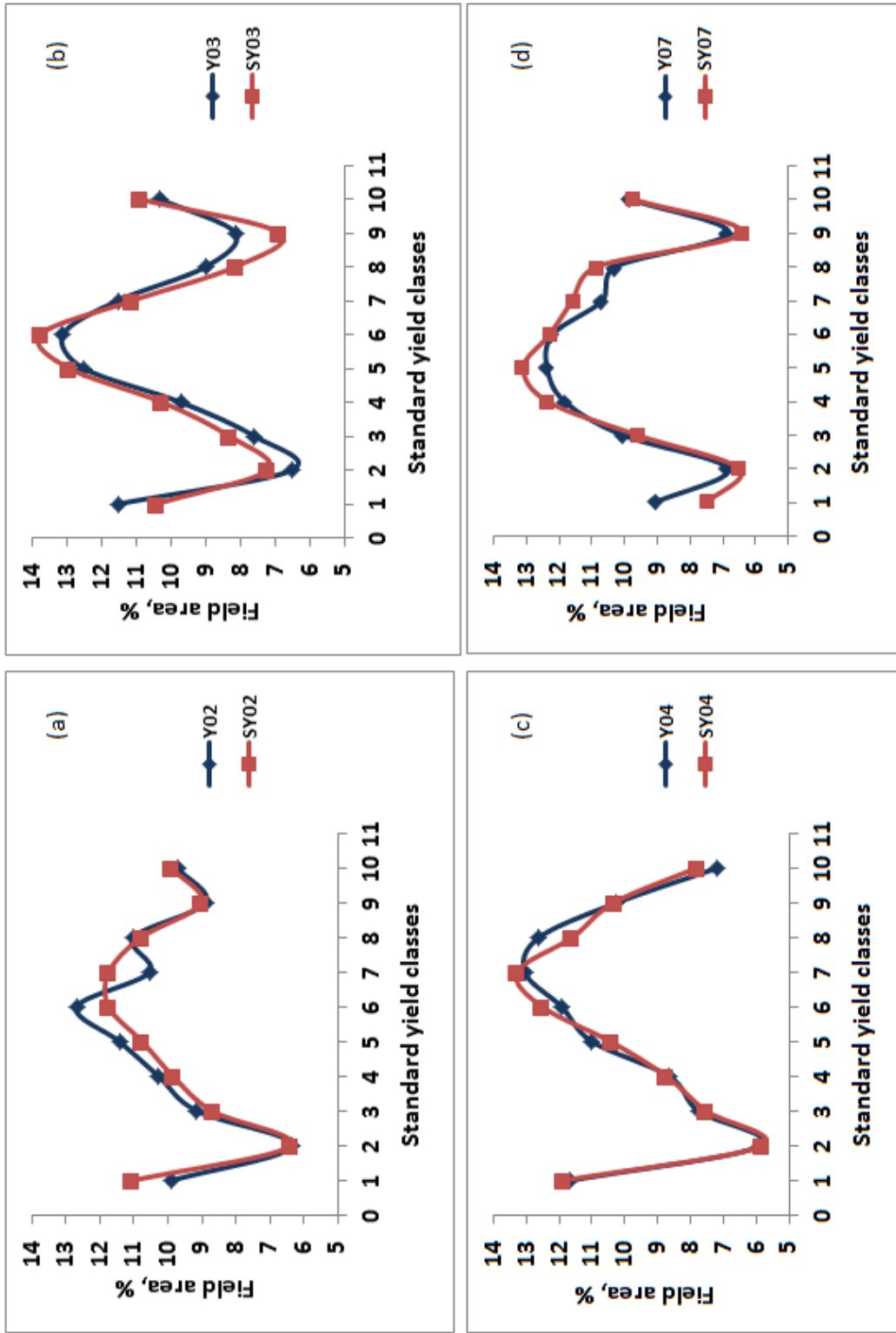


Figure 4.2: Field area percentage according to different standard yield classes and different initial point densities for stochastic simulation: (a) Azarento field; (b) Bemposta field.



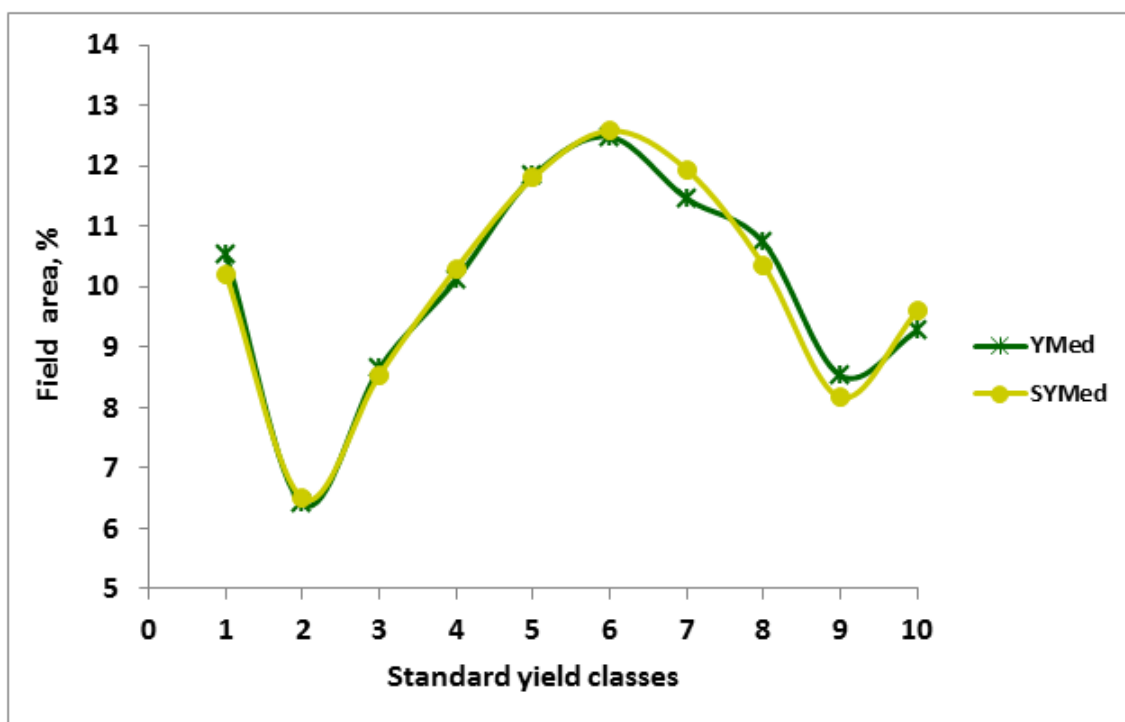
Y02; Y03; Y04; Y07 – Real yield 2002; 2003; 2004 and 2007; SY02; SY03; SY04; SY07 – Simulated yield 2002; 2003; 2004 and 2007

Figure 4.3: Real and simulated yield ($\approx 65\%$ points ha^{-1}) field area percentage according to different standard yield classes (Azarento field): (a) 2002; (b) 2003; (c) 2004; (d) 2007.

Table 4.11: Percentage differences of minimum, maximum and average yield values per yield class between real yield data and simulated yield data, considering $\approx 65\%$ points ha^{-1} of yield data.

Yield classes	YMin- SYMin (%)	YMax - SYMax (%)	YMed - SYMed (%)	YMin- SYMin (%)	YMax - SYMax (%)	YMed - SYMed (%)
	Azarento			Bemposta		
1	1.580	-0.210	0.327	0.54	0.85	1.07
2	0.040	-0.360	-0.095	0.11	-0.11	-0.25
3	0.170	0.450	0.108	-0.91	0.01	-0.59
4	-0.090	-0.520	-0.183	0.04	0.94	-0.05
5	0.570	-0.580	0.023	-1.23	0.77	-0.19
6	0.180	-0.650	-0.100	0.39	-0.87	-0.57
7	-0.570	-0.230	-0.480	-0.03	0.31	0.10
8	0.850	1.010	0.375	-1.19	-0.24	0.15
9	0.400	-0.090	0.362	-0.65	0.22	-0.15
10	-0.640	-0.590	-0.325	-1.61	1.90	0.47

YMin –yield minimum class percentage; YMax –yield maximum class percentage; SYMin – Simulated yield minimum class percentage; SYMax – Simulated yield maximum class



Ymed – average real yield; SYMed - Average simulated yield

Figure 4.4: Average real yield and simulated yield ($\approx 65\%$ points ha^{-1}) field area percentage according to different standard yield classes and considering 4 years (Azarento field).

Table 4.12: Field area percentage below the yield average according to 95%, 90%, 80%, 70%, 60% and 50% confidence levels, considering yield simulations from $\approx 65\%$ points ha^{-1} of real yield data.

Yield simulation data (number of simulations)	Confidence level					
	95%	90%	80%	70%	60%	50%
Azarento - field area (%)						
SY02 (100)	14.89	18.25	25.31	32.45	39.24	45.61
SY03 (100)	14.89	19.68	27.67	34.08	41.11	48.48
SY04 (100)	14.79	18.33	24.61	30.53	35.91	41.62
SY07 (100)	14.70	18.51	26.69	34.74	41.94	48.61
SY02+SY03 (200)	6.77	12.39	21.93	31.38	38.68	47.69
SY02+SY03+SY04 (300)	5.37	10.47	20.14	28.34	36.27	44.23
SY02+SY03+SY04+SY07 (400)	3.00	8.00	17.61	26.67	35.74	44.85
Bemposta - field area (%)						
SY02 (100)	18.52	23.50	31.59	38.59	44.53	50.54
SY03 (100)	16.35	19.42	25.03	31.25	37.72	43.60
SY04 (100)	14.78	19.23	26.57	33.16	39.70	45.50
SY06 (100)	13.00	15.86	21.37	27.82	34.93	41.56
SY07 (100)	19.76	24.46	31.30	36.97	41.61	45.93
SY08 (100)	13.31	16.43	22.35	28.67	34.27	40.39
SY10 (100)	17.14	21.89	30.07	37.26	44.03	51.11
SY02+SY03 (200)	8.34	13.28	23.11	31.29	38.36	47.35
SY02+SY03+SY04 (300)	3.42	7.35	16.82	25.63	36.16	45.55
SY02+SY03+SY04+SY06 (400)	2.10	5.45	14.91	24.55	34.45	44.22
SY02+SY03+SY04+SY06+SY07 (500)	1.51	4.65	14.33	24.79	34.33	44.75
SY02+SY03+SY04+SY06+SY07+SY08 (600)	1.02	4.06	13.36	23.55	33.57	43.11
SY02+SY03+SY04+SY06+SY07+SY08 +SY10(700)	0.84	4.17	13.39	23.98	34.45	44.07

Table 4.13: Field area percentage above-yield average according to 95%, 90%, 80%, 70%, 60% and 50% confidence levels, considering yield simulations from $\approx 65\%$ points ha^{-1} of real yield data.

Yield simulation data (number of simulations)	Confidence level					
	95%	90%	80%	70%	60%	50%
Azarento - field area (%)						
SY02 (100)	18.52	23.70	33.13	40.83	48.13	55.04
SY03 (100)	18.61	23.10	29.74	36.91	44.27	52.30
SY04 (100)	23.43	29.32	38.48	46.06	53.02	58.98
SY07 (100)	20.18	24.34	32.45	39.26	45.79	51.95
SY02+SY03 (200)	8.20	15.13	27.39	37.85	45.65	54.47
SY02+SY03+SY04 (300)	6.74	14.99	28.31	37.99	47.67	56.08
SY02+SY03+SY04+SY07 (400)	4.41	11.54	24.67	35.95	46.34	55.49
Bemposta - field area (%)						
SY02 (100)	23.53	27.35	33.11	38.70	44.31	49.96
SY03 (100)	19.89	25.07	34.79	43.13	50.33	56.85
SY04 (100)	25.88	29.58	37.06	42.94	49.01	55.07
SY06 (100)	26.20	31.90	40.50	47.19	53.26	59.09
SY07 (100)	29.61	34.11	40.58	45.48	50.07	54.44
SY08 (100)	28.60	33.99	42.13	48.59	54.37	60.26
SY10 (100)	23.09	26.97	33.66	39.40	44.34	49.76
SY02+SY03 (200)	11.33	17.14	27.95	37.31	45.93	55.05
SY02+SY03+SY04 (300)	7.20	12.29	23.61	34.11	44.34	54.78
SY02+SY03+SY04+SY06 (400)	6.88	12.85	24.49	36.07	46.46	56.05
SY02+SY03+SY04+SY06+SY07 (500)	7.11	13.12	24.38	35.54	45.71	55.48
SY02+SY03+SY04+SY06+SY07+SY08 (600)	6.88	12.93	24.75	36.32	46.74	57.07
SY02+SY03+SY04+SY06+SY07+SY08 +SY10(700)	6.68	12.58	24.30	35.17	45.35	56.05

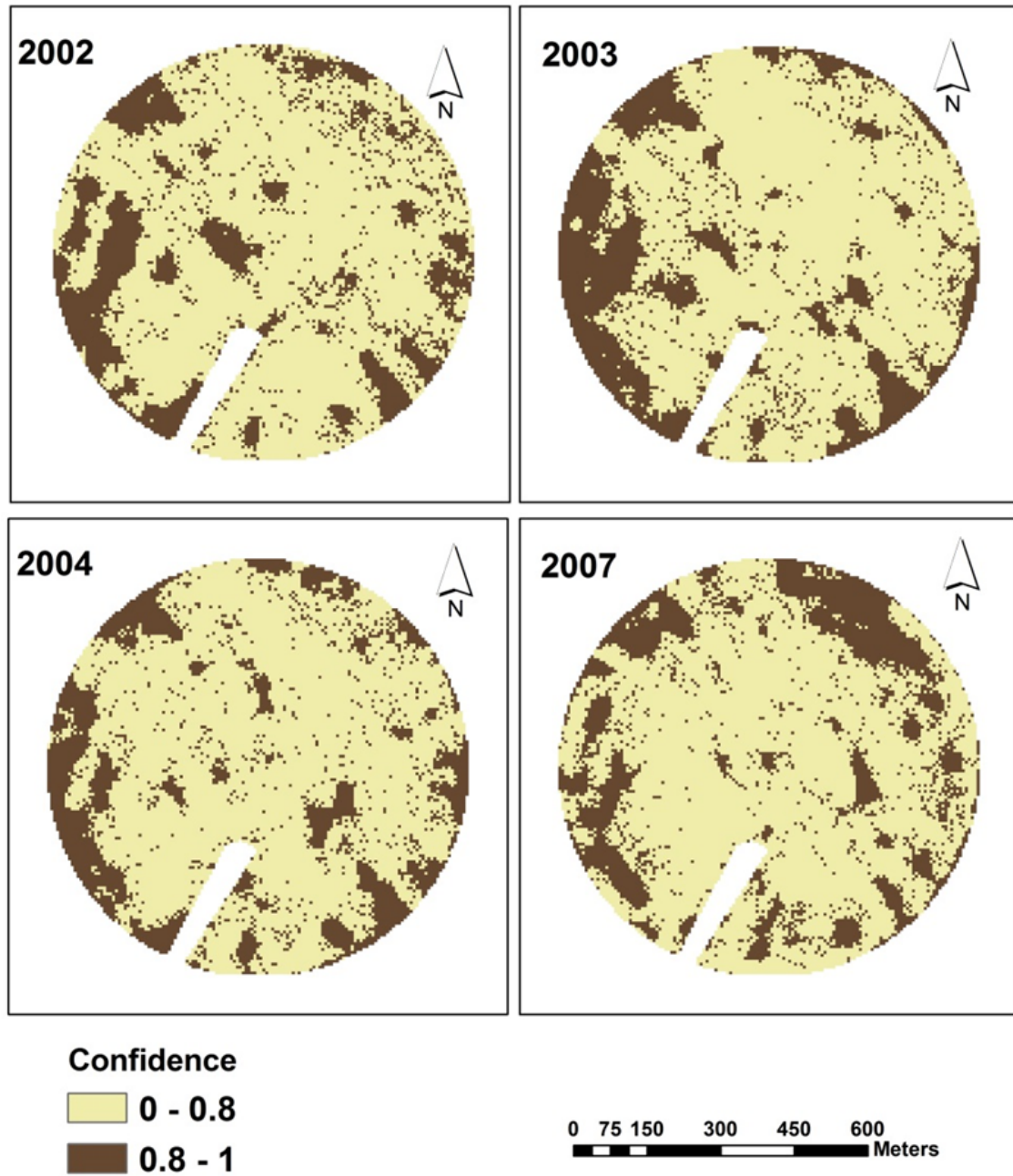


Figure 4.5: Below-average yield areas with 80% confidence considering 2002, 2003, 2004 and 2007 simulation data analyzed independently (Azarento field).

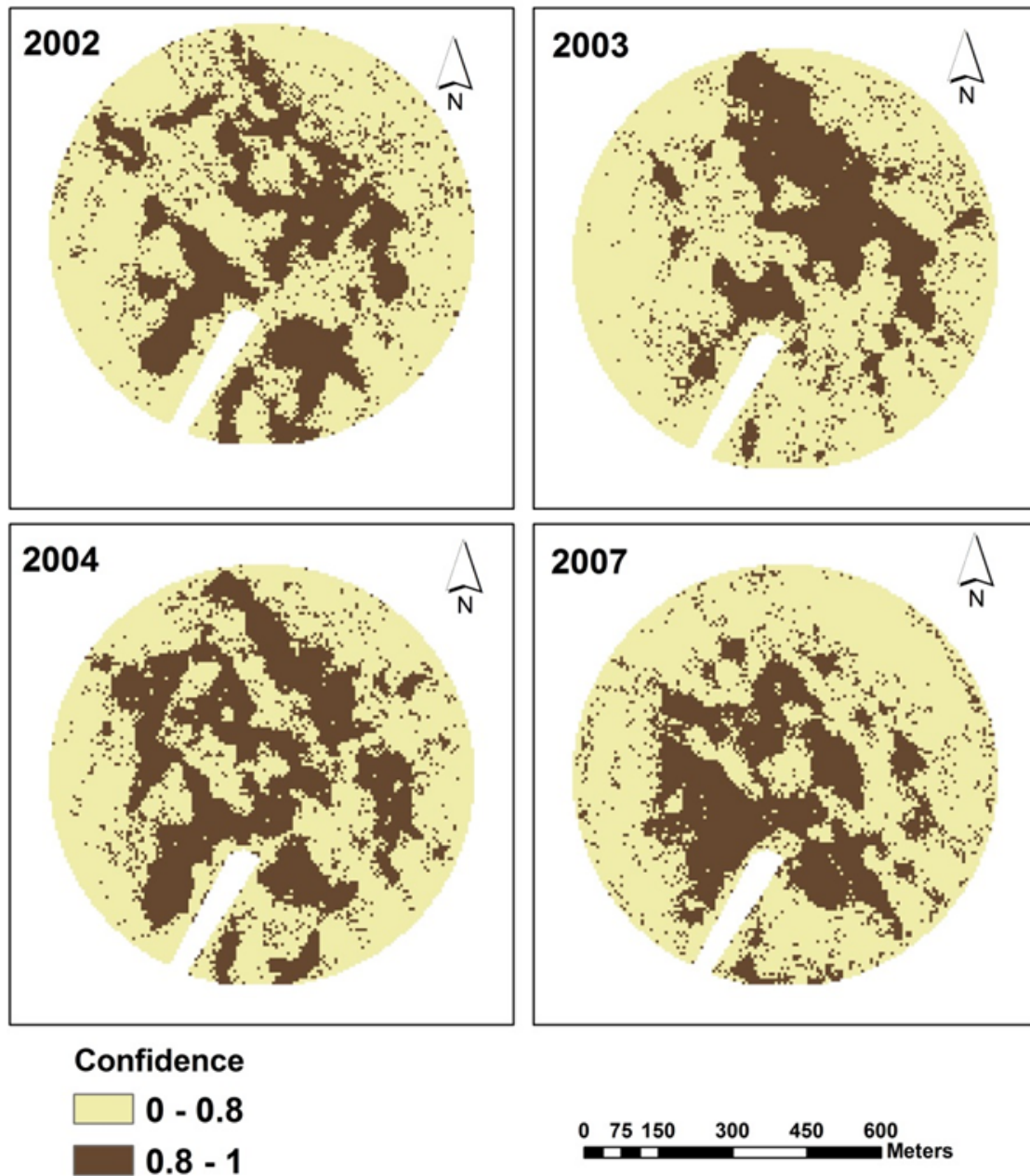


Figure 4.6: Above average yield areas with 80% confidence considering 2002, 2003, 2004 and 2007 simulation data analyzed independently (Azarento field).

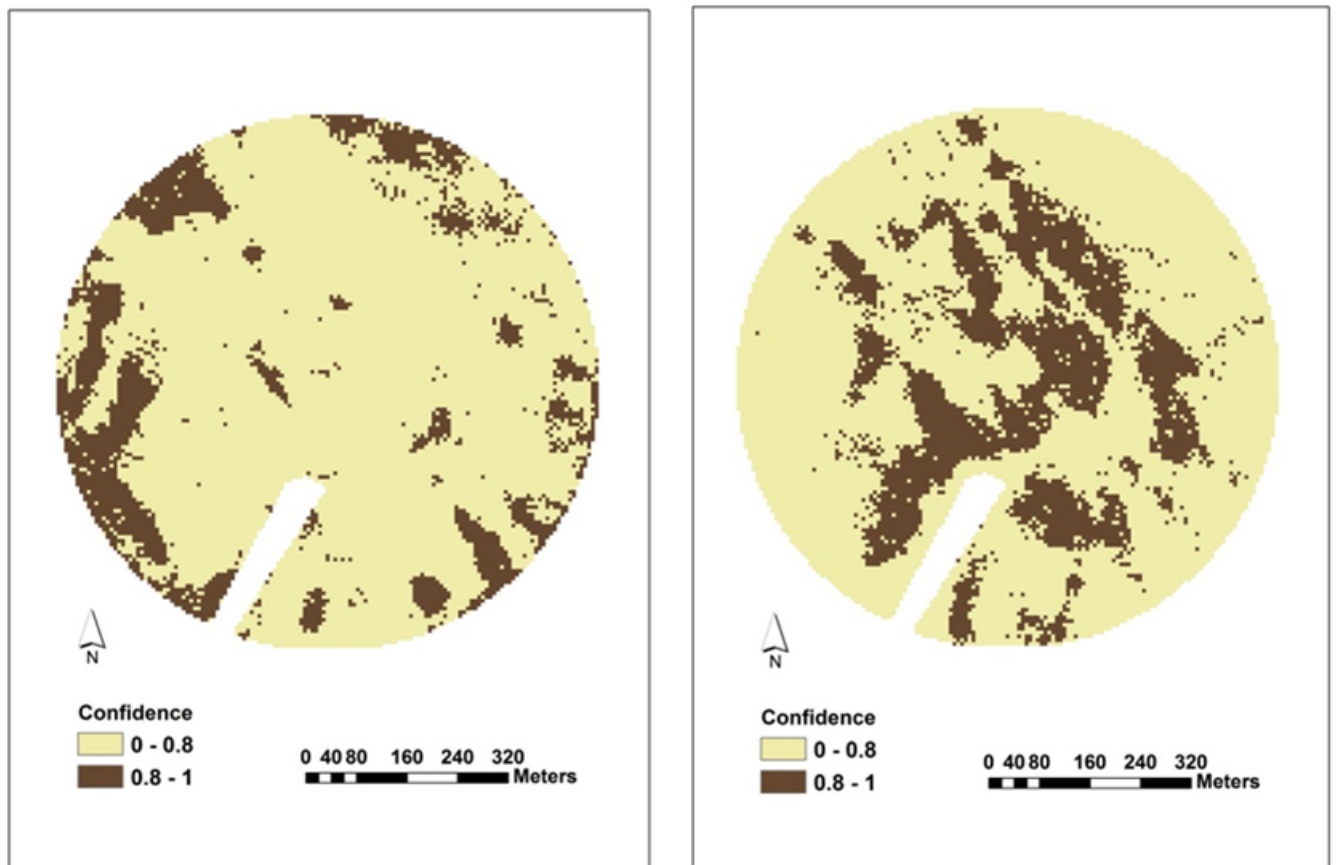


Figure 4.7: Below-average (a) and above-average (b) yield areas with 80% confidence considering 2002, 2003, 2004 and 2007 simulation yield data grouped together (Azarento field).

4.3.4 Yield classes and their occurrence probability

Considering the number of replications that can be obtained with stochastic simulation, it is relatively easy to calculate a certain probability from a yield estimate. Thus, it is possible to obtain with a certain statistical confidence the yield area that is associated with a certain yield class. With one year's data and with a 95% confidence level, the below-average Azarento field area is approximately 15%, regardless of the considered year (Table 4.12). However, considering two yield years simultaneously with the same statistical confidence level, the below-yield average field area is reduced to approximately 7% (Table 4.12).

Table 4.12 also shows that the Bemposta field has the same behavior as that of the Azarento field. However, for higher confidence levels, the average area decreases faster in the Bemposta field than in the Azarento field when adding another yield year over a span of seven years, reflecting a higher inter-annual yield variability for Bemposta compared to Azarento field.

Thus, including a new year's data, for the same statistical confidence level, the below average field percentage area normally decreases; however, this reduction is felt more quickly at higher statistical levels, such as 95%, than at lower statistical levels, such as 50% (Table 4.12).

The above-average yield areas (Table 4.13) present with similar behavior; however, for the same statistical confidence level, the fields show a greater area percentage, suggesting that above-average yield areas are more stable (trusted) from the point of view of multiyear productivity compared to the below-average yield areas.

With a set of 3 to 4 years' worth of data, introducing 1 year more does not appear to change the field area percentage regardless of the considered level of confidence (Tables 4.12 and 4.13). Considering previous results, one may say that 3 to 4 years' worth of data are required to make robust probabilistic previsions. This type of study (Tables 4.12 and 4.13) may be performed for any yield class and field and may thus support producers in their decision making: 1) it makes it possible to map with a given confidence level (producer risk profile) the yield areas under study (Figs. 4.5 and 4.6; for Bemposta field, see supplementary material - Appendix A); 2) considering the surrounding yield risk (e.g., international price of maize, international price of inputs, etc.), it enables producers to make safe decisions about which areas should or should not be subjected to production. In other words, with a relatively high surrounding risk (e.g., low international price of maize and relatively high input prices), the decision makers should consider higher levels of confidence (e.g., 80% - 90%) when making their decisions, and with a relatively low surrounding yield risk (e.g., high international maize price and moderate input prices), decision makers may consider lower levels of confidence (e.g., 60% - 70%) when making their decisions.

Considering the years 2002, 2003, 2004 and 2007 individually for the Azarento field and the areas with productivity below (Fig. 4.5) and above (Fig. 4.6) the yield average, at the 80% confidence level, it is possible to detect a multiyear spatial trend; however, there is still some spatial-temporal variability (the same occurred in Bemposta field (see supplementary material - Appendix A)). Considering the 4 (Azarento) and 7 (Bemposta) yield years that were analyzed together in a grouped way, the spatial variability below the (Fig. 4.7a) and above the (Fig. 4.7b) yield average for a statistical confidence level of 80% decreases, consolidating the below- and above-yield average areas surrounding a particular location (see supplementary material for the Bemposta field - Appendix A).

Although this technique can be used with only a year's worth of data, a greater number of years are without doubt the most beneficial from the statistical and the spatial confidence points of view. From what has been said in the previous paragraph, at least 3 to 4 years considered together are recommended to obtain robust probabilistic estimates.

4.4 Conclusions

It was found that i) the class yield percentage variation in yield stochastic simulation depends on the sampling density; ii) higher sampling densities in stochastic simulation, such as 150 to 250 yield points ha^{-1} , promote an over-estimation of low and high yield values compared to real yield data; iii) reducing the sampling density in stochastic simulation promotes the reduction of low and high values while increasing the values of the central classes compared to the real yield data; iv) the ideal point density for yield stochastic simulation in this particular study was approximately 65 points ha^{-1} compared to real yield data; v) the overall coincidence between real yield data and stochastic simulation yield data was greater when considering the multi-annual yield average; vi) the number of equi-probable surfaces that were generated by sequential Gaussian simulation helped to reproduce the main yield classes of uncertainty compared to those of real year yield data; vii) this approach permits the study of class yield probabilities for a particular position in the field and therefore to manage the yield risk and support future decisions; viii) 3 to 4 years of real yield data processed together are recommended to draw robust yield uncertainty maps by means of stochastic simulation; and ix) the innovative approach presented here may increase the agricultural field prior knowledge in the absence of long multi-year yield databases, promoting a better management strategy according to the producer risk profile and the international prices of maize and inputs.

5

Maize fertilization: soil phosphorous and potassium optimization - yield/input ratio

Grifo, A. R. L. & Marques da Silva, J. R. (2015). Maize fertilization: soil phosphorous and potassium optimization - yield / input ratio .
Submitted to Precision Agriculture

Abstract

This study aims to evaluate the agronomic, economic and environmental properties of maize phosphorus (P) and potassium (K) fertilization. The study was performed in a 56.5 ha experimental field, and different fertilization scenarios were proposed based on the yield/input ratio, taking into consideration the field surface yield and the actual maize price. Considering a 2015 maize price of 175 € t⁻¹ and the direct crop cost structure of about 1890 € ha⁻¹ (typical in the Mediterranean region), the break-even yield was ≈ 11 t ha⁻¹. The results indicate that i) in agricultural fields subject to uniform fertilization for many years, with variable nutrient extractions, the budget of soil inputs is also variable; ii) the yield/input ratio (e.g., P and K) can help farmers and managers optimize agronomic inputs and reduce economic and environmental risks; and iii) differential fertilization of this specific experimental field could save approximately 200 € ha⁻¹.

Keywords: phosphorus, yield/input ratio, break-even yield

5.1 Introduction

Maintaining a soil nutrient balance is fundamental for maintaining good soil health in all agricultural production systems. The increase of nutrient inputs to answer the demands for more food in a growing world population has contributed to the nutrient soil imbalance.

Phosphorus (P) is a nutrient commonly provided in all fertilization programs because it is an essential element for plant growth. However, the addition of P to soil and the consequent plant uptake requires knowledge of the P distribution and dynamic in the soil.

The soil P dynamics involve the interaction of microbes, plants and fauna, and to understand the processes involved, it is important to know the P behaviour. The immobilization, mineralization and redistribution of P depends upon the physico-chemical soil properties [SPdS⁺10, ST87]. Phosphorus can be found in the soil in organic and mineral forms, the latter more so than the former. The organic form can only be absorbed by plants after the mineralization process as it is dependent upon the mineral P availability; soil temperature; soil moisture content; appropriate balance between P, carbon, nitrogen and sulphur [San95, ST87]; residue management and cultivation practices [DEP98, WTC⁺11].

The mineral form, the main fraction of P in non-organic soils, is generally held with more or less energy and therefore is not directly available to plants; only a small part is available in the soil solution and can be readily utilized by plants [San95].

Soils rich in allophane minerals or in iron, aluminium oxides/hydroxides and in clay minerals, particularly the 1:1 type, have a great ability to adsorb phosphorus in forms that are not absorbable by plants [San95, Sha95]. The presence of high calcium carbonate (CaCO₃) and soil pH also dominate the P available to plants [San95, Sha95]. The precipitation of P essentially occurs when the soil pH is between 7.5 and 8. Above pH 8, the calcium is precipitated to form calcium carbonate, and calcium is thus removed. However, in very alkaline soils, less soluble secondary phosphates (H₂PO₄²⁻) predominate that are less absorbed by plants [San95, Sha95].

The studies of Horta et al. [HMMT13] in Mediterranean soils showed that P sorption processes depend upon the soil depth: predominantly, precipitation in C horizons; adsorption in A horizons; and both processes occurring in B horizons.

To achieve a correct understanding of soil P dynamic, it is also important to study the balance between the supplied and the available P [SPdS⁺10].

The phosphorus accumulation in soil, especially in the topsoil, due to its low mobility, is a consequence of the consecutive addition of phosphate fertilizers [WEF01]. This accumulation occurs mainly in inorganic forms, with different degrees of binding energy. However, the static nature of the phosphorus can be disturbed by man causing a higher bioavailability and mobility of this nutrient in the soil [San95].

The following are direct consequences of this phosphorus accumulation as a result of many years of excessive applications are: i) rising production costs; ii) uneven soil P distributions due to regular P applications and irregular plant extractions; and iii) eutrophication of water bodies and water reservoirs due to the P transferences between excessive soil concentrations and soil water runoffs [San95, Sha95, WEF01].

Thereby, it is fundamental to assess the potential soil phosphorus losses in different scenarios. Horta and Torrent [HT07] evaluated the ability of the Olsen method to predict the P release capacity in runoff and drainage water for acid soils with different parent materials and indicated as the threshold levels of 20 to 50 mg Kg⁻¹ of soil. On basic rocks soils, under a sub-humid Mediterranean climate, Horta et al. [HMMT13] showed a eutrophication risk when the P values exceed 13 mg Kg⁻¹ (Olsen method) in runoff and surface waters.

According to Torrent et al. [TBGS07], the proportion of soils falling into high P classes was generally great and has consistently increased from 1980 until recent years. A great effort is being made to reduce the inputs of some fertilizers, to avoid over-enrichment and to achieve more sustainable practices of land use. One of the goals of P variable rate applications is to have adequate levels of P in the field, improving its efficiency [SPdS⁺10].

Potassium in soils is mainly in the following mineral forms: a) structural K of minerals; b) fixed K or interlayer K (fixed in 2:1 layer clay minerals, such as illite and montmorillonite); c) exchangeable K; and d) K in soil solution [San95]. These forms constitute a dynamic system in equilibrium with a reversible transfer between them but only a minor part of soil K is in solution.

The availability of K differs greatly with soil type and is affected by physico-chemical properties of the soil [JK08]. When K fertilizer is applied to a soil, K enters in the soil solution and then equilibrates the different K mineral forms depending, mainly, on the amount and type of clay, the total cation exchange capacity, and soil pH [AEJ04, San95, SSS14, Sha90].

Like other nutrients, K in the soil solution is directly taken by plants, but is also easily dragged by leaching because it has no chemical retention [San95]. However, K in the soil solution represents a very small fraction of the total K in soil and its leaching does not result directly in eutrophication (Alfaro et al. 2004; Santos 1995). [AJG04, San95]. Alfaro et al. (2004) showed that the amount of potassium leaching losses was related to the soil type, but the chemistry of the soil was not as important as its hydrology in controlling the dynamics of K leaching.

According to Jalali et al. (2008) the movement of K in soil is markedly affected by the extent of sorption by soil. These authors found a significant relationship between K leaching and simple measurements of exchangeable K. Therefore, such relationships can provide useful estimates of leaching and thus aid in the control of losses.

Although K is little dragged by leaching in well supplied colloids soils, K over-fertilization can lead to nutritional imbalances with other cations, reducing the absorption of Ca and Mg (ionic antagonism).

Therefore it should be avoided excess K levels in soil and it should be included agricultural practices that enhance the efficiency of nutrient conversion and reduce the losses, e.g. using site-specific management.

The within-field P and K spatial variation is a key issue for minimizing fertilization costs and reducing P eutrophication risks.

This study aims to improve the economic, agronomic and environmental efficiency of maize production based

on: i) the maize international market price fluctuations; ii) the yield level from which profit can be generated (break-even yield); and iii) the yield/input ratio. The article focus is on phosphorous, but the same methodology can be adopted for other crop inputs, such as potassium, water, etc.

5.2 Materials and methods

5.2.1 Study field

The investigated field has 56.5 ha and is located in the “Herdade de Cego” farm near Fronteira (Lat: +39.09307; Long: -7.611332) in the Alentejo region of southern Portugal. The climate of this area is typically Mediterranean (Csa climate according to the Koppen classification). The average annual rainfall is 600 mm (20 years), with a hot dry season from June to September with maximum temperatures that occasionally exceed 40°C. The winters are mild, with minimum temperatures rarely below 0°C.

The field predominant soils are classified as Luvisols and Vertisols [FAO14]. The farmer used a reduced tillage system involving a small subsoiler (300 mm in depth) prior to sowing.

The considered yield years were 2002, 2004 and 2007, and maize was sown in late April/early May and harvested in September/October. Because maize is grown under irrigation, year-to-year yield variation should not occur based on water availability.

A CLAAS LEXION 450 combine harvester (produced by CLAAS, Harsewinkel, Germany) was used and was equipped with a combine electronic board information system (CEBIS), providing instantaneous yield and grain moisture data with less than 5% error. The combine harvester was equipped with a 6 m cutting header; a differential GPS Pilot; a grain photoelectric sensing (the magnitude of signal of the light receptor is used to determine the flow rate of the grain); and a grain moisture sensor (by sensing the dielectric properties of the harvested grain), which were near the top of the clean grain elevator. The yield data were cleaned to remove errors as described in Blackmore and Moore [BM99] (see subsection 3.2.1), and the weight of the collected grain was adjusted for grain moisture (140 g kg⁻¹ of moisture).

5.2.2 Digital elevation model

Elevation data collected by a “Trimble RTK/PP-4700” global position system (GPS) were used for a topographical survey of the irrigated area. The track points were collected approximately every 5 m, with 5 m spacing between swaths and an accuracy of ±2 cm vertically and horizontally. An irregular network of triangles (TIN) was calculated on the basis of the point data. A digital elevation model (DEM) was generated on a 6 m grid from point elevations using the 3D Analyst extension in the ArcGis software. Terrain attributes, such as elevation and slope, were calculated from the DEM using ArcGis 9.3. The altitude varies from 196 m to 230 m and the slope from 0 to 22% (Fig. 5.1a).

5.2.3 Apparent soil electrical conductivity measurements (EC_a survey)

The apparent soil electrical conductivity (EC_a) was measured using a Veris 2000XA Mapping System (Veris Technol., Salina, Kansas, US) equipped with a GPS receiver.

The (EC_a) sensor consisted of four aligned rotating coulter on a tool bar. The Veris 2000XA was attached to a farm tractor that crossed the field on bare soil at a speed of 10 km h⁻¹ along parallel tracks 10-15 m apart. The

coulter-electrodes penetrated the soil surface approximately 6 cm. Geo-referenced data points were logged every second (approximately 3 m of travel), and the assumed depth for conductivity measured with the coulter was 0.60 m (Veris Technol., Salina, Kansas, US). Data with negative values and data with the same coordinates were removed because they indicate poor soil-sensor contact and sensor immobilization, respectively. Measurements were made in autumn, and the moisture content varied from 17.8% to 19.3%. A EC_a surface (Fig. 4.1b) with 6 m resolution grid was obtained considering an ordinary kriging interpolation and the variogram structural properties (Table 4.1).

5.2.4 Soil sampling and laboratory procedures

Before the spring-summer crops and basal fertilization, 120 soil samples were taken at a depth of 0-20 cm (Fig. 5.1a).

Ten strata were selected for soil sampling based on the stratified sampling strategies of Hirzel and Guisan [HG02]. The strata were built from three sources of spatial information: soil apparent electrical conductivity (EC_a); elevation and yield.

Equal-stratified sampling was used, with each stratum having twelve sampling points. For each stratum, the 12 points were randomly generated, with a minimum distance of 3 m between the sampling points (Fig. 5.1a). Based on these procedures, performed with the ArcGIS 9.3 software (ESRI, Redlands, USA [ESR09]), soil samples were collected with a mechanical probe.

At each of the sampling points, a composite (1 Kg) sample was obtained by mixing four subsample soil cores within 2-3 m around the designated sampling point of the topsoil (0-20 cm). The core samples were dried under forced air at 35°C for 48 hours, and stones and debris were removed and sieved through a 2 mm mesh sieve before analyses.

The collected soil samples were analysed for bioavailable phosphorus ($mg(P_2O_5) Kg^{-1}$) and potassium ($mg(K_2O) Kg^{-1}$) by the Égner-Riehm method.

5.2.5 Data analysis

The summary statistics for yield grain maize, phosphorus and potassium were calculated to detect the presence of global outliers and trends and to describe the variation of the yield in the three considered years using SPSS software (IBM Corp., Armonk, New York, USA [IBM10]).

Data normality was tested by skewness and kurtosis after taking into account the normal distribution of data when the skewness ranges between -1 and 1 [Oli10, PdJBBA14, KMKP06].

Local outliers were eliminated by considering the Voronoi analysis (ArcGISTM: Geostatistical Analyst tool; (ESRI, Redlands, USA[ESR09]). The cluster method was used to identify those cells that are dissimilar to their surrounding neighbours. When a cluster equalled -1, it was considered to be a local outlier [ESR09].

The maize yield spatial structural analysis, soil properties and EC_a were performed using the SpaceStatTM software (BioMedware, Ann Arbor, USA [Bio12]) and ArcGISTM: Geostatistical Analyst (ESRI, Redlands, USA[ESR09]). The trend analysis tool in Arcmap was used to explore the global trends in the data. The trends were analysed based on the direction and the order of the line that fitted the trend. The yield data revealed no trend or isotropic behaviour [IS89, Oli10]. Phosphorus (P) and potassium (K) showed a quadratic trend removed by second-order polynomials [JVKL03].

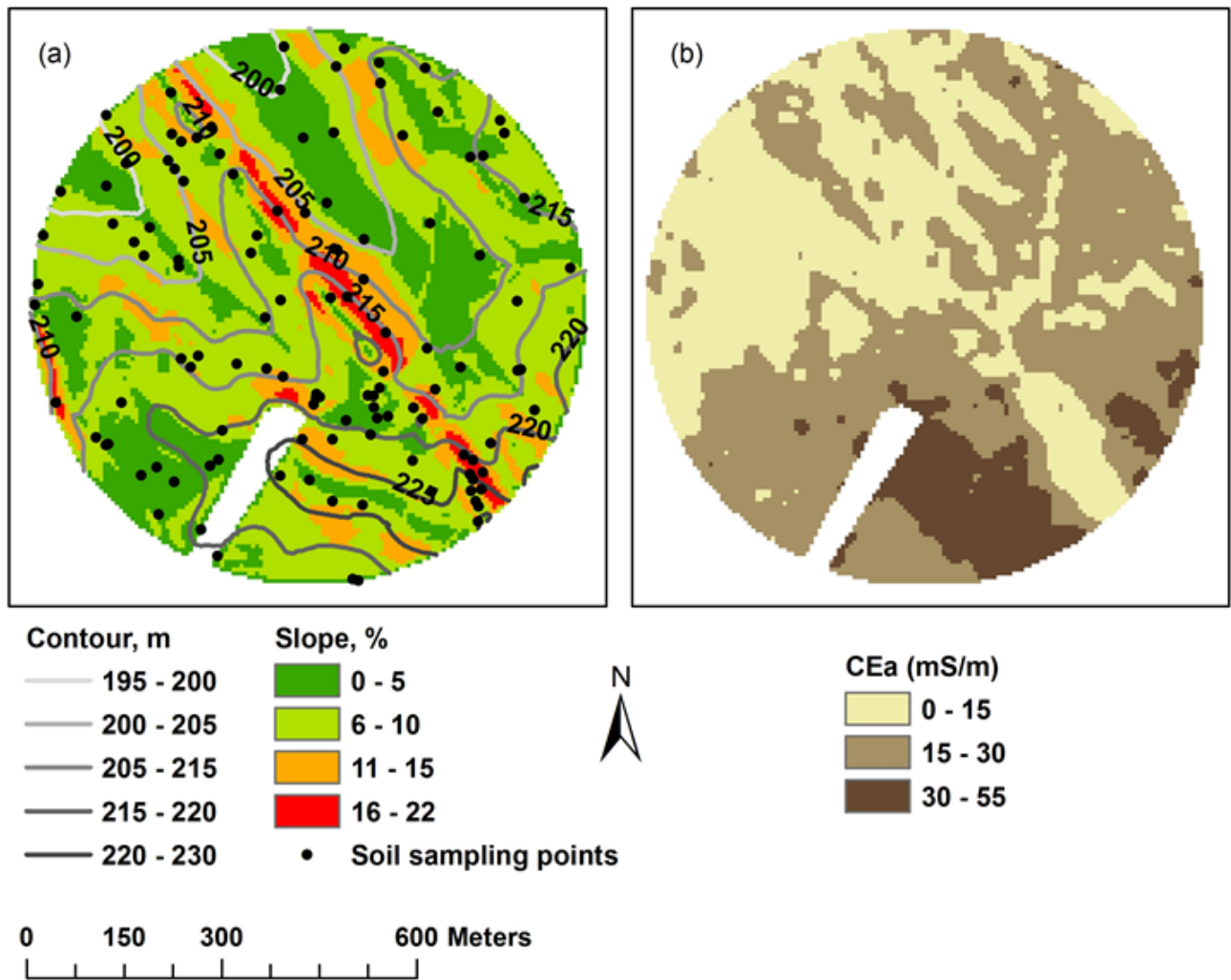


Figure 5.1: (a) Digital elevation model (DEM): contour, slope and soil sampling points; (b) EC_a spatial distributionm.

The experimental omnidirectional variograms were calculated to determinate how samples were related to each other in space using Matheron's equation [Oli10]. The experimental omnidirectional variograms were fitted to standard models to capture the main characteristics of maize productivity and soil properties [Goo98b, Goo99, Oli10]. This was accomplished by minimizing the weighted sum of squares (WSS) of the differences between the experimental and theoretical variogram models and considering the study area and prior knowledge [Goo99]. Following cross-validation statistics, the choice of the best model was based on the lowest root mean square error [ESR09, IS89].

Spatial yield and potassium variation were characterized by spherical models (2 structures) and phosphorus and EC_a variation by exponential models (Table 5.1). The interpolation of the considered variables was performed by ordinary kriging in a 6 m x 6 m grid, and all maps were drawn using ArcGISTM: Spatial/3D analyst tools (ESRI, Redlands, USA [ESR09]). The spatial dependence was calculated with spatial class ratios that were similar to those that were presented in previous work [CMP⁺94].

Table 5.1: Phosphorus, potassium, apparent soil electrical conductivity and yield of 2007 data variogram parameters.

Variable	Lag (m)	Nr. Lags	Model	Nugget Effect Co	Sill	Range (m)	SD ¹ (%)	SDD ²
Phosphorus	25	10	Exponential	650	2200	159	22.8	Strong
Potassium	25	8	Exponential	985	2980	65	24.8	Strong
CEa	2	30	Exponential	5.9	36.5	102	13.9	Strong
Yield 2007	6	40	Spherical	0.37	0.429	49.6	34.3	Mod
					0.41	313.1		

¹SD=Spatial Dependence (Co/Co+C): (SD<25%=strong spatial dependency (Strong); SD between 25 and 75%=moderate spatial dependence (Mod.); SD>75% weak spatial dependence; SD≈ 100%= random); ²SDD=Spatial dependence degree (Cambardella et al. 1994); ECa apparent soil electrical conductivity

The yield temporal variance at a specific field point [BGF03] for the three analysed years was calculated considering the following equation equation [BGF03, MS06]:

$$\delta_i^2 = \frac{\sum_{i=2}^{i=n} (Y_{t,i} - \bar{Y}_t)^2}{n} \quad (5.1)$$

Where δ_i^2 is the yield temporal variance at a specific field point i ; t is time in years (2002-2004-2007); $Y_{t,i}$ is the yield for year t at point i ; n is the number of observed years; and \bar{Y}_t is the mean yield for the whole field for years n .

From the temporal variance, the standard temporal deviation has been estimated. The low values of the standard temporal deviation indicate areas of the field where the yield changes little over time [BGF03]. These results allow one to build a standard temporal deviation map (Fig. 5.2b).

5.2.6 Yield/input ratio

The ratio between yield and inputs of phosphorus (P_{yr}) and potassium (K_{yr}) is the ratio of the productivity of the previous year and the concentration of the nutrient in the soil before the new crop cycle. This aids in determining which parts of the field have the greatest productivity per unit of available nutrient. The yield/input ratio and yield data can be brought together to optimize field nutrition.

As an example (case study), the yield/phosphorus (P_{yr}) and yield/potassium (K_{yr}) ratios were calculated considering the 2007 yield as follows: 2007 yield ($t\ ha^{-1}$)/soil nutrient concentration ($mg\ Kg^{-1}$).

5.2.7 Crop budget

The maize production costs (without amortizations) were $1890\ \text{€}\ ha^{-1}$ (2015 prices) based on the farm crop management structure under study (see supplementary material - Appendix B). The break-even yield was calculated considering the previous crop costs and an expected maize price of $175\ \text{€}\ t^{-1}$ (2015 prices). The break-even yield was $10.77\ t\ ha^{-1}$: this indicates the yield level from which we can generate profit, i.e., the point at which expenses and revenue are equal.

5.3 Results

5.3.1 Productivity maps of P and K

In the study field (Fig. 5.1), a variable average yield distribution was observed in space and time (Fig. 5.2a). Some areas were more temporally stable than others, characterized by a temporal standard deviation from 0.1 to $9.3\ t\ ha^{-1}$ (Fig. 5.2b). Considering the average yield of the three studied years (2002, 2004 and 2007), the minimum and maximum yield varied between 0.5 and $20\ t\ ha^{-1}$. However, the field average yield was similar in the three considered years (average $\approx 12.5\ t\ ha^{-1}$), (Table 5.2; Fig. 5.2a).

The field spatial and temporal yield variability induces differential soil nutrient extraction and consequently differential soil nutrient concentrations for regular field fertilization; sometimes, more productive places are less fertile in terms of the soil nutrient concentrations.

The experimental field soil phosphorus and potassium bioavailability changes in space (Fig. 5.3a and 5.3b), and this can be the result of: i) geological and pedological complex processes; ii) differential nutrient extractions, mentioned above; or iii) differential nutrient immobilization depending on the soil type and its constituents [AEO03, BJPG03, Sha95, WEF01].

The average soil P and K contents were, respectively $119\ mg\ Kg^{-1}$ and $135\ mg\ Kg^{-1}$, with P ranging from $36\ mg\ Kg^{-1}$ to $266\ mg\ Kg^{-1}$ (standard deviation: $\sigma_P=32\ mg\ Kg^{-1}$) and potassium ranging from $48\ mg\ Kg^{-1}$ to $425\ mg\ Kg^{-1}$ (standard deviation: $\sigma_K=36\ mg\ Kg^{-1}$). As mentioned above, this high P and K spatial variability (Figs. 5.3a and 5.3b) likely results from P and K differential extractions (see Fig. 5.2a for different potential extractions) that are not compensated for with many years of fertilizing uniformly.

Given the above and assuming the fertilizers' optimization, two types of information were considered to calculate differential fertilization maps: i) a yield map (in this particular example the 2007 yield map was considered, rather similar to the yield average map in Fig. 5.2a); and ii) a bioavailability inputs map (e.g., Figs. 5.3a and 5.3b), which in this case was obtained with the methodology described in subchapter 5.2.5.

Table 5.2: Grain yield summary statistics for the Azarento field.

Year	Mean t ha ⁻¹	Standard deviation t ha ⁻¹	Minimum t ha ⁻¹	Maximum t ha ⁻¹	Coefficient of variation	Skewness
2002	12.57	4.966	0.505	20.2	0.395	-0.292
2004	12.66	3.833	0.506	19.9	0.303	-0.664
2007	12.55	3.582	0.503	19.6	0.285	-0.464

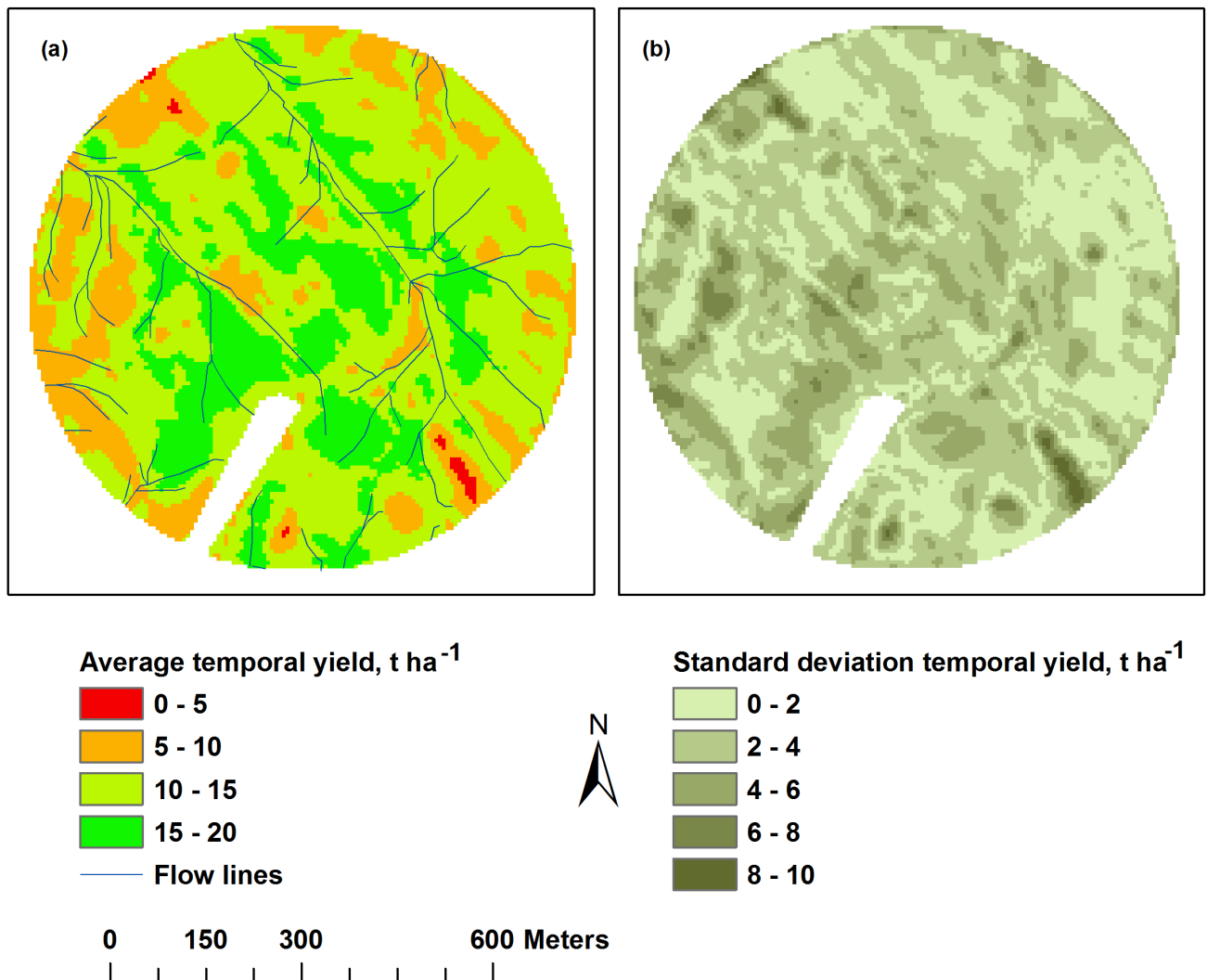


Figure 5.2: Maize yield spatial statistics: (a) yield average and (b) yield standard deviation.

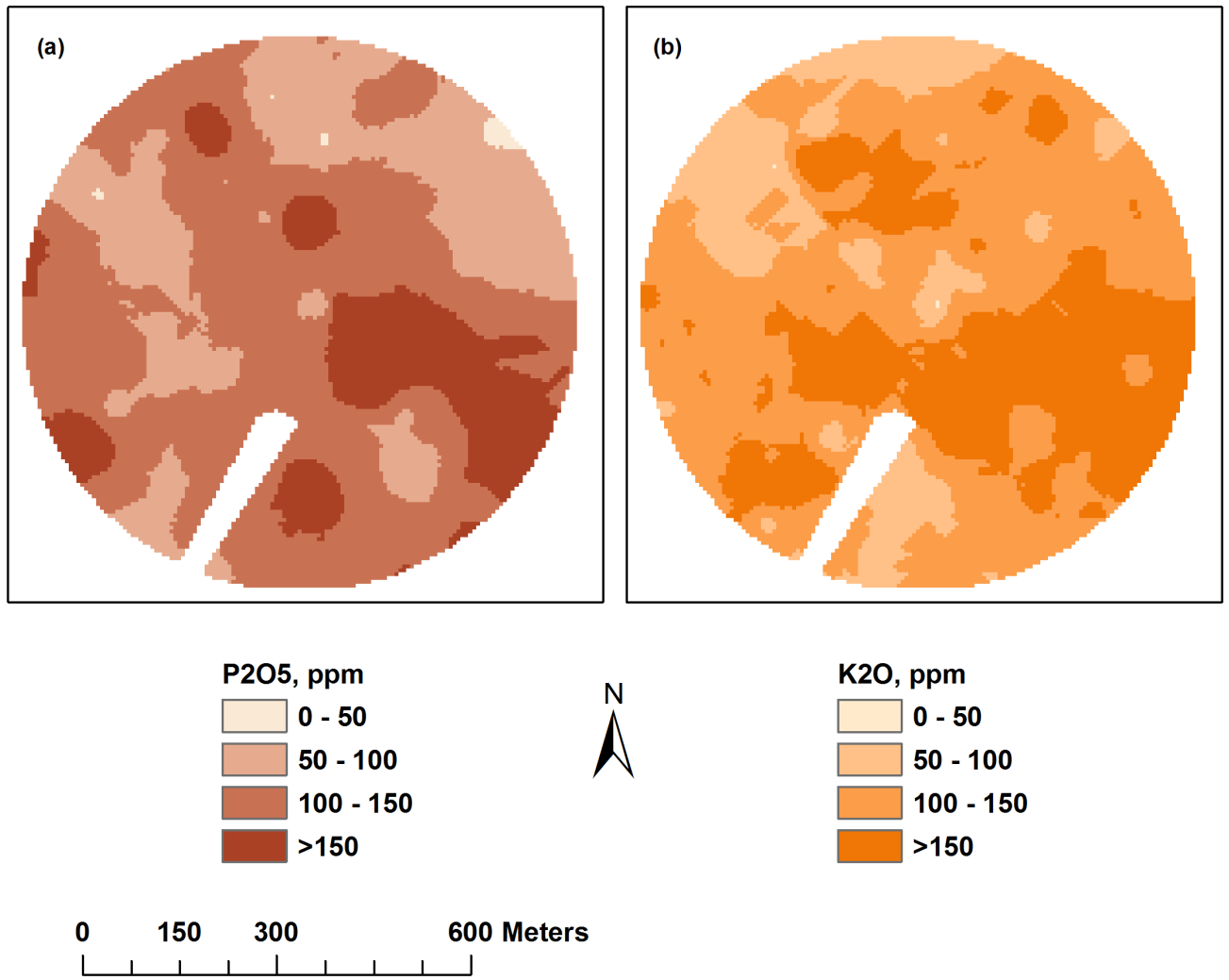


Figure 5.3: The soil (a) phosphorus and (b) potassium spatial distribution.

5.3.2 Yield/nutrient input ratio of phosphorus and potassium

Considering a yield map (e.g., 2007 yield) and the available nutrients map from the experimental field (e.g., Figs. 5.3a and 5.3b), it is possible to calculate the ratio between yield and phosphorus (P_{yr} , $t\ ha^{-1}\ (mg\ Kg^{-1})^{-1}$, Fig.5.4a) and the ratio between yield and potassium (K_{yr} , $t\ ha^{-1}\ (mg\ Kg^{-1})^{-1}$, Fig. 5.4b), dividing the yield by the inputs availability.

With the yield/P and yield/K ratios, it is possible to understand which field areas have higher yield returns per unit of inputs availability and thus understand if the differential allocation of nutrients can be managed more efficiently when considering the desired productivity and the soil richness inputs threshold.

Figures 5.2, 5.3 and 5.4 show that the same yield/input ratio can be achieved with different yield and soil inputs concentration levels. In view of the above, it was considered relevant to calculate the 2015 break-even of the field, i.e., the productivity from which there is a positive net income, which in this particular case, given the assumptions presented in chapter 5.2, is $10.77\ t\ ha^{-1}$.

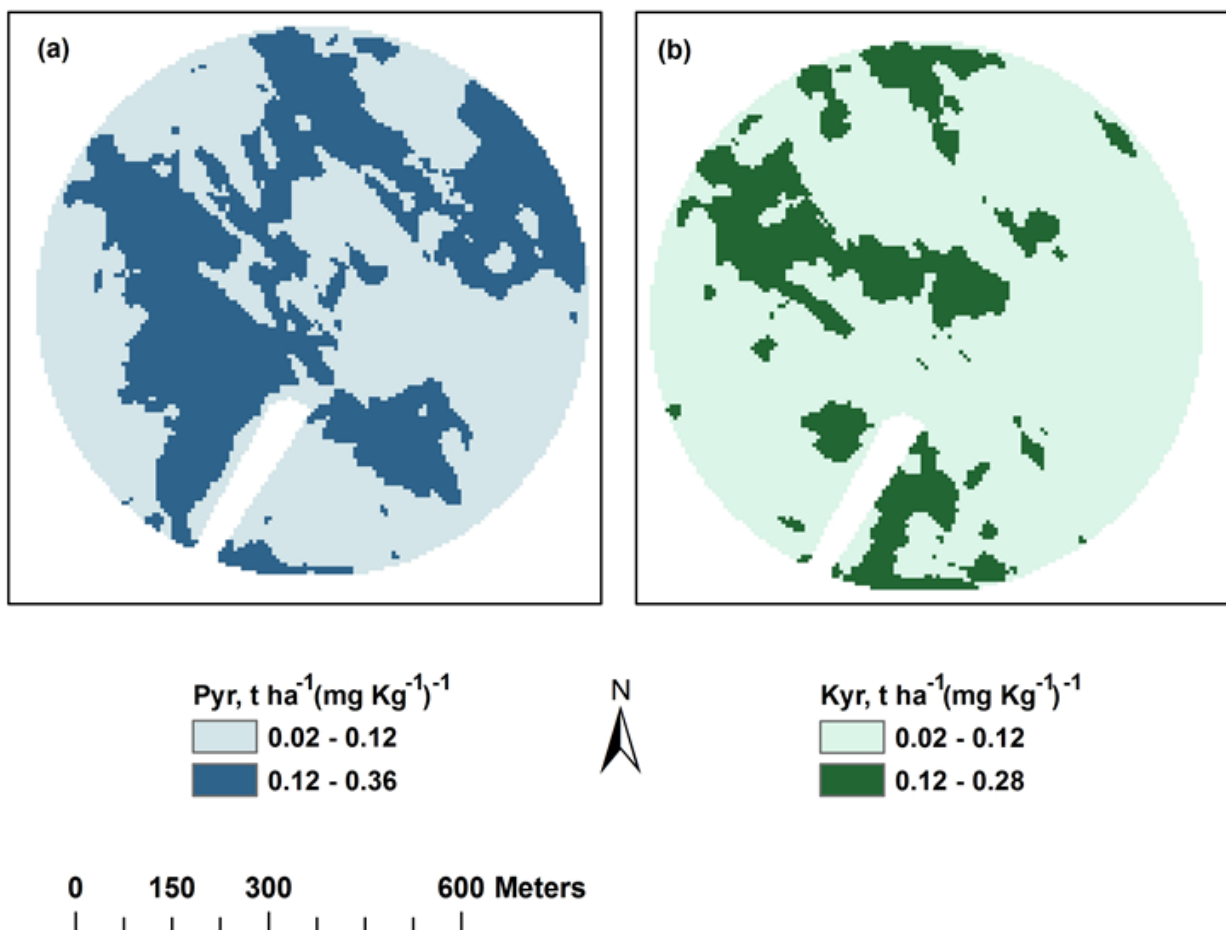


Figure 5.4: Spatial distribution of the yield/input ratio of (a) phosphorus (P_{yr}) and (b) potassium (K_{yr}).

Considering the above, the experimental field was divided in 5 zones that were obtained by considering the yield surface and the yield/input ratio surface. A threshold value of $0.12\ t\ ha^{-1}\ (mg\ Kg^{-1})^{-1}$ was used to consider a good yield, and the nutrient soil concentration threshold values (P and K) were $18\ t\ ha^{-1}$ and $150\ mg\ Kg^{-1}$

respectively. The following example is focused on P, but the same procedure can be used for any other input.

Zone 1 – field cells with yields below the break-even and with yield/input ratio below 0.12 t ha⁻¹ (mg Kg⁻¹)⁻¹.

Zone 1 represents approximately 23% of the field, and it is characterized by low yield values (mean ≈ 9 t ha⁻¹) and high values of bioavailable phosphorus (Figs. 5.3a, 5.4a and 5.5; Table 5.3). On average, the P content was 125 mg Kg⁻¹, ranging between 60 and 266 mg Kg⁻¹ (Table 5.3). For this field region and for K, the average concentration was 129 mg Kg⁻¹, ranging between 48 and 319 mg Kg⁻¹ (Fig. 5.3b; Table 5.4). The average richness levels of P and K in this particular region made it possible to conclude that the limiting yield factor may not be associated with their soil availability but rather with other yield-controlling factors, such as irrigation.

Zone 2 – field cells with yields below the break-even and with yield/input ratio above 0.12 t ha⁻¹ (mg Kg⁻¹)⁻¹.

Zone 2 represents approximately 2.95% of the field, and it is characterized by low productivity values (mean ≈ 10 t ha⁻¹) and low values of bioavailable phosphorus (Figs. 5.3a, 5.4a, and 5.5; Table 5.3). This area shows, respectively, a P and K average concentration of 70 mg Kg⁻¹ and 112 mg Kg⁻¹ (Figs. 5.3a and 5.3b; Tables 5.3 and 5.4). Any positive change in the price of maize (lowering of the break-even line) can result in a marked decrease of this area or even in its extinction.

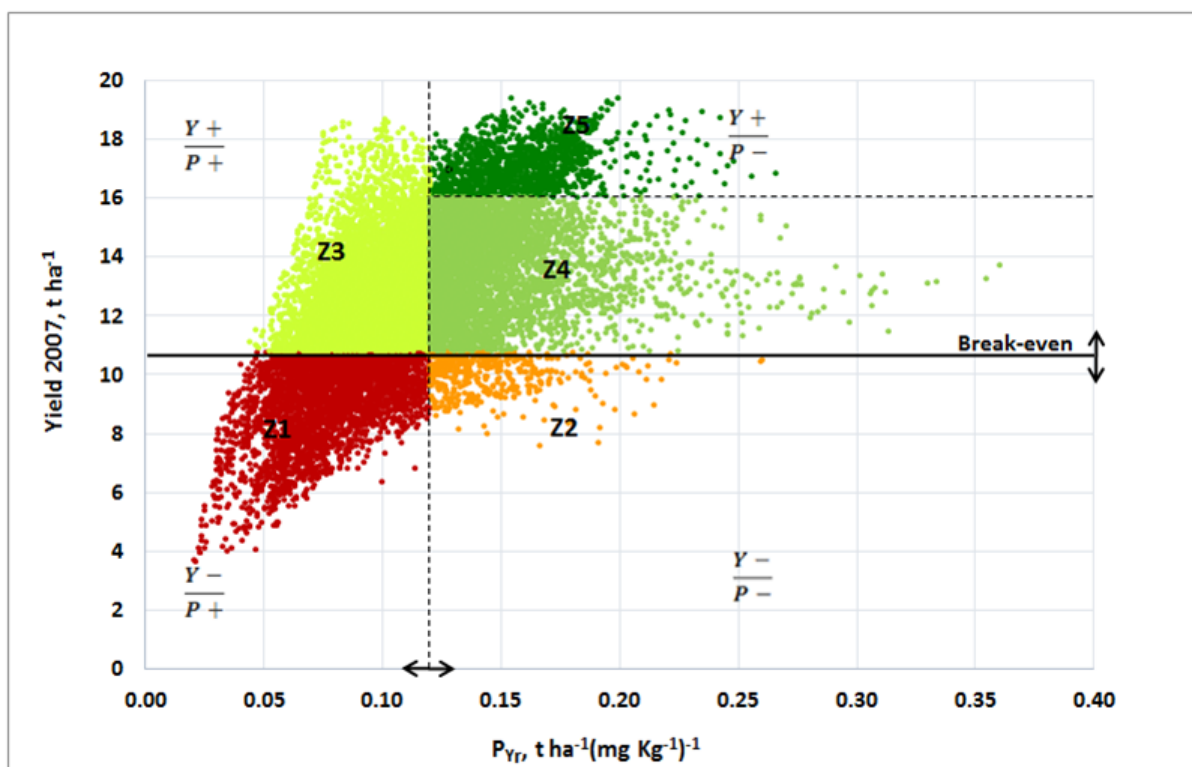


Figure 5.5: Yield/phosphorus ratio zones (Z1, Z2, Z3, Z4 and Z5) according the 2007 maize yield; (Y+ higher yield; Y- lower yield; P+ higher phosphorus soil concentration; P- lower phosphorus soil concentration).

Zone 3 – field cells with yields above the break-even and with yield/input ratio below 0.12 t ha⁻¹(mg Kg⁻¹)⁻¹.

Zone 3 represents approximately 36.78% of the field, and it is characterized by medium to high productivity values (average ≈ 13 t ha⁻¹) (Figs. 5.2a, 5.5; Table 5.2). The average contents of bioavailable P and K in the soil were identical, approximately 141 mg Kg⁻¹ (Figs. 5.3a and 5.3b; Tables 5.2 and 5.3), but with different standard deviations ($\sigma_P=26.76$ mg Kg⁻¹ and $\sigma_K=39.51$ mg Kg⁻¹). However, in general, the levels of these nutrients were high, and only in rare cases were the concentrations slightly less than 100 mg Kg⁻¹, causing the yield/P and yield/K low ratios.

Zone 4 and 5 – field cells with yields above the break-even and with yield/input ratio above 0.12 t ha⁻¹(mg Kg⁻¹)⁻¹.

Zones 4 and 5 represent approximately 37.09% (Z4=28.35%; Z5=7.84%) of the field and are characterized by productivity values between 10.77 and 16 t ha⁻¹ in Z4 and above 16 t ha⁻¹ in Z5 (Figs. 5.2a and 5.5; Tables 5.3 and 5.4).

Although on average the phosphorus contents differ little between the two zones (Z4 ≈ 95 mg Kg⁻¹; Z5 ≈ 110 mg Kg⁻¹, (Fig. 5.3a; Table 5.3)), there were a larger number of sites in Z4, particularly those with lower yield, that recorded levels of P always less than 100 mg Kg⁻¹.

For K values, there were on average higher values in Z5 (150 mg Kg⁻¹) than in Z4 (129 mg Kg⁻¹), and while the Z4 lowest values of K always followed the lowest P values, the same did not occur in Z5 (Fig. 5.3b; Table 5.4). In Z4, the lowest values of P and K were mainly in the places of lower productivity.

The Z4 and Z5 zones showed high yield/input ratios because there were low nutrient contents in the soil when compared with the Z3 zone (Figs. 5.4a and 5.5; Table 5.3).

Table 5.3: Soil P levels and yield/P ratio according to Z1, Z2, Z3, Z4 and Z5 zones.

Zone	Yield	Area	Yield	Min.	Max.	Aver.	Min.	Max.	Aver.
			Average	P	P	P	P _{yr}	P _{yr}	P _{yr}
	t ha ⁻¹	% (ha)	t ha ⁻¹	mg Kg ⁻¹	mg Kg ⁻¹	mg Kg ⁻¹	*	*	*
Z1	<10.77	23.18 (13.10)	9.09	60	266	125	0.020	0.120	0.077
Z2	<10.77	2.95 (1.67)	10.00	40	89	70	0.120	0.260	0.145
Z3	>10.77	36.78 (20.79)	13.03	91	251	140	0.044	0.120	0.095
Z4	>10.7 and <16	28.35 (16.03)	13.63	36	133	94	0.120	0.360	0.148
Z5	>16	8.74 (4.94)	17.10	63	148	110	0.120	0.266	0.158

Min. minimum; Max. maximum; Aver. average; P_{yr} yield/P ratio; *t ha⁻¹ (mg Kg⁻¹)⁻¹

Table 5.4: Soil K levels and yield/K ratio according to Z1, Z2, Z3, Z4 and Z5 zones.

Zone	Yield t ha ⁻¹	Area % (ha)	Yield Average t ha ⁻¹	Min. K mg Kg ⁻¹	Max. K mg Kg ⁻¹	Aver. K mg Kg ⁻¹	Min. K _{yr} *	Max. K _{yr} *	Aver. K _{yr} *
Z1	<10.77	23.18 (13.10)	9.09	48	319	129	0.024	0.218	0.075
Z2	<10.77	2.95 (1.67)	10.00	49	163	112	0.057	0.206	0.093
Z3	>10.77	36.78 (20.79)	13.03	51	425	142	0.030	0.224	0.098
Z4	>10.7 and <16	28.35 (16.03)	13.63	51	293	129	0.050	0.284	0.113
Z5	>16	8.74 (4.94)	17.10	62	277	150	0.058	0.270	0.119

Min. minimum; Max. maximum; Aver. average; (K_{yr} yield/K ratio; *t ha⁻¹ (mg Kg⁻¹)⁻¹

5.4 Discussion

5.4.1 Differential fertilization - decision making

As seen in Fig. 5.5 (e.g., Z1, Z2, Z3, Z4 e Z5), it is possible to infer that the form and size of these areas can be different every year either by the movement of the break-even line (parallel to the X-axis) or by the movement of the line that defines the yield/input ratio threshold determined by the farm manager (parallel to the Y-axis). The break-even line can move depending upon the maize price and/or changes in the production costs, and the yield/input ratio threshold line can be moved depending on the market risk, including the economic contingency of the company and the changing yield/input ratio technical requirements.

As an example and considering a fixed cost structure, one may say that the threshold break-even line falls when the price of maize goes up (more areas have positive net income) or the threshold line rises when the price of maize goes down (fewer areas have positive net income) (Fig.5.5). The yield/input ratio threshold line will move more to the right if the market risk is higher and the financial availability of the company is smaller, and the opposite is also true.

Normally, the farm manager faces two extreme situations from the standpoint of maize production cycles: i) low international maize price; ii) and high international maize price.

Maize low International prices

When the farm manager must make decisions about P and K fertilization opportunities in a cost-cutting situation, he should consider the following: (1) first, it is important to determine whether both nutrients have the same yield/input ratio, and this is achieved considering the results of Fig. 5.6. This figure shows that the yield/input ratios of P and K in this field are very similar (points almost equally distributed above and below the unit slope line). However, if there were a greater number of points on the quadrant of yield/P when compared to yield/K (Fig. 5.6), then the farm manager could consider fertilizing only with P in a cost reduction perspective; and (2) after deciding which macro-nutrient or macro nutrients he should use, it is essential to look at Fig. 5.5 (P example). In this figure, it is possible to realize that the fertilization areas, in a cost-cutting situation, are the areas that have higher yield/input ratios and are above the break-even line; in short, they are like the Z4 and Z5 zones.

High international price of maize

When the farm manager must make decisions about P and K fertilization opportunities in a favourable price situation, he must consider the same methodology presented above to be efficient, but at the same time he can take additional risks to maximize yield. In this particular situation, the farm manager could consider fertilizing Z3, Z4 and Z5 zones. He could also consider fertilizing Z2 and Z1 zones (in this order); however, these zones have yield-controlling factors that are independent from nutrients, and while they are not controlled, it is environmentally and economically unreasonable to fertilize them.

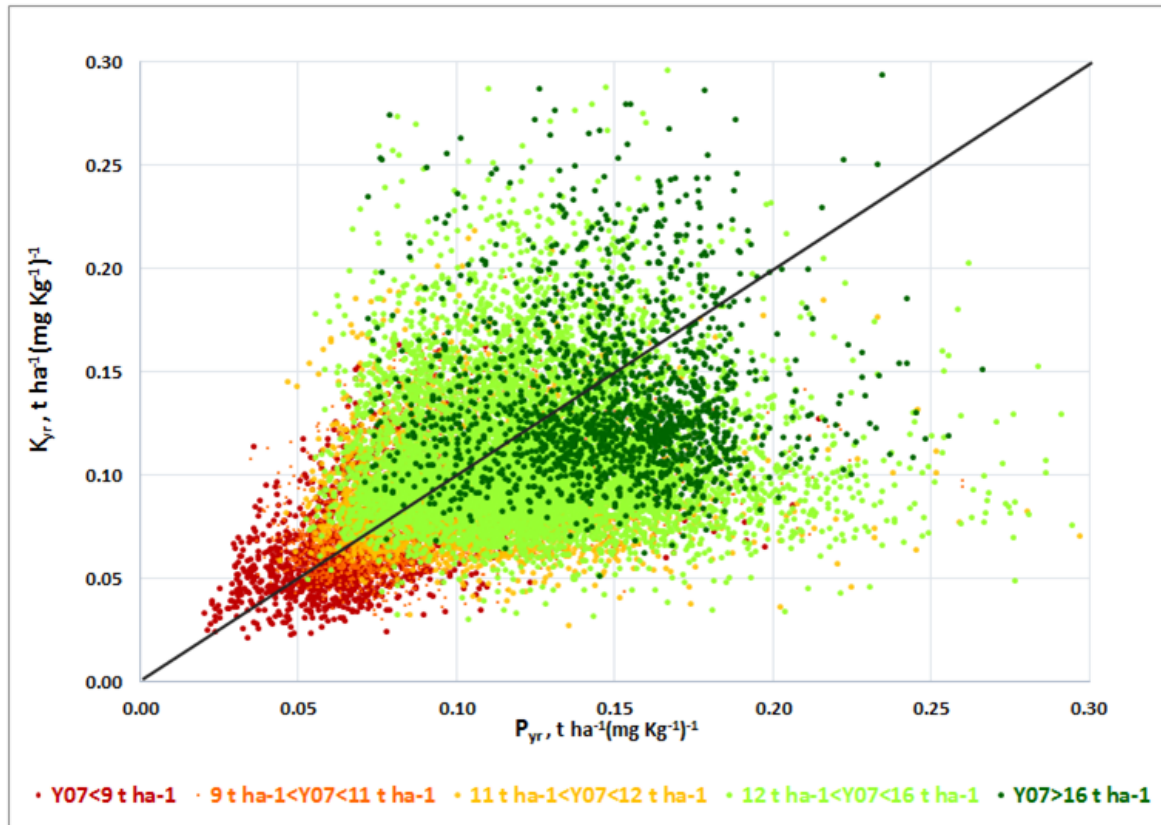


Figure 5.6: One-to-one straight line comparison between yield/phosphorus ratio (P_{yr}) and yield/potassium ratio (K_{yr}).

5.4.2 Differential fertilization - economic aspects

To realize the economic impact that a differential fertilization strategy would have in this particular field, it is necessary to consider the following assumptions:

- (1) the farm manager will fertilize with P and K;
- (2) the Z1 zone ($\approx 23\%$ of the field area) is not fertilized because it is under the break-even; presents medium to very high soil bioavailable P and K contents, and it is susceptible to other yield controls (Fig. 5.7; Tables 5.3 and 5.4);
- (3) the Z2 zone ($\approx 2.95\%$ of the field area) is not fertilized because it is under the break-even and it is susceptible

to other yield controls (Fig. 5.7);

(4) the Z3 zone fertilization ($\approx 37\%$ of the area of the field), when performed, is always with the objective of maintaining the soil fertility level, which here is relatively high. For this particular zone, an expected average yield of approximately 13 t ha^{-1} was considered (Fig. 5.7; Tables 5.3 and 5.4);

(5) the Z4 ($\approx 28.35\%$ of the area of the field) and the Z5 ($\approx 8.74\%$ of the area of the field) zone fertilizations considered their average production potentials, which were, respectively 13.6 t ha^{-1} and 17 t ha^{-1} (Fig. 5.7; Tables 5.3 and 5.4).

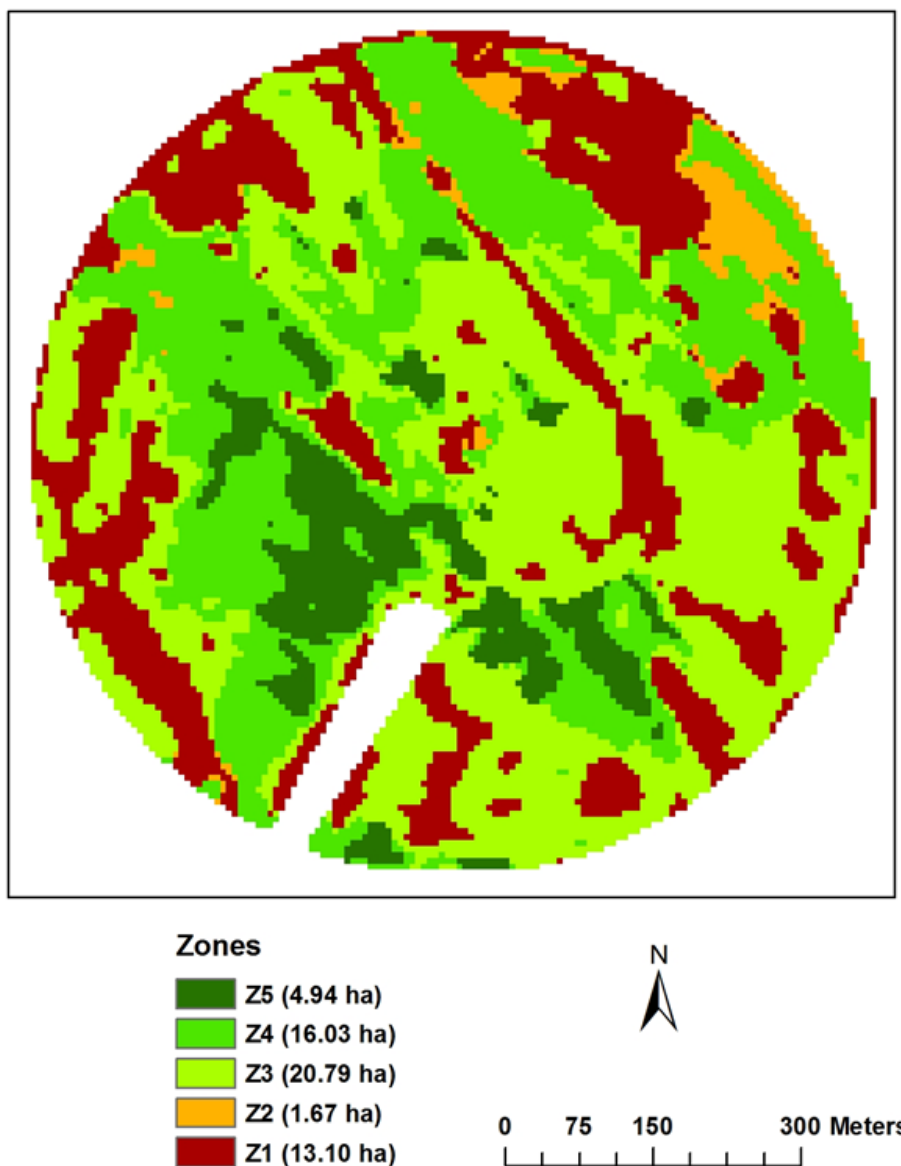


Figure 5.7: Management zones (Z1, Z2, Z3, Z4 and Z5) according to the 2007 maize yield and yield/input ratio of $0.12 \text{ t ha}^{-1} (\text{mg Kg}^{-1})^{-1}$.

The following scenarios were also considered:

Scenario 1 (S_1) - based on the farm manager's normal strategy, a P and K constant and uniform application

based on a yield target average of approximately 15 t ha^{-1} was considered. This scenario was considered as the reference scenario;

Scenario 2 (S_2) - In all aspects similar to scenario 1; however, the yield target average was considered to be 12.6 t ha^{-1} , the real field multi-annual average productivity;

Scenario 3 (S_3) - considering a variable rate application of P and K to maximize production (maize high price) and return, thus fertilizing zones Z3, Z4 and Z5 (Fig. 4.7). The particular zones' average yield were considered as the target yield for these particular zones ($Z3=13.03 \text{ t ha}^{-1}$, $Z4=13.63 \text{ t ha}^{-1}$ and $Z5=17.10 \text{ t ha}^{-1}$);

Scenario 4 (S_4) - considering a variable rate application of P and K to minimize costs (maize low price) and maximize return, thus fertilizing zones Z4 and Z5 (Fig. 4.7) with the following yield targets: $Z4=13.63 \text{ t ha}^{-1}$ and $Z5=17.10 \text{ t ha}^{-1}$, the average yield for these particular zones.

Scenario 1 showed high fertilization costs (15263 €, Table 5.5) that reflect an excessive fertilization (Table 5.6) driven by an average target yield above the real yield temporal average. The nutrients distribution is conducted in a constant and uniform way, and because of that it is agronomically (Z1 and Z3), economically (Z1 and Z2) and environmentally (Z1, Z2 and Z3) inefficient (Table 5.6). These inefficient phosphate applications are the main cause of their accumulation in agricultural soils [MM02], promoting P diffusive pollution [Sha95, WEF01] and leading in most cases to eutrophication processes [MM02].

In scenario 2, the fertilization costs fell 59% (6218 €, Table 5.5), as did the amount of applied nutrients (Table 5.6). Despite the amendment in relation to scenario 1 (yield target close to the yield average of the field), the nutrients distribution continues to be conducted in a constant and uniform way and is therefore agronomically, economically and environmentally inefficient (Table 5.6).

In scenario 3, the costs were reduced when compared to the reference scenario (S_1) by approximately 61% (5932 €, Table 5.5), despite the fact that the number of fertilizer units was increased (Table 5.6) in the Z3, Z4 and Z5 zones compared to the same zones of scenario 2. In short, scenario 3 would approximately reach the fertilization costs of scenario 2 but would be agronomically and environmentally more efficient.

In scenario 4, the scenario with a low maize prices situation, only Z4 and Z5 zones are fertilized (Tables 5.5 and 5.6). This strategy would reduce field fertilization costs by approximately 73% (4051 €, Table 5.5) when compared to scenario 1 (S_1), increasing the economic, agronomic and environmental inputs' efficiency.

It could be argued that this fertilization strategy (Table 5.6), used for a long time, would decrease the field fertility level. This may not be possible because a nutrient soil reduction immediately promotes a yield/input ratio rise, causing the cells from Z3 areas to migrate to Z4 or Z5 (Fig. 5.5) areas, provided that they are above the break-even line.

The savings ($\approx 200 \text{ € ha}^{-1}$) presented in scenario 4 only consider the costs associated with P and K, but using the same methodology to improve nitrogen applications can significantly increase the savings.

5.5 Conclusions

The results of this study suggest the following: i) to optimize maize inputs and reduce economical risks, the following relevant information is needed: yield maps, input maps, costs associated with the activity and the expected maize price; ii) from previous information, it is possible to derive the yield/input ratios and the break-even productivity, setting up a differential fertilization strategy; iii) the best savings scenario ($\approx 200 \text{ € ha}^{-1}$) considered the differential fertilization in areas above the break-even productivity and above a yield/phosphorus ratio of $0.12 \text{ t ha}^{-1} (\text{mg Kg}^{-1})^{-1}$; and (iv) this differential fertilization strategy achieves the best economic, agronomic and environmental efficiency.

Table 5.5: Fertilization scenarios.

Scenarios	S ₁	S ₂	S ₃	S ₄
Zone (ha)	Average yield	Average yield	Average yield	Average yield
		t ha ⁻¹	t ha ⁻¹	t ha ⁻¹
Z1 (13.10)	15.00 (F)	12.60 (F)	9.09 (NF)	9.09 (NF)
Z2 (1.67)	15.00 (F)	12.60 (F)	10.00 (NF)	10.00 (NF)
Z3 (20.79)	15.00 (F)	12.60 (F)	13.03 (F)	13.03 (NF)
Z4 (16.03)	15.00 (F)	12.60 (F)	13.63 (F)	13.63 (F)
Z5 (4.94)	15.00 (F)	12.60 (F)	17.10 (F)	17.10 (F)
Fertilized area, ha	56.53	56.53	41.76	20.97
Total fertilizer costs, €	15263	6218	5932	4051
Fertilizer cost per ha, € ha ⁻¹	270	110	105	72
Cost reduction compared to S ₁ , %	0%	59%	61%	73%

NF not fertilized; F fertilized; S₁ scenario 1; S₂ scenario 2; S₃ scenario 3; S₄ scenario 4

Table 5.6: Fertilizer units applied in each scenario.

Zone	Scenario 1		Scenario 2		Scenario 3		Scenario 4	
	PFU	KFU	PFU	KFU	PFU	KFU	PFU	KFU
	(Kg ha ⁻¹)	(Kg ha ⁻¹)	(Kg ha ⁻¹)	(Kg ha ⁻¹)	(Kg ha ⁻¹)	(Kg ha ⁻¹)	(Kg ha ⁻¹)	(Kg ha ⁻¹)
Z1	135	90	37.5	55	-	-	-	-
Z2	135	90	37.5	55	-	-	-	-
Z3	135	90	37.5	55	22.5	54.0	-	-
Z4	135	90	37.5	55	71.3	77.5	71.3	77.5
Z5	135	90	37.5	55	97.5	107.0	97.5	107.0

PFU Phosphorus Fertilizer Units (P₂O₅); KFU Potassium Fertilizer Units (K₂O)

6

General Discussion, Future Work and Conclusions

6.1 General discussion

The ultimate goal of the agricultural production system is to be economically, environmentally and socially sustainable. This dissertation presents three different approaches used to determine yield and field variability, which can support management decisions within the framework of precision agriculture.

Crop yields are the integrated result of all of the factors that affect crop growth and productivity [DHB04], so the analysis of crop yields in space and time may provide useful information about which factors interact and how they influence crop yields. With this in mind, the principal component analysis (PCA) multivariate technique was used in the first study to extract information from two fields (Azarento and Bemposta) about the maize produced over a certain number of years. This study demonstrated that the use of PCA effectively identified spatial and temporal trends and assisted in the identification of areas with higher and lower risks to production. The analysis showed that the first (PC1) and second components (PC2) together accounted for 88.8% and 77.3% of the variance in the yield data from the Azarento and Bemposta fields, respectively. Although only a small

portion of these values relates to the variance explained by PC2 (11.9% in Azarento and 13.2% in Bemposta), this component was fundamental to the identification of the regions with different yields and possibly different management potentials.

The meaning of the PC2 values presented in the respective maps (Chapter 3) was better understood through the analysis and interpretation of the parabolic association between PC2 and the temporal standard deviation of the yield. The low and high PC2 values corresponding to low or high yields indicated areas with high temporal yield variability. These areas have a higher potential production risk, and as Diker et al. [DHB04] emphasized, special attention should be paid to them in the subsequent years to identify the yield-limiting factors and, if possible, amend the problem.

The areas with intermediate PC2 values (between 2 and 4) presented a low yield temporal standard deviation, which means that they were more stable over time. These results are consistent with those reported by Blackmore et al. [BGF03] and Marques da Silva [Mar06], who defined different zones based on yield temporal standard deviation.

Our approach indicates another possible application of this multivariate technique that may be important to the identification of areas of high yield stability over time. Therefore, the novelty of the present work is not in the PCA itself, but in its application to the study of yield variability on agricultural fields.

To implement the PCA, it is necessary to have data from several years of crop productivity, but this is not always the case. Therefore, the second paper proposed another approach that is particularly suitable for these situations. Considering the absence of multi-year data, the main goal of this research was to estimate the spatial and temporal uncertainty in maize yield using stochastic simulation techniques (sequential Gaussian simulation (SGS)) to reduce the economic risk to the fields.

Currently, the availability of yield monitors makes it easy to obtain data at high densities, so to determine the influence of data density on the stochastic simulation results, 30, 65, 125 and 150 to 250 of the initial data points ha^{-1} were tested. The results showed that sampling density affected the stochastic yield simulation results. Under the conditions of this study, the ideal point density for the stochastic yield simulation was approximately 65 points ha^{-1} compared to the real yield data.

By comparing the simulation results with the real yield data, it was possible to verify that higher sampling densities promoted an over-estimation of the low and high yields (yield border classes). In contrast, a lower sampling density promoted an over-estimation around the average yield (central classes) and a reduction in the yield border classes.

At 65 points ha^{-1} , the results of the stochastic simulations performed for each year's yield in both fields revealed a strong correlation between the percentage of the field area per class of the real yield and the simulated yield data. Combining both fields and taking all years and classes into account, 80% of the differences between the real yield and the simulated yield data per yield class were reduced to less than 1 percentage point. These results suggest that stochastic simulation is a useful tool for interpreting trends in yield that permits the mapping and identification of focal areas based on a number of repetitions.

The number of equi-probable surfaces that were generated by the sequential Gaussian simulation was used to calculate a certain probability from a yield estimate with a certain degree of statistical confidence. Considering any given year and any confidence level, the results were similar for both fields if each year was analyzed individually. Both fields showed a greater area percentage with above-average yield at all confidence levels, suggesting that these areas were more stable than those with below-average yields (Chapter 4).

In both fields, the field area percentages were very different depending on the level of confidence. The parcel area percentages were high at low confidence levels (50% and 60%), and area percentages were low for high confidence levels (90% and 95%), (Chapter 4).

Including data for a new year, the percentages of the below- and above-average field areas normally decreased but did so more quickly at higher levels of statistical significance (95% and 90%). Nevertheless, despite taking more than one year into account, from 3 to 4 years, the results revealed that the introduction of one year has not changed the field area percentage at any level of confidence (Chapter 4).

This study suggests that stochastic simulation can help farm managers as a decision support tool as probability maps with different confidence levels allow farmers to make decisions based on production risk. For example, accounting for the international price of maize will influence the break-even yield point.

Another way to reduce economic and environmental risks is to focus on the management of inputs. In Mediterranean regions, including Portugal, excessive phosphorus is commonly applied to the soil [TBGS07]; the normal strategy is to evenly apply P and K based on an average yield target. Normally, the applied P moves slowly into the soil, and its accumulation increases the risk of water eutrophication due to leaching [Sha95].

With this in mind, the third study examined different fertilization scenarios based on yield/input ratios by taking the field surface yield, the soil input maps (derived from the EC_a maps and others) and the actual maize price into consideration.

The experimental field presented high spatial variability in soil P and K (Chapter 5), which was probably due to the differential extraction rates of P and K, which had not been corrected due to many years of uniform fertilization. The study indicated that crop yield does not always increase with increasingly higher values of P and K, so the yield spatial variability cannot be attributed to P and K because the concentrations of these nutrients in the Azarento soil were relatively high and therefore not limiting factors to plant growth. Taking these results into account, the field was divided into 5 zones (Chapter 5) depending on maize yield, the yield/phosphorus ratio ($0.12 \text{ t ha}^{-1} (\text{mg Kg}^{-1})^{-1}$) and yield break-even (10.77 t ha^{-1}) values.

The different characteristics of each zone made it possible to calculate a P and K variable rate fertilizer application in accordance with the break-even line and the yield/input ratio threshold, as determined by the farm manager, whose movements depend on the price of maize and the market risk, respectively. Being unable to change certain yield-limiting factors, some of them structural, the rationing of nutrients, in particular phosphorus, can help farmers increase productivity in highly yield/input ratio areas by increasing the phosphorus reserves in the soil; P can be saved where the yield/input ratio is low through interactions with other yield-limiting factors, such as areas with poor drainage, excessive slopes and soil structure problems.

As was highlighted in this work, it is possible to reduce risks and achieve the best economic, agronomic and environmental efficiency if fertilization is in accordance with the productive potential of each zone and if the non-fertilization areas are below break-even and/or below a defined yield/input ratio value for P or another input. This strategy is supported by Zhang et al. [ZWW02] who advises that when certain parts of a field always produce below the break-even line, they must be isolated for the development of site-specific management.

This work presented a methodology that allows for the optimization of agronomic, economic and environmental inputs based on the yield break-even, the yield/input ratios and the variable rate inputs application. Considering only P and K, the savings could reach 200 € ha^{-1} (2015 maize and input prices) when compared with traditional fertilization application.

6.2 Future work

This work positively contributes to better crop management to minimize environmental problems and increase economic returns. However, some issues have remained unresolved during this research but are challenging topics for future investigation.

Future research should address the following topics:

- 1- N is responsible for half of the cost of NPK in maize productions, so how can N differential management applications be optimized? Through proximal, drone-mounted N sensors? Intelligent N fertilizers? Future work should aim to reduce the same amount of N when compared to PK;
- 2- The yield/input ratios technique can be applied to other type of inputs, such as water, seed density, etc., which would allow farmers to be more conscious about their fields and the variability in spatial and temporal economic risks while optimizing their activities at the same time;
- 3 – Minimal and direct seedling, herbicide optimization, and proximal drone-transported NDVI sensors can play an important role in the optimization of maize economics because high yield/input ratios in productive areas should not be limited by a high concentration of weeds. Therefore yield/herbicide ratios should also be considered in the future.

6.3 Conclusions

Precision agriculture has provided farmers with greater awareness about the spatial and temporal variability in soil and yield, even in small areas. Farmers are increasingly concerned about trying to adjust production inputs to local needs and to improve the profitability of crop production.

One of the main contributions of the current dissertation was to reveal different approaches to soil management and yield variability.

The exploratory multivariate technique, principal component analysis (PCA), allowed the study of the spatial and temporal variability in maize yield and demonstrated its usefulness as a technique to delineate management zones for site-specific treatments. Average temporal yield was indicated by the first PCA axis, and temporal yield stability was indicated by the second PCA axis. This information made it possible to identify four management zones: i) zones of high productivity (high PC1 values) that are stable over time (intermediate PC2 values); ii) zones of high productivity (high PC1 values) but unstable over time (low or high PC2 values); iii) zones of low productivity (low PC1 values) that are stable over time (intermediate PC2 values); iv) zones of low productivity (low PC1 values) that are unstable over time (low or high PC2 values).

When PCA is applied to multiple years of yield data, it can be a powerful tool in decision-making processes and in the selection of agricultural fields, or parts of agricultural fields if considering their temporal redundancy. The results indicate that field areas with higher PC1 and median PC2 values should be chosen by producers to optimize production factors and reduce economic risk.

The stochastic simulation represented the spatial and temporal heterogeneity in yield in a probabilistic way. The use of historic crop yield data (4 and 7 years for the Azarento and Bemposta fields, respectively) made it possible to display time trends and verify the inter-annual yield variability. In Mediterranean environments, 3 to 4 years of real yield data processed together will allow for the creation of robust yield uncertainty maps to better manage the yield risk and support future decisions.

This knowledge is important in the absence of long-term, multi-year yield databases in that it will help farmers define the most appropriate strategies for their fields and respective crops in advance. The simulation, combined with other techniques, statistical or not, can be a powerful risk management tool that can complement the decisions of the producer. Due to the costs of intensive sampling and soil analysis and the limited life of the results, this technique has the potential to help farmers when they do not know the history of a field.

Usually P and K fertilizer applications are greater than crop removal, which normally causes nutrient accumulation in the soil over time.

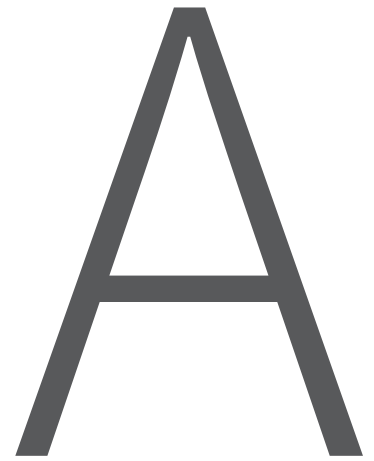
During the study, it was demonstrated that the yield/phosphorus ratio and the field yield break-even point were effective for the design of variable input rate applications, thus improving resource-use efficiencies.

Site-specific P and K management allowed for the distribution of both fertilizers within the field only where it was needed, and it avoided nutrient deficiencies or excesses while providing greater agronomic and economic returns and profitability.

This work suggests that variable input management optimization requires i) a yield map, ii) input maps (derived with intelligent sampling based on soil EC_a surveys), and iii) the international product price and the crop account.

With the savings from P and K variable rate applications, a farmer with 250 ha could pay for the VRT fertilization (liquid) equipment in one year.

In short, inefficient processes should not be allowed in agriculture, especially when technology is available and affordable.



Figures

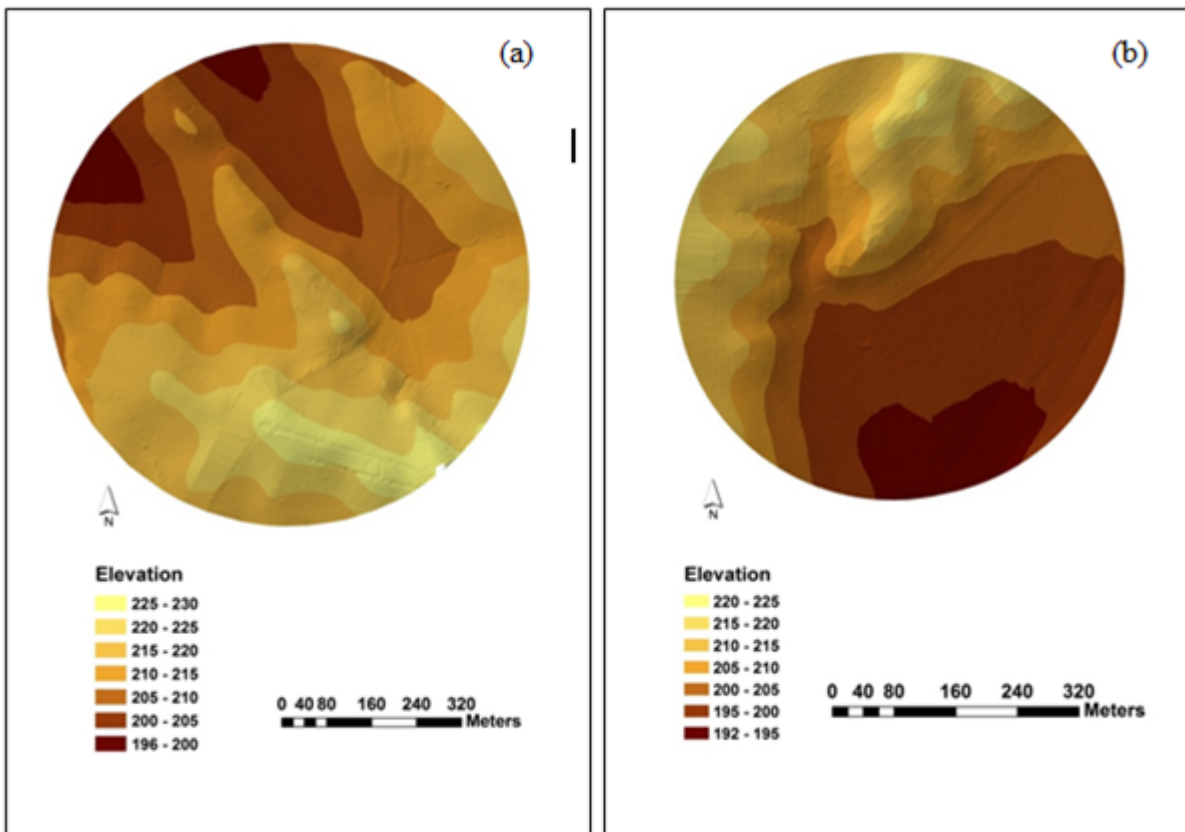
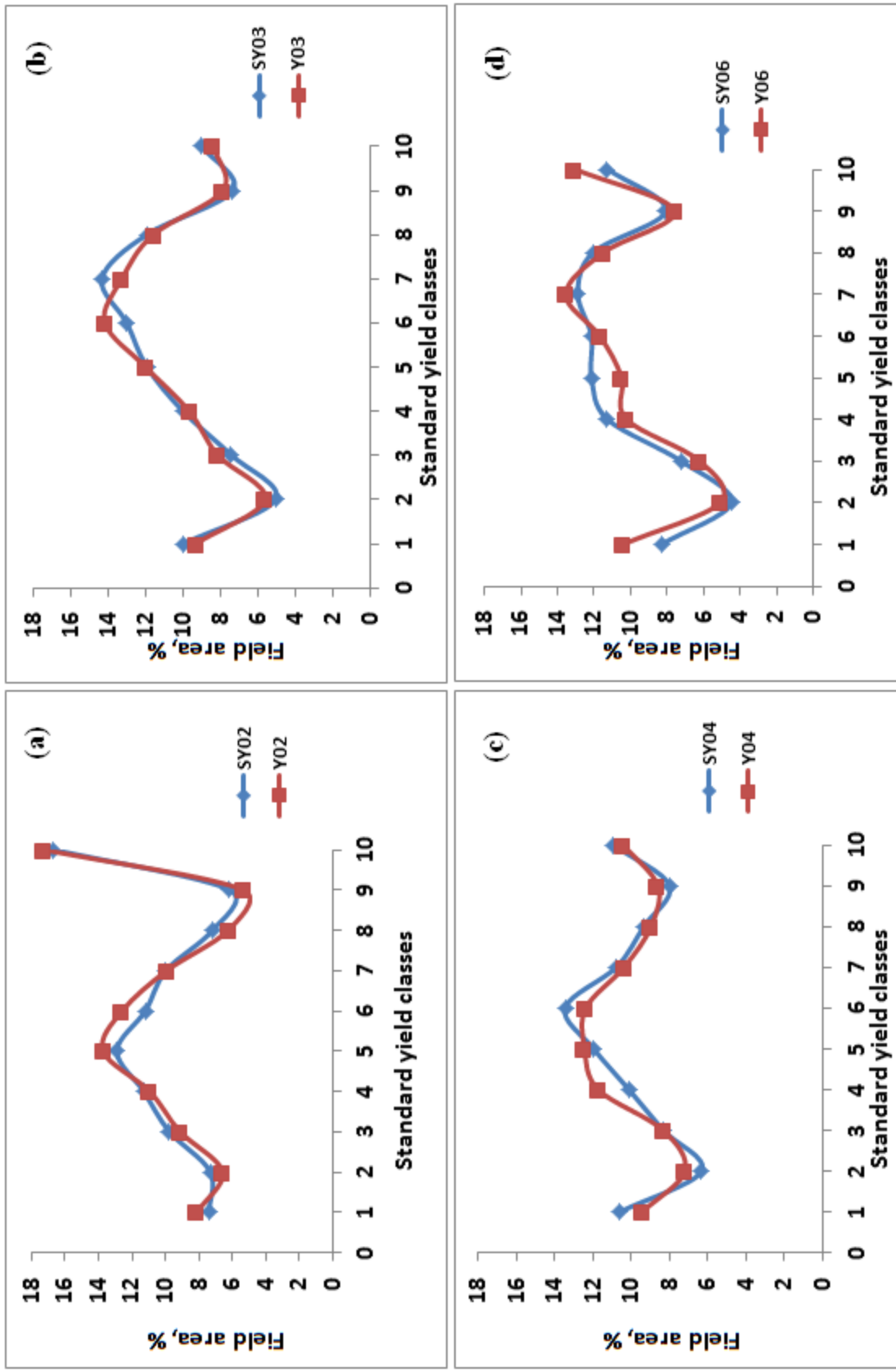
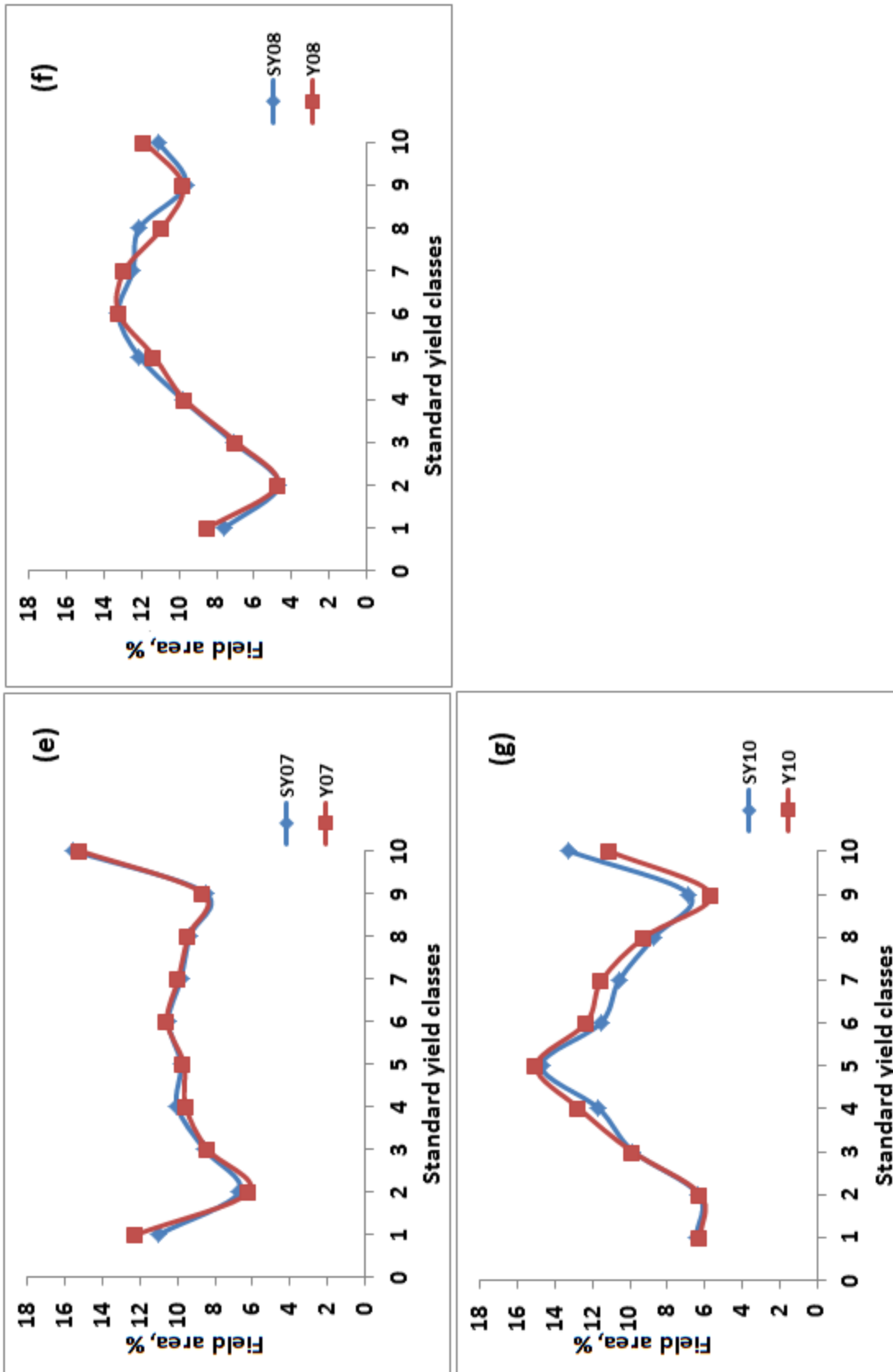


Figure A.1: DEMs for: (a) Azarento field; b) Bemposta field.



Y02; Y03; Y04; Y06 – Real yield 2002; 2003; 2004 and 2006; SY02; SY03; SY04; SY06 – Simulated yield 2002, 2003, 2004 and 2006

Figure A.2: Real and simulated yield (≈ 65 points ha^{-1}) field area percentage according to different standard yield classes Bemposta field: (a) 2002; (b) 2003; (c) 2004; (d) 2006.



Y07; Y08; Y10 – Real yield 2007, 2008 and 2010; SY06, SY07; SY08; SY10 – Simulated yield 2007, 2008 and 2010

Figure A.3: Real and simulated yield (≈ 65 points ha^{-1}) field area percentage according to different standard yield classes Bemposta field: (e) 2007; (f) 2008; (g) 2010.

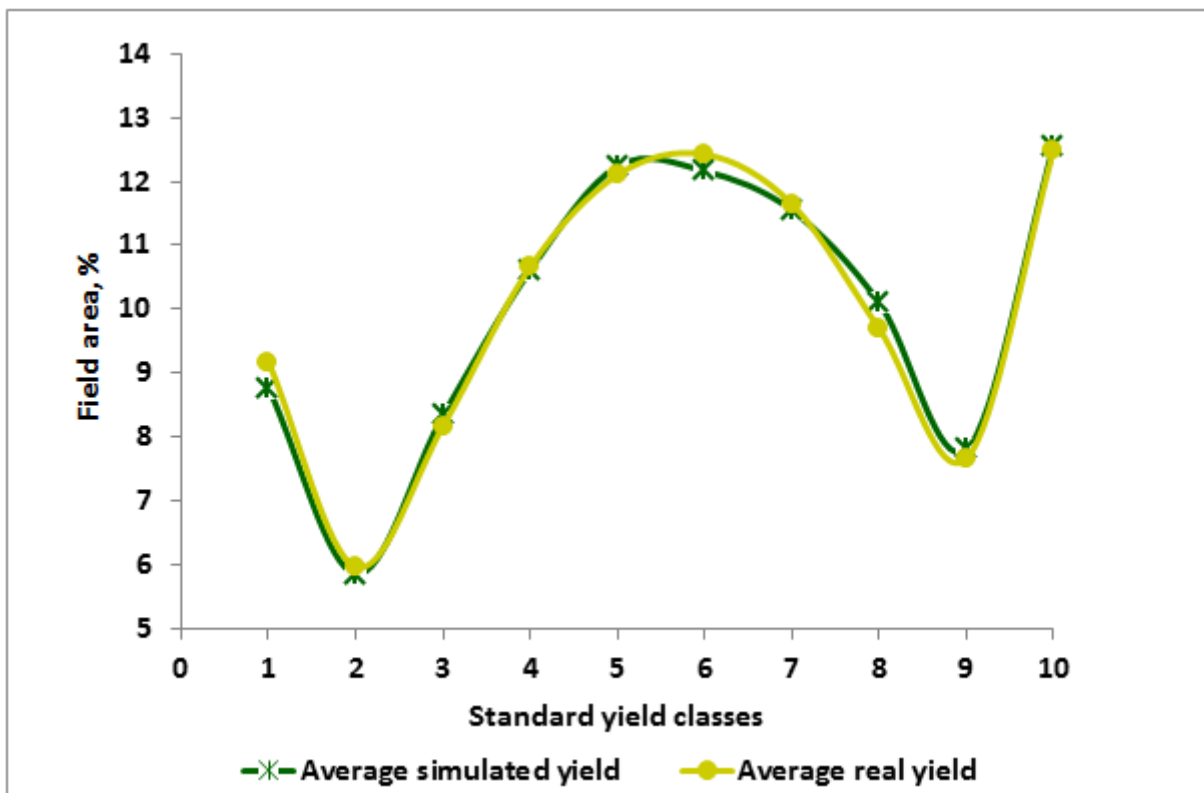


Figure A.4: Average real yield and simulated yield ($\approx 65 \text{ points ha}^{-1}$) field area percentage according to different standard yield classes and considering 7 years (Bemposta field).

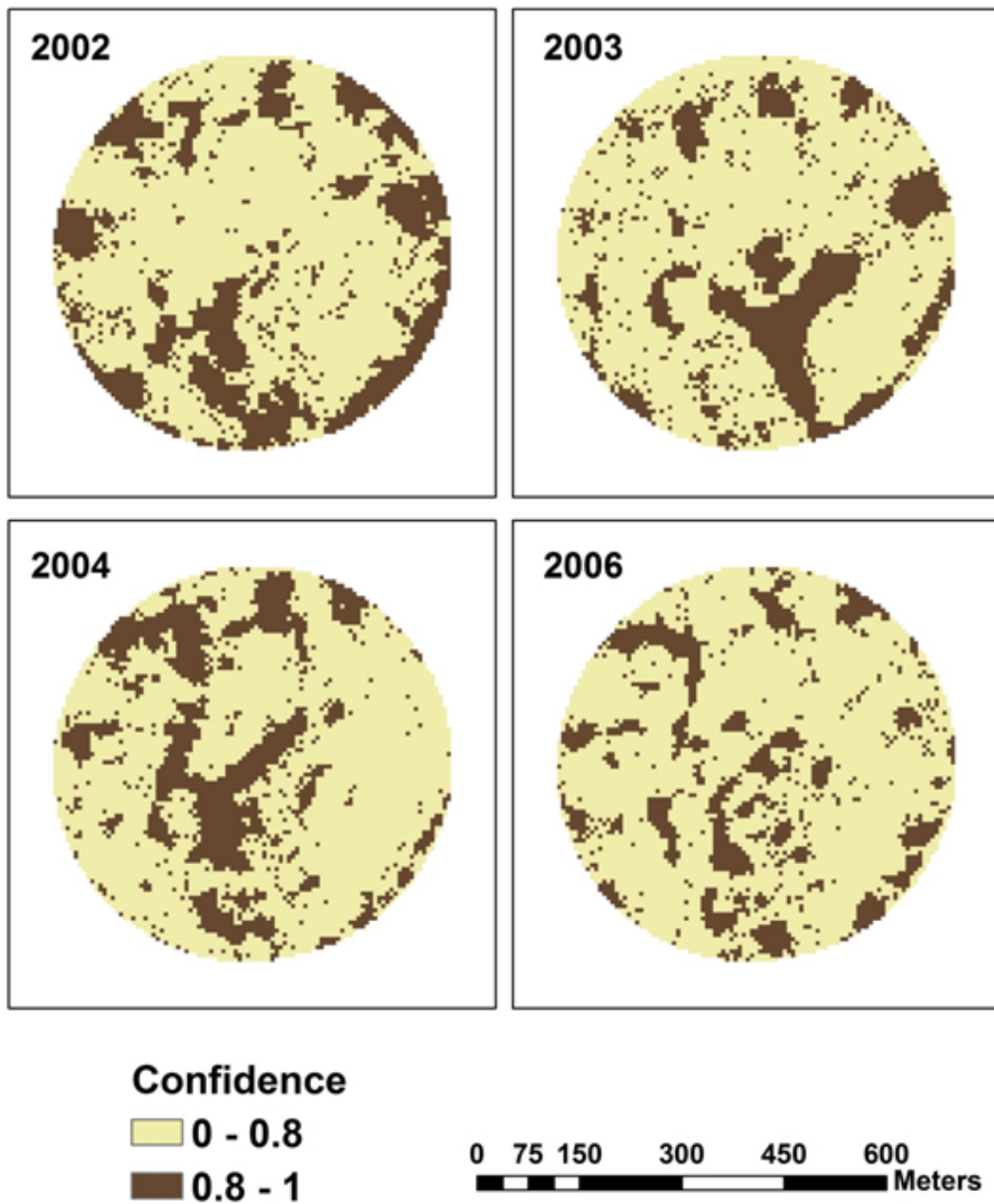


Figure A.5: Below average yield areas with 80% of confidence considering 2002, 2003, 2004 and 2006, simulation data analyzed independently (Bemposta field)

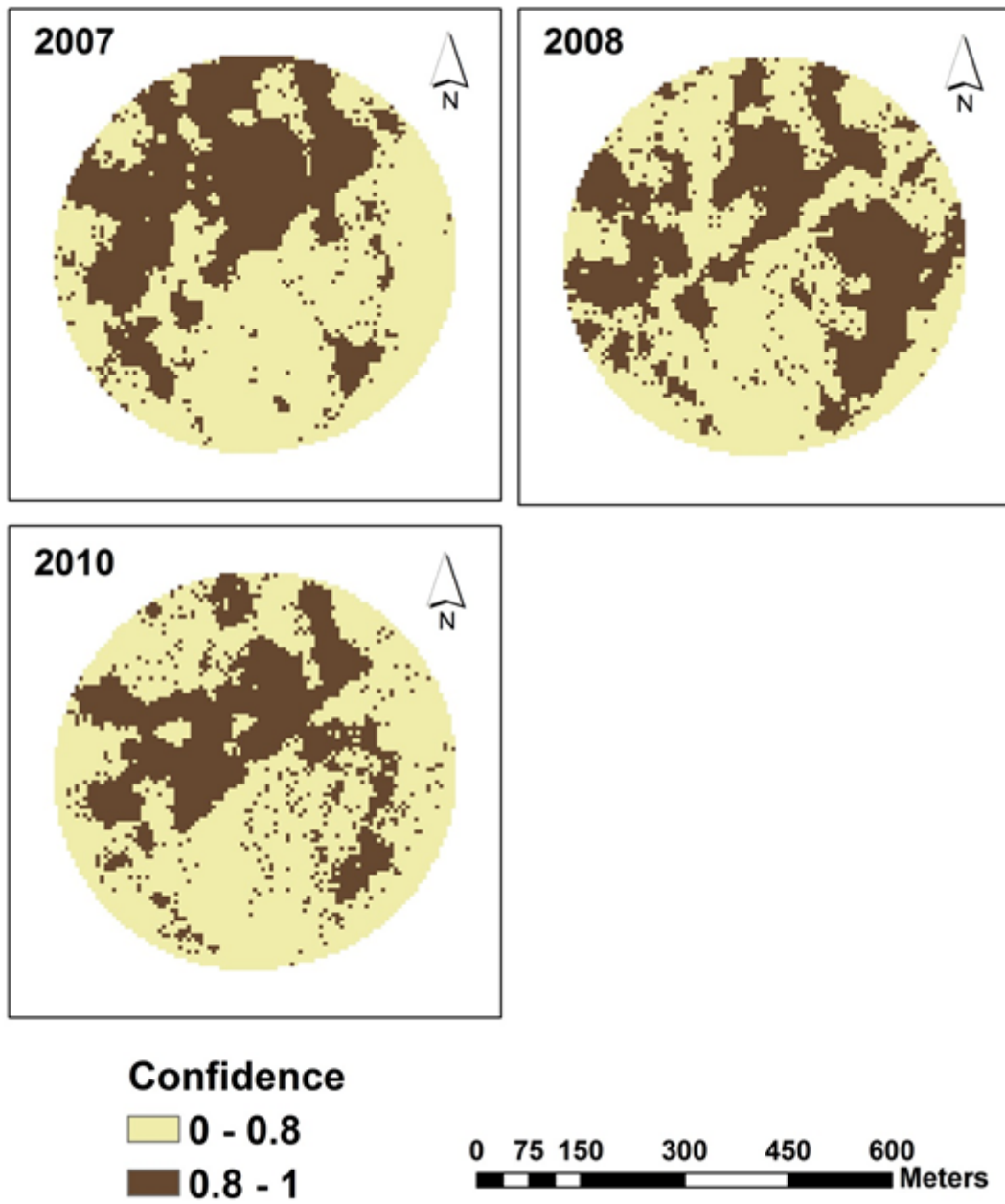


Figure A.6: Below average yield areas with 80% of confidence considering 2007, 2008 and 2010 simulation data analyzed independently (Bemposta field)

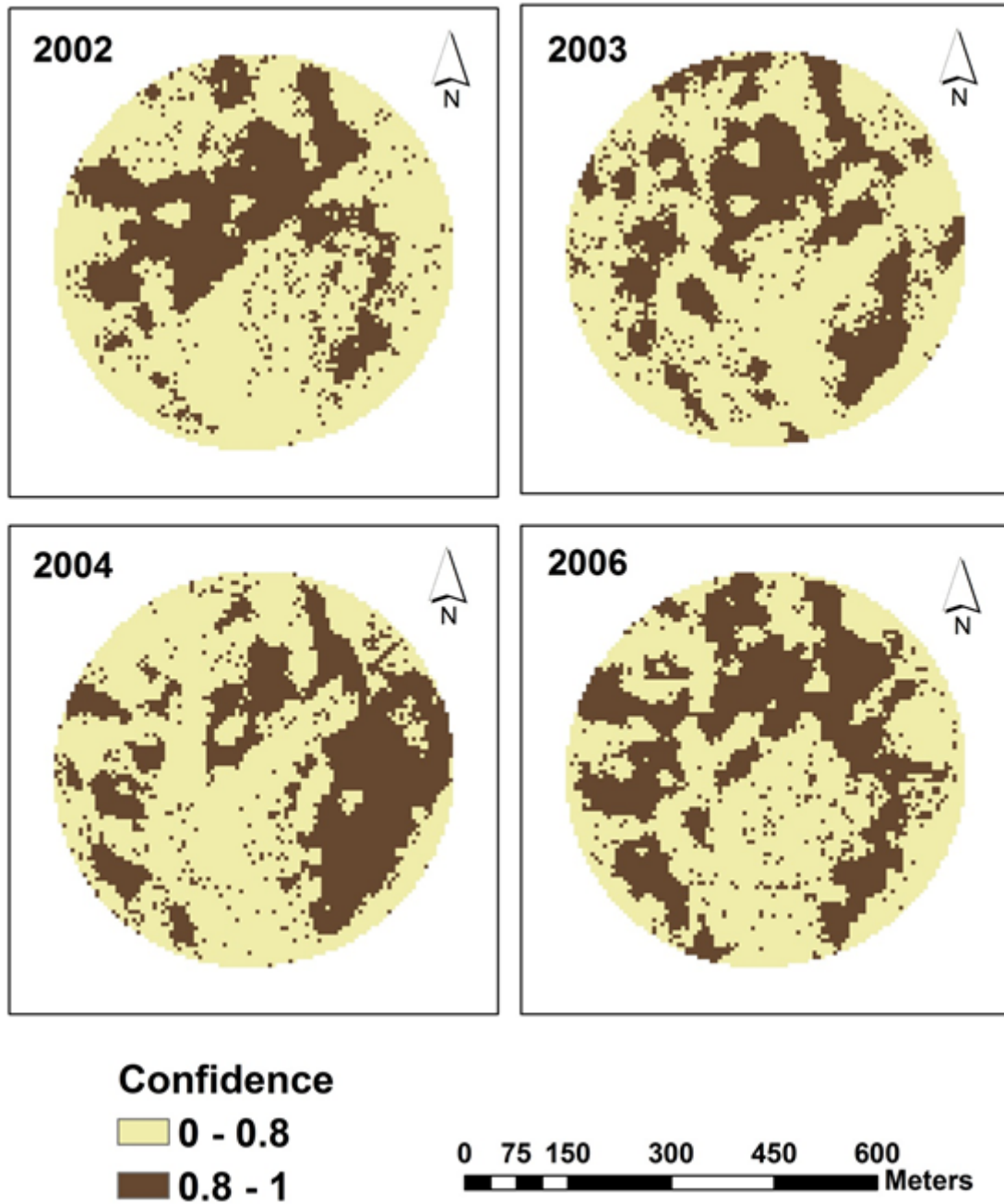


Figure A.7: Above average yield areas with 80% of confidence considering 2002, 2003, 2004 and 2006 simulation data analyzed independently (Bemposta field).

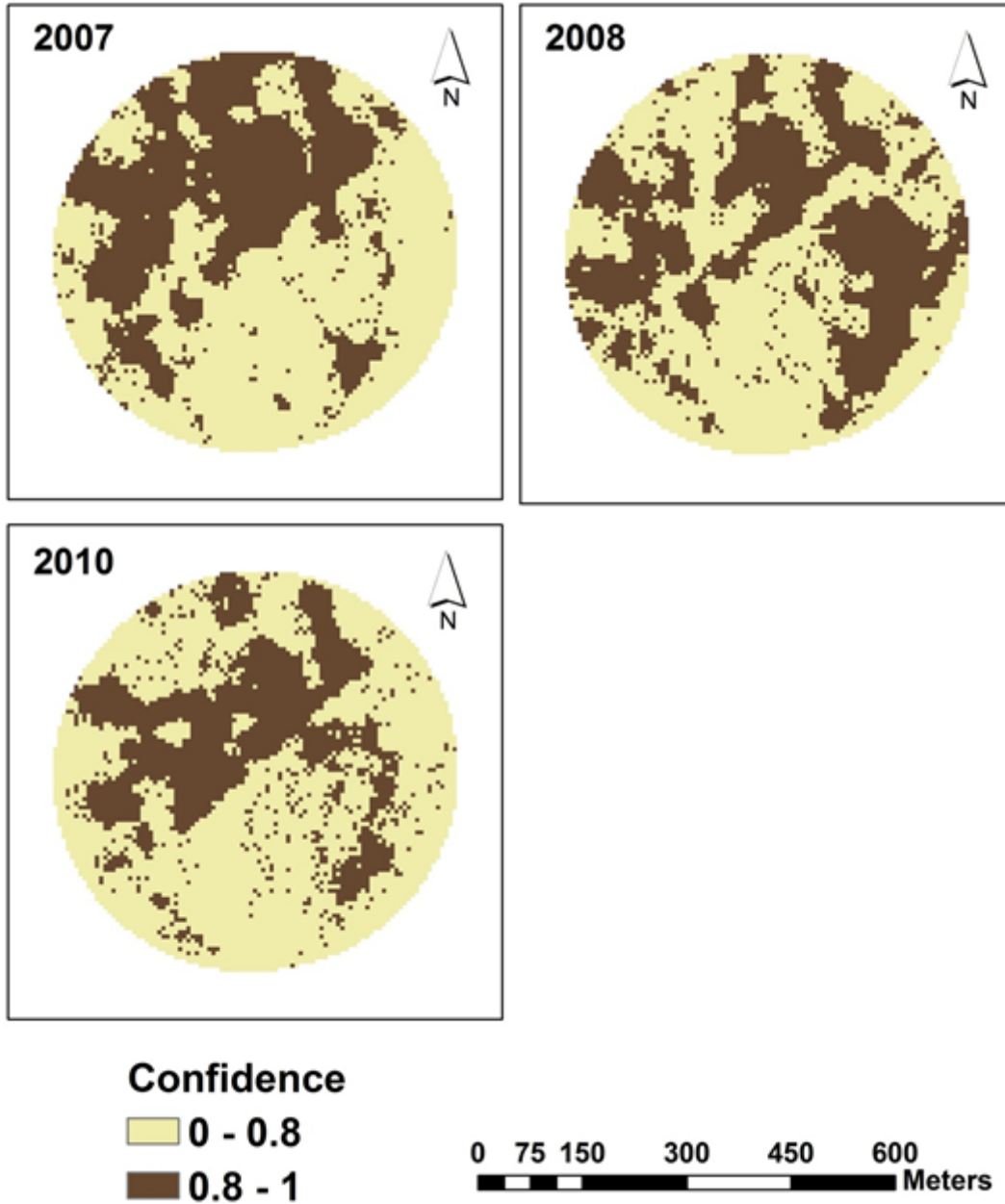


Figure A.8: Above average yield areas with 80% of confidence considering 2007, 2008 and 2010 simulation data analyzed independently (Bemposta field).

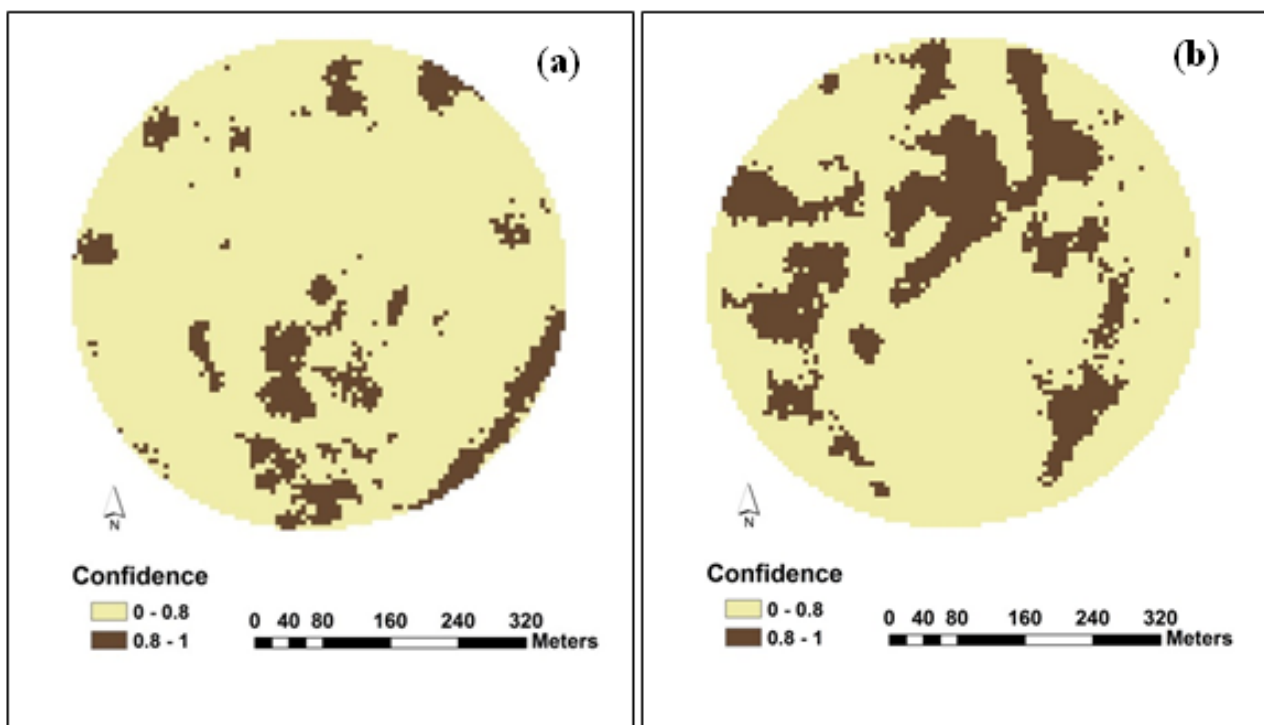


Figure A.9: Below average (a) and above average (b) yield areas with 80% of confidence considering 2002, 2003, 2004, 2006, 2007, 2008 and 2010 simulation yield data grouped together (Bemposta field)

B

Maize production costs

Table B.1: Maize production costs

Maize production costs : breakeven calculation basis			
Herdade do Cego - Azarento Field			
CROP: grain maize		Field area (m²)	565380
		Yield (dry weight)*	12,6 ton ha⁻¹
		Price	175 € ha⁻¹
	Quantity	Unit price	Value
COSTS OF PRODUCTION:			
SEEDS			
FAO 600 (doses)	1,8	130	234
FERTILIZERS			
Humifosfato 15 (ton)	0,9	300	270
Nitro+Zn (ton)	0,8	305	244
PESTICIDES			
Total herbicide (L)	3	3,5	10,5
Residual herbicide (L)	4	13,6	54,4
Post-emergent herbicide (L)	3	10	30
Insecticide (2 applications)	0,6	63	37,8
TRACTION			
Products applications	4	15	60
Mobilization-Fertilization	1	80	80
Sowing	1	40	40
soil cultivation	1	40	40
Harvest	1	85	85
Transport (ton)**	14,06	4	56,2
Irrigation / energy / water	7500	0,033	247,5
OUTROS			
Land Rental***	1	100	100
Reviews and repairs	1	100	100
Dryer****	14,06	14	196,8
PRODUCTION COST			1886,3 € ha⁻¹

*average of the three years of maize yield considered

*Transport with a very short distance (dryer is owned by the farmer)

**The farmer manager owns the land. Therefore it was considered a rental but low price

*** Reference moisture 14%; moisture at harvest 23%

Depreciation: not counted because the services were calculated as if they were rented

Bibliography

- [AAR⁺09] W Aimrun, M S M Amin, M Rusnam, D Ahmad, M M Hanafi, and A R Anuar. Bulk soil electrical conductivity as an estimator of nutrients in the maize cultivated land. *European Journal of Scientific Research*, 31(1):37–51, 2009.
- [Ada06] Viacheslav I Adamchuk. Characterizing Soil Variability Using On-the-Go Sensing Technology. *Site-Specific Management Guidelines, SSMG*, 44:1–4, 2006.
- [AEJ04] M Askegaard, J Eriksen, and A E Johnston. Sustainable management of potassium. In P. Schjøning and B. T. S. Elmholt, editors, *Managing Soil Quality—challenges in modern agriculture*, chapter Chapter 6, pages 85–102. 2004.
- [AEO03] M Askegaard, J Eriksen, and J E E Olesen. Exchangeable potassium and potassium balances in organic crop rotations on a coarse sand. *Soil Use and Management*, 19(2):96–103, 2003. DOI:10.1111/j.1475-2743.2003.tb00287.x.
- [AES06] Barry J Allred, M Reza Ehsani, and Dharmendra Saraswat. Comparison of electromagnetic induction, capacitively-coupled resistivity, and galvanic contact resistivity methods for soil electrical conductivity measurement. *Applied Engineering in Agriculture*, 22(2):215–230, 2006.
- [AHMU04] Viacheslav I Adamchuk, J W Hummel, M T Morgan, and S K Upadhyaya. On-the-go soil sensors for precision agriculture. *Computers and Electronics in Agriculture*, 44(1):71–91, 2004. DOI:10.1016/j.compag.2004.03.002.
- [AJG04] M. A Alfaro, S. C. Jarvis, and P. J. Gregory. Factors affecting potassium leaching in different soils. *Soil Use and Management*, 20(2):182–189, 2004.
- [AKA⁺11] Ali Ashraf Amirinejad, Kalpana Kamble, Pramila Aggarwal, Debashis Chakraborty, Sanatan Pradhan, and Raj Bala Mittal. Assessment and mapping of spatial variation of soil physical health in a farm. *Geoderma*, 160(3-4):292–303, 2011. DOI:10.1016/j.geoderma.2010.09.021.
- [Ame07] E Amezketa. Soil salinity assessment using directed soil sampling from a geophysical survey with electromagnetic technology: A case study. *Spanish Journal of Agricultural Research*, 5(1):91–101, 2007.
- [AZK07] Sh Ayoubi, S Mohammad Zamani, and F Khormali. Spatial variability of some soil properties for site specific farming in northern Iran. *International Journal of Plant Production*, 1(2):225–236, 2007.

- [BBP02] William D Batchelor, Bruno Basso, and Joel O Paz. Examples of strategies to analyze spatial and temporal yield variability using crop models. *European Journal of Agronomy*, 18(1-2):141–158, 2002. DOI:10.1016/S1161-0301(02)00101-6.
- [BBSM07] Bruno Basso, Matteo Bertocco, Luigi Sartori, and Edward C. Martin. Analyzing the effects of climate variability on spatial pattern of yield in a maize-wheat-soybean rotation. *European Journal of Agronomy*, 26(2):82–91, 2007. DOI:10.1016/j.eja.2006.08.008.
- [BCC⁺09] Bruno Basso, D Cammarano, D Chen, G Cafiero, M Amato, G Bitella, R Rossi, and F Basso. Landscape position and precipitation effects on spatial variability of wheat yield and grain protein in southern Italy. *Journal of Agronomy and Crop Science*, 195(4):301–312, 2009. DOI:10.1111/j.1439-037X.2008.00351.x.
- [BGF03] Simon Blackmore, Richard J Godwin, and Spyros Fountas. The analysis of spatial and temporal trends in yield map data over six years. *Biosystems Engineering*, 84(4):455–466, 2003. DOI:10.1016/S1537-5110(03)00038-2.
- [Bio12] BioMedware. SpaceStat. Washington, USA: Geospatial Research and Software., 2012.
- [BJCK00] A Bakhsh, D B Jaynes, T S Colvin, and R S Kanwar. Spatio-Temporal Analysis of Yield Variability for a Corn-Soybean Field in Iowa. *Transactions of the ASAE/ Am. Soc. Agr. Eng.*, 43(1993):31–38, 2000.
- [BJPG03] L Blake, A E Johnston, P R Poulton, and K W T Goulding. Changes in soil phosphorus fractions following positive and negative phosphorus balances for long periods. *Plant and Soil*, 254(2):245–261, 2003. DOI:10.1023/A:1025544817872.
- [BKE09] Ali Bozkurt, Cengiz Kurtulus, and Hasan Endes. Measurements of apparent electrical conductivity and water content using a resistivity meter. *International Journal of Physical Sciences*, 4(12):784–795, 2009.
- [Bla00] Simon Blackmore. The interpretation of trends from multiple yield maps. *Computers and Electronics in Agriculture*, 26(1):37–51, 2000. DOI:10.1016/S0168-1699(99)00075-7.
- [BM99] Simon Blackmore and Mark Moore. Remedial Correction of Yield Map Data. *Precision Agriculture*, 1:53–66, 1999. DOI:10.1023/A:1009969601387.
- [BRP⁺01] Bruno Basso, J T Ritchie, F J Pierce, R P Braga, and J W Jones. Spatial validation of crop models for precision agriculture. *Agricultural Systems*, 68(2):97–112, 2001. DOI:10.1016/S0308-521X(00)00063-9.
- [CaEF⁺12] Luísa Conceição, Pilar B Elorza, Ricardo Freixial, Susana Dias, and Constantino U Valero. Effects of different soil management practices on soil mechanic resistance and seed depth placement in a maize crop in Alentejo, Portugal Mediterranean region. In *International Conference of Agricultural Engineering*, July, CIGR Ageng2012, Valencia., 2012.
- [CC08] Raffaele Casa and Annamaria Castrignanò. Analysis of spatial relationships between soil and crop variables in a durum wheat field using a multivariate geostatistical approach. *European Journal of Agronomy*, 28(3):331–342, 2008. DOI:10.1016/j.eja.2007.10.001.
- [CGWA03] M S Cox, P D Gerard, M C Wardlaw, and M J Abshire. Variability of Selected Soil Properties and Their Relationships with Soybean Yield. *Soil Science Society of America Journal*, 67(4):1296, 2003. DOI:10.2136/sssaj2003.1296.
- [CK99] C A Cambardella and D L Karlen. Spatial Analysis of Soil Fertility Parameters. *Precision Agriculture*, 1(1):5–14, 1999. DOI:10.1023/a:1009925919134.

- [CL03] D L Corwin and S M Lesch. Application of soil electrical conductivity to precision agriculture: Theory, principles, and guidelines. *Agronomy Journal*, 95(3):455–471, 2003. DOI:10.2134/agronj2003.4550.
- [CL05a] D L Corwin and S M Lesch. Apparent soil electrical conductivity measurements in agriculture. *Computers and Electronics in Agriculture*, 46(1-3 SPEC. ISS.):11–43, 2005. DOI:10.1016/j.compag.2004.10.005.
- [CL05b] D L Corwin and S M Lesch. Characterizing soil spatial variability with apparent soil electrical conductivity: I. Survey protocols. *Computers and Electronics in Agriculture*, 46(1-3 SPEC. ISS.):103–133, 2005. DOI:10.1016/j.compag.2004.11.002.
- [CL05c] D L Corwin and S M Lesch. Characterizing soil spatial variability with apparent soil electrical conductivity: Part II. Case study. *Computers and Electronics in Agriculture*, 46(1-3 SPEC. ISS.):135–152, 2005. DOI:10.1016/j.compag.2004.11.003.
- [CLOK06] D L Corwin, S M Lesch, J D Oster, and S R Kaffka. Monitoring management-induced spatio-temporal changes in soil quality through soil sampling directed by apparent electrical conductivity. *Geoderma*, 131(3-4):369–387, 2006. DOI:10.1016/j.geoderma.2005.03.014.
- [CLS+08] D L Corwin, S M Lesch, P J Shouse, Soppe R, and E Ayars. Delineating Site-Specific Management Units Using Geospatial ECa Measurements. In M R Allred, B J; Daniels, J J and Ehsani, editor, *Handbook of Agricultural Geophysics*, chapter 16, pages 247–254. CRC Press, Boca Raton, FL, 2008.
- [CMP+94] C. a. Cambardella, T. B. Moorman, T. B. Parkin, D. L. Karlen, J. M. Novak, R. F. Turco, and a. E. Konopka. Field-Scale Variability of Soil Properties in Central Iowa Soils. *Soil Science Society of America Journal*, 58(5):1501–1511, 1994. DOI:10.2136/sssaj1994.03615995005800050033x.
- [CO05] Z L Carroll and Margaret A Oliver. Exploring the spatial relations between soil physical properties and apparent electrical conductivity. *Geoderma*, 128(3-4 SPEC. ISS.):354–374, 2005. DOI:10.1016/j.geoderma.2005.03.008.
- [DCT+12] Mariangela Diacono, Annamaria Castrignanò, Antonio Troccoli, Daniela De Benedetto, Bruno Basso, and Pietro Rubino. Spatial and temporal variability of wheat grain yield and quality in a Mediterranean environment: A multivariate geostatistical approach. *Field Crops Research*, 131:49–62, 2012. DOI:10.1016/j.fcr.2012.03.004.
- [DEP98] John W Doran, E T Elliott, and K Paustian. Soil microbial activity, nitrogen cycling, and long-term changes in organic carbon pools as related to fallow tillage management. *Soil and Tillage Research*, 49(1-2):3–18, 1998. DOI:10.1016/S0167-1987(98)00150-0.
- [DHB04] K Diker, D F Heermann, and M K Brodahl. Frequency analysis of yield for delineating yield response zones. *Precision Agriculture*, 5(5):435–444, 2004. DOI:10.1007/s11119-004-5318-9.
- [DMV07] Nicola Di Virgilio, Andrea Monti, and Gianpietro Venturi. Spatial variability of switchgrass (*Panicum virgatum* L.) yield as related to soil parameters in a small field. *Field Crops Research*, 101(2):232–239, 2007. DOI:10.1016/j.fcr.2006.11.009.
- [EDNW00] Roger A Eigenberg, John W Doran, J A Nienaber, and B L Woodbury. Soil conductivity maps for monitoring temporal changes in an agronomic field. In Proc 8th Int'l Symp Animal, Agricultural and Food Processing Wastes, Oct 9–11, 2000, Des Moines, Iowa. *Usda*, pages 249–265, 2000.
- [EMP01] Daniel R Ess, Mark T Morgan, and Samuel D Parsons. Implementing Site-Specific Management : Variable Rate Application. *Precision Agriculture*, SSM-2-W:1–9, 2001.

- [ESR09] ESRI. ARCGIS 9.3.3., 2009.
- [FAO14] FAO. World reference base for soil resources 2014. International soil classification system for naming soils and creating legends for soil maps. World Soil Resources Reports 106. Food and Agriculture Organization of the United Nations. Rome 2014., 2014.
- [FB04] H J Farahani and G W Buchleiter. Temporal stability of soil electrical conductivity in irrigated sandy fields in Colorado. *Transactions of the American Society of Agricultural Engineers*, 47(1):79–90, 2004.
- [Fri05] Shmulik P Friedman. Soil properties influencing apparent electrical conductivity: A review. *Computers and Electronics in Agriculture*, 46(1-3 SPEC. ISS.):45–70, 2005. DOI:10.1016/j.compag.2004.11.001.
- [FWWB00] K L Fleming, D G Westfall, D W Wiens, and M C Brodahl. Evaluating farmer defined management zone maps for variable rate fertilizer application. *Precision Agriculture*, 2(2):201–215, 2000. DOI:10.1023/A:1011481832064.
- [GAHT09] Robert Grisso, Mark Alley, David Holshouser, and Wade Thomason. Precision farming tools: soil electrical conductivity. *Virginia Cooperative Extension, Publication 442-508*, 2009.
- [GMB12] Wenxuan Guo, Stephan J Maas, and Kevin F Bronson. Relationship between cotton yield and soil electrical conductivity, topography, and Landsat imagery. *Precision Agriculture*, 13(6):678–692, 2012. DOI:10.1007/s11119-012-9277-2.
- [Goo98a] Pierre Goovaerts. Accounting for estimation optimality criteria in simulated annealing. *Mathematical Geology*, 30(5):511–534, 1998. DOI:10.1023/A:1021738027334.
- [Goo98b] Pierre Goovaerts. Geostatistical tools for characterizing the spatial variability of microbiological and physico-chemical soil properties. *Biology and Fertility of Soils*, 27(4):315–334, 1998. DOI:10.1007/s003740050439.
- [Goo99] Pierre Goovaerts. Geostatistics in soil science: state-of-art and perspectives. *Geoderma*, 89:1–45, 1999. DOI:10.1016/S0016-7061(98)00078-0.
- [Goo00] Pierre Goovaerts. Estimation or simulation of soil properties? An optimization problem with conflicting criteria. *Geoderma*, 97(3-4):165–186, 2000. DOI:10.1016/S0016-7061(00)00037-9.
- [HABF13] H H Huang, Viacheslav I Adamchuk, I I Boiko, and R F Ferguson. Effect of sampling patterns and interpolation methods on prediction quality of soil variability mapping. In John V. Stafford, editor, *Precision agriculture'13*, pages 243–250. Wageningen Academic Publishers., 2013. DOI:10.3920/978-90-8686-778-3_28.
- [HG02] Alexandre Hirzel and Antoine Guisan. Which is the optimal sampling strategy for habitat suitability modelling. *Ecological Modelling*, 157(2-3):331–341, 2002. DOI:10.1016/S0304-3800(02)00203-X.
- [HJ00] J W Hansen and J W Jones. Scaling-up crop models for climate variability applications. *Agricultural Systems*, 65(1):43–72, 2000. DOI:10.1016/S0308-521X(00)00025-1.
- [HMC03] Ronnie W Heiniger, Robert G McBride, and David E Clay. Using soil electrical conductivity to improve nutrient management. *Agronomy Journal*, 95(3):508–519, 2003. DOI:10.2134/agronj2003.0508.
- [HMMT13] C Horta, F Monteiro, M Madeira, and J Torrent. Phosphorus sorption and desorption properties of soils developed on basic rocks under a subhumid Mediterranean climate. *Soil Use and Management*, 29(SUPPL.1):15–23, 2013. DOI:10.1111/j.1475-2743.2012.00405.x.

- [HMT⁺00] N J Hartsock, T G Mueller, G W Thomas, R I Barnhisel, K L Wells, and Shearer S A. Soil Electrical Conductivity Variability. In W.E. Robert, P.C., Rust, R.H., Larson, editor, *Proceedings of the 5th International Conference On Precision Agriculture (vol 5)*, Madison, 2000. ASA and SSSA, Madison, WI.
- [Hot33] H Hotelling. Analysis of a Complex of Statistical Variables in to Principal Components. *Journal of educational psychology*, 24(6):417–441, 1933. DOI:10.1037/h0071325.
- [HT07] M C Horta and J Torrent. Phosphorus Desorption Kinetics in Relation To Phosphorus Forms and Sorption Properties of Portuguese Acid Soils. *Soil Science*, 172(8):631–638, 2007. DOI:10.1097/ss.0b013e3180577270.
- [HYE⁺04] C B Hedley, I J Yule, C R Eastwood, T G Shepherd, and G Arnold. Rapid identification of soil textural and management zones using electromagnetic induction sensing of soils. *Australian Journal of Soil Research*, 42(4):389–400, 2004.
- [IBM10] IBM Corp. IBM SPSS Statistics for windows, Version 19.0, 2010.
- [IS89] E H Isaaks and R M Srivastava. *An Introduction to Applied Geostatistics*. Oxford: Oxford University Press., 1989. DOI:10.1016/0040-1951(74)90006-7.
- [ITJ⁺05] Javed Iqbal, John A Thomasson, Johnie N Jenkins, Phillip R Owens, and Frank D Whisler. Spatial Variability Analysis of Soil Physical Properties of Alluvial Soils. *Soil Science Society of America Journal*, 69(4):1338, 2005. DOI:10.2136/sssaj2004.0154.
- [IVL⁺11] M M Islam, M Van Meirvenne, E Loonstra, E Meerschman, P De Smedt, F Meeuws, E Van De Vijver, and T Saey. Key properties for delineating soil management zones. In *The Second Global Workshop on Proximal Soil Sensing*, 16-18 May 2011, Montreal, 2011.
- [Jac80] J E Jackson. Principal components and factor analysis: Part II - additional topics related to principal components. *Journal of Quality Technology*, 13(1), 1980.
- [JCK05] Dan B Jaynes, Tom S Colvin, and Thomas C Kaspar. Identifying potential soybean management zones from multi-year yield data. *Computers and Electronics in Agriculture*, 46(1-3 SPEC. ISS.):309–327, 2005. DOI:10.1016/j.compag.2004.11.011.
- [JED⁺05] Cinthia K Johnson, Roger A Eigenberg, John W Doran, B J Wienhold, B Eghball, and B L Woodbury. Status of soil electrical conductivity studies by central state researchers. *Transactions of the Asae*, 48(3):979–989, 2005.
- [JK08] M. Jalali and Z. Kolahchi. Ability of sorption–desorption experiments to predict potassium leaching from calcareous soils. *Journal of Plant Nutrition and Soil Science*, 171(5):785–794, 2008.
- [JKS⁺05] W K Jung, N R Kitchen, Kenneth A Sudduth, R J Kremer, and P P Motavalli. Relationship of Apparent Soil Electrical Conductivity to Claypan Soil Properties. *Soil Science Society of America Journal*, 69(3):883–892, 2005. DOI:10.2136/sssaj2004.0202.
- [JVKL03] K. Johnston, J. M. Ver Hoef, K. Krivoruchko, and N. Lucas. *ArcGIS 9 - Using ArcGIS Geostatistical Analyst. Gis by Esri*. 2003.
- [Kai70] H F Kaiser. A second generation little jiffy. *Psychometrika*, 35:401–415, 1970.
- [KB00] A N Kravchenko and D G Bullock. Correlation of Corn and Soybean Grain Yield with Topography and Soil Properties. *Agronomy Journal*, 92:75–83, 2000.
- [KB02] A N Kravchenko and D G Bullock. Spatial Variability of Soybean Quality Data as a Function of Field Topography: 1. Spatial Data Analysis. *Crop Science*, 42:804–815, 2002.

- [KBW⁺09] Jürgen Kühn, Alexander Brenning, Marc Wehrhan, Sylvia Koszinski, and Michael Sommer. Interpretation of electrical conductivity patterns by soil properties and geological maps for precision agriculture. *Precision Agriculture*, 10(6):490–507, 2009. DOI:10.1007/s11119-008-9103-z.
- [KCJ⁺03] Thomas C Kaspar, Thomas S Colvin, Daniel B Jaynes, Douglas L Karlen, David E James, David W Meek, Daniel Pulido, and Howard Butler. Relationship between six years of corn yields and terrain attributes. *Precision Agriculture*, 4(1):87–101, 2003. DOI:10.1023/A:1021867123125.
- [KKKM11] J Kumhálová, F Kumhála, M Kroulík, and Š Matějková. The impact of topography on soil properties and yield and the effects of weather conditions. *Precision Agriculture*, 12(6):813–830, 2011. DOI:10.1007/s11119-011-9221-x.
- [KMKP06] M Kroulík, M Mimra, F Kumhála, and V Prošek. Mapping spatial variability of soil properties and yield by using geostatic method. *Research in Agricultural Engineering*, 2006(1):17–24, 2006.
- [KO03] Ruth Kerry and Margaret A Oliver. Variograms of ancillary data to aid sampling for soil surveys. *Precision Agriculture*, 4(3):261–278, 2003. DOI:10.1023/A:1024952406744.
- [KPF⁺04] Thomas C Kaspar, D J Pulido, T E Fenton, T S Colvin, D L Karlen, D B Jaynes, and D W Meek. SITE-SPECIFIC ANALYSIS Relationship of Corn and Soybean Yield to Soil and Terrain Properties. *Agronomy Journal*, 96:700–709, 2004.
- [KR74] H F Kaiser and J Rice. NoLittle Jiffy, Mark IV. *Educational and Psychological Measurement*, 34:111–117, 1974.
- [KSM⁺05] N R Kitchen, Kenneth A Sudduth, D B Myers, ST Drummond, and SY Hong. Delineating productivity zones on claypan soil fields using apparent soil electrical conductivity. *Computers and Electronics in Agriculture*, 46(1-3 SPEC. ISS.):285–308, 2005. DOI:10.1016/j.compag.2004.11.012.
- [KWG88] R G Kachanoski, I J Van Wesenbeeck, and E G Gregorich. Estimating spatial variations of soil water content using noncontacting electromagnetic inductive methods. *Canadian Journal of Soil Science*, 68(4):715–722, 1988. DOI:10.4141/cjss88-069.
- [KWJ89] T Kosaki, K Wasano, and A S R Juo. Multivariate statistical analysis of yield-determining factors. *Soil Science Plant Nutrition*, 35(4):597–607, 1989. DOI:10.1080/00380768.1989.10434795.
- [KZN⁺14] J Kumhálová, F Zemek, P Novák, O Brovkina, and M Mayerová. Use of Landsat images for yield evaluation within a small plot. *Plant Soil Environment*, 60(11):501–506, 2014.
- [LCD99] E D Lund, C D Christy, and P E Drummond. Practical Applications of Soil Electrical Conductivity Mapping. In: (Ed.) J. V. Stafford, *precision Agriculture '99: Proceedings of the 2nd European Conference on Precision Agriculture*, Sheffield Academic Press, Sheffield, UK, (July):771–779, 1999.
- [LCD00] E D Lund, C D Christy, and P E Drummond. Using yield and soil electrical conductivity (EC) maps to derive crop production performance information. In *Veris Technologies. Salina KS Presented at the Proceedings of the 5th International Conference on Precision Agriculture*, Bloomington, Minnesota, USA, 16-19 July, 2000. American Society of Agronomy, pages 1–10, 2000.
- [LGBC06] Johanna Link, Simone Graeff, William D Batchelor, and Wilhelm Claupein. Spatial variability and temporal stability of corn (*Zea mays* L.) grain yields – relevance of grid size. *Archives of Agronomy and Soil Science*, 52(4):427–439, 2006. DOI:10.1080/03650340600775487.
- [LGC04] Johanna Link, Simone Graeff, and Wilhelm Claupein. Spatial and temporal stability of corn grain yields in the Upper Rhine Valley. In *4th International Crop Science Congress*, Brisbane, Australia, 2004.

- [LMP95] L Lebart, A Morineau, and M Piron. *Statistique exploratoire multidimensionnelle*. Paris, 1995.
- [LWH01] E D Lund, M C Wolcott, and G P Hanson. Applying nitrogen site-specifically using soil electrical conductivity maps and precision agriculture technology. In *In proceedings of the 2nd International Nitrogen Conference on Science and Policy Oct. 14-18. Potomac, MD*, pages 1–10, 2001.
- [LWHT10] J Lofton, D C Weindorf, B Haggard, and B Tubana. Nitrogen variability: a need for precision agriculture. *Agricultural Journal*, 5(1):6–11, 2010.
- [MA05] J R Marques da Silva and C Alexandre. Spatial variability of irrigated corn yield in relation to field topography and soil chemical characteristics. *Precision Agriculture*, 6(5):453–466, 2005. DOI:10.1007/s11119-005-3679-3.
- [Mar06] J R Marques da Silva. Analysis of the Spatial and Temporal Variability of Irrigated Maize Yield. *Biosystems Engineering*, 94(3):337–349, 2006. DOI:10.1016/j.biosystemseng.2006.03.006.
- [MBA⁺02] Stephen Machado, E D Bynum, T L Archer, R J Lascano, L T Wilson, J Bordovsky, E Segarra, K Bronson, D M Nesmith, and W Xu. Spatial and temporal variability of corn growth and grain yield: Implications for site-specific farming. *Crop Science*, 42(5):1564–1576, 2002. DOI:10.2135/cropsci2002.1564.
- [MF11] José Paulo Molin and G C Faulin. The influence of soil moisture on the spatial and temporal variability of soil electrical conductivity. In *In Proceeding of The Second Global Workshop on Proximal Soil Sensing*, pages 12–15, Montreal, 2011.
- [MHS⁺03] T G Mueller, N J Hartsock, T S Stombaugh, S A Shearer, P L Cornelius, and R I Barnhisel. Soil electrical conductivity map variability in limestone soils overlain by loess. *Agronomy Journal*, 95(3):496–507, 2003. DOI:10.2134/agronj2003.0496.
- [MKR⁺05] M Mzuku, R Khosla, R Reich, D Inman, F Smith, and L MacDonald. Spatial Variability of Measured Soil Properties across Site-Specific Management Zones. *Soil Science Society of America Journal*, 69(5):1572, 2005. DOI:10.2136/sssaj2005.0062.
- [MM02] P P Motavalli and R J Miles. Soil phosphorus fractions after 111 years of animal manure and fertilizer applications. *Biology and Fertility of Soils*, 36(1):35–42, 2002. DOI:10.1007/s00374-002-0500-6.
- [MMRS05] Y Miao, D J Mulla, P C Robert, and J V Stafford. Combining soil-landscape and spatial-temporal variability of yield information to delineate site-specific management zones. In *In Precision agriculture'05. Papers presented at the 5th European Conference on Precision Agriculture, Uppsala, Sweden*, pages 811–818. Wageningen Academic Publishers., 2005.
- [MRSM12] J R Marques da Silva, Francisco J Rebollo, Adélia Sousa, and Paulo Mesquita. Yield potential probability maps using the Rasch model. *Biosystems Engineering*, 111(4):369–380, 2012. DOI:10.1016/j.biosystemseng.2012.01.002.
- [MRSP10] B Murteira, C S Ribeiro, J A Silva, and C Pimenta. *Introdução à estatística (Introduction to statistics)*. Lisboa, 2010.
- [MS06] J R Marques da Silva and L L Silva. Relationship between Distance to Flow Accumulation Lines and Spatial Variability of Irrigated Maize Grain Yield and Moisture Content at Harvest. *Biosystems Engineering*, 94(4):525–533, 2006. DOI:10.1016/j.biosystemseng.2006.04.011.
- [MS08] J R Marques da Silva and L L Silva. Evaluation of the relationship between maize yield spatial and temporal variability and different topographic attributes. *Biosystems Engineering*, 101(2):183–190, 2008. DOI:10.1016/j.biosystemseng.2008.07.003.

- [MTM10] F J Moral, J M Terrón, and J R Marques da Silva. Delineation of management zones using mobile measurements of soil apparent electrical conductivity and multivariate geostatistical techniques. *Soil and Tillage Research*, 106(2):335–343, 2010. DOI:10.1016/j.still.2009.12.002.
- [NMMK12] Mehdi Nourzadeh, Mohammad Hossein Mahdian, Mohammad Jafar Malakouti, and Kazem Khavazi. Investigation and prediction spatial variability in chemical properties of agricultural soil using geostatistics. *Archives of Agronomy and Soil Science*, 58(5):461–475, 2012. DOI:10.1080/03650340.2010.532124.
- [NPD⁺11] Marcos Rafael Nanni, Fabrício Pinheiro Povh, José Alexandre Melo Demattê, Roney Berti De Oliveira, Marcelo Luiz Chicati, and Everson Cezar. Optimum size in grid soil sampling for variable rate application in site-specific management. *Scientia Agricola*, 68(3):386–392, 2011. DOI:10.1590/S0103-90162011000300017.
- [Oli10] M A Oliver. *An overview of geostatistics and precision agriculture. In Geostatistical Applications for Precision Agriculture*. Springer Netherlands, 2010. DOI:10.1007/978-90-481-9133-8.
- [OSn07] Rodrigo A Ortega and Oscar A Santibáñez. Determination of management zones in corn (*Zea mays* L.) based on soil fertility. *Computers and Electronics in Agriculture*, 58(1):49–59, 2007. DOI:10.1016/j.compag.2006.12.011.
- [PC13] Nahuel Raúl Peralta and José Luis Costa. Delineation of management zones with soil apparent electrical conductivity to improve nutrient management. *Computers and Electronics in Agriculture*, 99:218–226, 2013. DOI:10.1016/j.compag.2013.09.014.
- [PCCB13] Nahuel Raúl Peralta, José Luis Costa, Mauricio Castro, and Mónica Balzarini. Delimitación de zonas de manejo con modelos de elevación digital y profundidad de suelo. *Interciencia*, 38(6):418–424, 2013.
- [PdJBBA14] Thomas Panagopoulos, Jorge de Jesus, Dan Blumberg, and Jiftah Ben-Asher. Spatial Variability of Durum Wheat Yield as Related to Soil Parameters in an Organic Field. *Communications in Soil Science and Plant Analysis*, 45(15):2018–2031, 2014. DOI:10.1080/00103624.2014.919311.
- [Pea04] K Pearson. On the Theory of Contingency and its Relation to Points in Space. *Philosophical Magazine*, 2(11):559–572, 1904.
- [PGZ⁺07] J L Ping, C J Green, R E Zartman, K F Bronson, and T F Morris. Spatial Variability of Soil Properties, Cotton Yield, and Quality in a Production Field. *Communications in Soil Science and Plant Analysis*, 39(1-2):1–16, 2007. DOI:10.1080/00103620701758840.
- [PJABa06] T Panagopoulos, J Jesus, M D C Antunes, and J Beltrão. Analysis of spatial interpolation for optimising management of a salinized field cultivated with lettuce. *European Journal of Agronomy*, 24(1):1–10, 2006. DOI:10.1016/j.eja.2005.03.001.
- [PPCA13] Mariano Paggi, Nahuel Raúl Peralta, Mirta Calandroni, and Virginia Aparicio. Identificación de series de suelos mediante el uso de sensores de conductividad eléctrica aparente en el sudeste bonaerense. *Ciencia del Suelo (Argentina)*, 31(2):175–188, 2013.
- [PSM⁺05] J M N O Peça, João M Serrano, J R Marques da Silva, P Palma, M Carvalho, D Crespo, and C Novas. Variable Rate Application of Fertilizer in a Permanent Pasture - An Account of the First Year of Experimental Tests in Portugal. In *5th conference of the European federation for information technology in agriculture, food and environment*, pages 1241–1245, July 25–28, Vila Real, Portugal., 2005.
- [RCL99] J D Rhoades, F Chanduvi, and S Lesch. *Soil salinity assessment: methods and interpretation of electrical conductivity measurements*. Rome, 1999.

- [Rem02] N Remy. Stanford Geostatistical Modeling Software. Leland Stanford University, 2002.
- [RMSA89] J D Rhoades, Nahid A Manteghi, P J Shouse, and W J Alves. Estimating Soil Salinity from Saturated Soil-Paste Electrical Conductivity. *Soil Science Society of America Journal*, 53(2):428–433, 1989. DOI:10.2136/sssaj1989.03615995005300020067x.
- [RPPLS11] J Ramon Rodríguez-Pérez, Richard E Plant, Jean Jacques Lambert, and David R Smart. Using apparent soil electrical conductivity (EC a) to characterize vineyard soils of high clay content. *Precision Agriculture*, 12(6):775–794, 2011. DOI:10.1007/s11119-011-9220-y.
- [San95] J Quelhas Santos. *Fertilização e poluição: reciclagem agro-florestal de resíduos orgânicos. (Fertilization and pollution: agro-forestry recycling organic waste)*. Lisboa, 1995.
- [SCMaC08] Zigomar M Souza, Domingos G Pellegrino Cerri, P G Magalhães, and M C C Campos. Correlação dos atributos físicos e químicos do solo com a produtividade de cana-de-açúcar. *Revista de Biologia e Ciências da Terra*, 8(2):183–190, 2008.
- [SD07] Kenneth A Sudduth and Scott T Drummond. Yield editor: Software for removing errors from crop yield maps. *Agronomy Journal*, 99(6):1471–1482, 2007. DOI:10.2134/agronj2006.0326.
- [Sha90] Andrew N. Sharpley. Reaction of fertilizer potassium in soils of differing mineralogy. *Soil Science*, 149(1):44–51, 1990.
- [Sha95] Andrew N Sharpley. Soil phosphorus dynamics: agronomic and environmental impacts. *Ecological Engineering*, 5(2-3):261–279, 1995. DOI:10.1016/0925-8574(95)00027-5.
- [SHG⁺08] Jürgen Schellberg, Michael J Hill, Roland Gerhards, Matthias Rothmund, and Matthias Braun. Precision agriculture on grassland: Applications, perspectives and constraints. *European Journal of Agronomy*, 29(2-3):59–71, 2008. DOI:10.1016/j.eja.2008.05.005.
- [SKB⁺03] Kenneth A Sudduth, N R Kitchen, G a Bollero, D G Bullock, and W J Wiebold. Comparison Of Electromagnetic Induction And Direct Sensing Of Soil Electrical Conductivity. *Agronomy Journal*, 95(3):472–482, 2003. DOI:10.2134/agronj2003.4720.
- [SKW⁺] Kenneth A Sudduth, N R Kitchen, W J Wiebold, W D Batchelor, A Bollero, G Bullock, D E Clay, H L Palm, F J Pierce, R T Schuler, and K D Thelen.
- [Soa06] A Soares. *Geoestatística para as Ciências da Terra e do Ambiente. Coleção Ensino da Ciência e da Tecnologia*. Lisboa, IST Press, 2 edition, 2006.
- [SPC13] M Simón, Nahuel Raúl Peralta, and J L Costa. Relación entre la conductividad eléctrica aparente con propiedades del suelo y nutrientes. *Ciencia del suelo*, 31(1):45–55, 2013.
- [SPdS⁺10] João M Serrano, J O Peça, J R Marques da Silva, Shakib Shahidian, and Mário Carvalho. Phosphorus dynamics in permanent pastures: Differential fertilizing and the animal effect. *Nutrient Cycling in Agroecosystems*, 90(1):63–74, 2010. DOI:10.1007/s10705-010-9412-2.
- [SPMS10] João M Serrano, J O Peça, J R Marques da Silva, and S Shaidian. Mapping soil and pasture variability with an electromagnetic induction sensor. *Computers and Electronics in Agriculture*, 73(1):7–16, 2010. DOI:10.1016/j.compag.2010.03.008.
- [SSdS14] João M Serrano, Shakib Shahidian, and José Marques da Silva. Spatial and temporal patterns of apparent electrical conductivity: DUALEM vs. Veris sensors for monitoring soil properties. *Sensors (Switzerland)*, 14(6):10024–10041, 2014. DOI:10.3390/s140610024.

- [SSL⁺04] Aaron R Schepers, John F Shanahan, Mark A Liebig, James S Schepers, Sven H Johnson, and Arivaldo Luchiari. Appropriateness of Management Zones for Characterizing Spatial Variability of Soil Properties and Irrigated Corn Yields across Years. *Agronomy Journal*, 96(1):195–203, 2004. DOI:10.2134/agronj2004.0195.
- [SSM13] João M Serrano, Shakib Shahidian, and José R Marques da Silva. Comparing the DUALEM and VÉRIS sensors for mapping soil properties. In John V. Stafford, editor, *Precision agriculture'13*, pages 25–32. Wageningen Academic Publishers, 2013.
- [SSMds14] João M Serrano, S Shahidian, and J R Marques da silva. Soil phosphorus retention in a Mediterranean pasture subjected to differential management. *European Journal of Soil Science*, 65(4):562–572, 2014. DOI:10.1111/ejss.12141.
- [SSS14] João M Serrano, J Marques Da Silva, and S Shahidian. Spatial and temporal patterns of potassium on grazed permanent pastures-Management challenges. *Agriculture, Ecosystems and Environment*, 188:29–39, 2014.
- [ST87] J W B Stewart and H Tiessen. Dynamics of soil organic phosphorus. *Biogeochemistry*, 4(1):41–60, 1987. DOI:10.1007/BF02187361.
- [Sud99] Kenneth A Sudduth. Engineering technologies for precision farming. In *International Seminar on Agricultural Machinery Technology for Precision Farming*, May 17,(5-27):Rural Development Administration, Suwon, Korea, 1999.
- [SWB⁺00] Z Shi, K Wang, Js Bailey, C Jordan, and Aj Higgins. Sampling strategies for mapping soil phosphorus and soil potassium distributions in cool temperate grassland. *Precision Agriculture*, pages 347–357, 2000. DOI:10.1023/A:1012399915193.
- [TBGS07] J Torrent, E Barberis, and F Gil-Sotres. Agriculture as a source of phosphorus for eutrophication in southern Europe. *Soil Use and Management*, 23(SUPPL. 1):25–35, 2007. DOI:10.1111/j.1475-2743.2007.00122.x.
- [TL05] J Triantafilis and S M Lesch. Mapping clay content variation using electromagnetic induction techniques. *Computers and Electronics in Agriculture*, 46(1-3 SPEC. ISS.):203–237, 2005. DOI:10.1016/j.compag.2004.11.006.
- [Toz09] Peter R Tozer. Uncertainty and investment in precision agriculture - Is it worth the money? *Agricultural Systems*, 100(1-3):80–87, 2009. DOI:10.1016/j.agry.2009.02.001.
- [TWEG03] J C Taylor, G A Wood, R Earl, and R J Godwin. Soil factors and their influence on within-field crop variability, Part II: Spatial analysis and determination of management zones. *Biosystems Engineering*, 84(4):441–453, 2003. DOI:10.1016/S1537-5110(03)00005-9.
- [VBJ02] John Vann, Olivier Bertoli, and Scott Jackson. An Overview of Geostatistical Simulation for Quantifying Risk by. *Geostatistical Association of Australasia symposium “Quantifying Risk and Error”*, (March):1–12, 2002.
- [VPG03] Sidney Rosa Vieira and Antonio Paz-Gonzalez. Analysis of the spatial variability of crop yield and soil properties in small agricultural plots. *Bragantia*, 62(1):127–138, 2003. DOI:10.1590/S0006-87052003000100016.
- [VS⁺08] Udayakantha W a Vitharana, Marc Van Meirvenne, David Simpson, Liesbet Cockx, and Josse De Baerdemaeker. Key soil and topographic properties to delineate potential management classes for precision agriculture in the European loess area. *Geoderma*, 143(1-2):206–215, 2008. DOI:10.1016/j.geoderma.2007.11.003.

- [WEF01] Paul J A Withers, A C Edwards, and R H Foy. Phosphorus cycling in UK agriculture and implications for phosphorus loss from soil. *Soil Use and Management*, 17(3):139–149, 2001. DOI:10.1111/j.1475-2743.2001.tb00020.x.
- [WTC⁺11] Yi Wang, Cong Tu, Lei Cheng, Chunyue Li, Laura F Gentry, Greg D Hoyt, Xingchang Zhang, and Shuijin Hu. Long-term impact of farming practices on soil organic carbon and nitrogen pools and microbial biomass and activity. *Soil and Tillage Research*, 117:8–16, 2011. DOI:10.1016/j.still.2011.08.002.
- [YLK⁺01] Junta Yanai, Choung Keun Lee, Toshikazu Kaho, Michihisa Iida, Tsutomu Matsui, Mikio Umeda, and Takashi Kosaki. Geostatistical analysis of soil chemical properties and rice yield in a paddy field and application to the analysis of yield-determining factors. *Soil Science and Plant Nutrition*, 47(2):291–301, 2001. DOI:10.1080/00380768.2001.10408393.
- [ZSJ⁺10] Xiaodong Zhang, Lijian Shi, Xinhua Jia, George Seielstad, and Craig Helgason. Zone mapping application for precision-farming: A decision support tool for variable rate application. *Precision Agriculture*, 11(2):103–114, 2010. DOI:10.1007/s11119-009-9130-4.
- [ZWW02] Naiqian Zhang, Maohua Wang, and Ning Wang. Precision agriculture—a worldwide overview. *Computers and Electronics in Agriculture*, 36(2-3):113–132, 2002. DOI:10.1016/S0168-1699(02)00096-0.



UNIVERSIDADE DE ÉVORA
INSTITUTO DE INVESTIGAÇÃO
E FORMAÇÃO AVANÇADA

Contactos:

Universidade de Évora
Instituto de Investigação e Formação Avançada — IIFA
Palácio do Vimioso | Largo Marquês de Marialva, Apart. 94
7002 - 554 Évora | Portugal
Tel: (+351) 266 706 581
Fax: (+351) 266 744 677
email: iifa@uevora.pt